High-Fidelity FSI Simulations and V&V of Vertical and Oblique Flexible Plate Slamming

Riccardo Pellegrini[1,2], Matteo Diez[2], Zhaoyuan Wang[3], and Frederick Stern[3]

[1] Visiting postdoc at IIHR-Hydroscience & Engineering, University of Iowa, Iowa City, IA, USA

[2]National Research Council, Institute of Marine Engineering (INM), Rome, Italy

[3]IIHR-Hydroscience & Engineering, University of Iowa, Iowa City, IA, USA

Funding for this work is provided by the Office of Naval Research, Ship Systems and Engineering Research Division (Code 331), under the direction of Dr. Robert Brizzolara, Grant N00014-20-1-2259 under administration. Dr. Riccardo Pellegrini is partially supported through CNR-INM project ATOM.

Outline

- Introduction (3)
  - Motivation, background, objectives, and approach
- Physical problem and EFD (2)
- Hydroelasticity parameters (4)
- CFD/CSD/FSI methods and setup (5)
- Overview validation (7)
- Stagnation point model derivation and analysis (7)
- Energy equation derivation and analysis (11)
- MDO for reduced slamming response (6)
- Conclusions and future research (1)

Introduction - Motivation

- Achievement of weight reduction without loss of structural safety in the design of high-speed vessels
  - Slamming phenomenon must be considered
- High-fidelity computational fluid and structural dynamics (CFD/CSD) are used for load prediction in realistic operating conditions
- Challenges include multi-phase flow and fluid structure interaction (FSI) for hydroelastic phenomena
- Simplified geometries are used to decouple physical phenomena and investigate the underlying physics of the slamming

Search and Rescue, Patrolling

https://www.youtube.com/watch?v=Sx57-LnuuFs

Commercial activities

https://www.youtube.com/watch?v=bZSM5ZbdpWw

Introduction - Background

- Analytical, numerical, and experimental investigations on slamming of wedges, plates, and other simplified geometries have been performed in the last century
- Main findings are:
  - Self-similar flow models are a reasonable approximation for 2D investigations
  - Gravity is important for low-speed water entry
  - There exists a high-pressure ridge moving along the wet surface during the slam
  - The velocity of the spray root is not constant
  - Impact loads scale with the normal to the body surface velocity
  - Elastic structures can exhibit:
    - Spray separation
    - Increase of the total load
    - Reduction of the local pressure
    - Cavitation and/or ventilation
  - For elastic plates, the significance of the hydroelasticity is a function of the wetting time and the first eigenfrequency

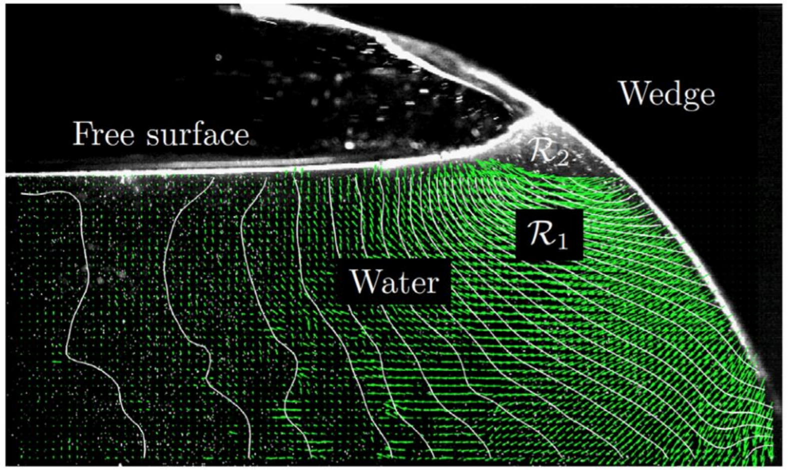

Fig. 4. Example of a high speed image with overlaid PIV measurement and relative contour lines. The wedge considered here has an average deadrise angle $\beta_0 = 35^\circ$ and deadrise angle at the keel of $2\beta_0$.

Panciroli, R., A. Shams, and M. J. O. E. Porfiri. "Experiments on the water entry of curved wedges: High speed imaging and particle image velocimetry." Ocean Engineering 94 (2015): 213-222.

Example of water slam with large deflection and air entrapment

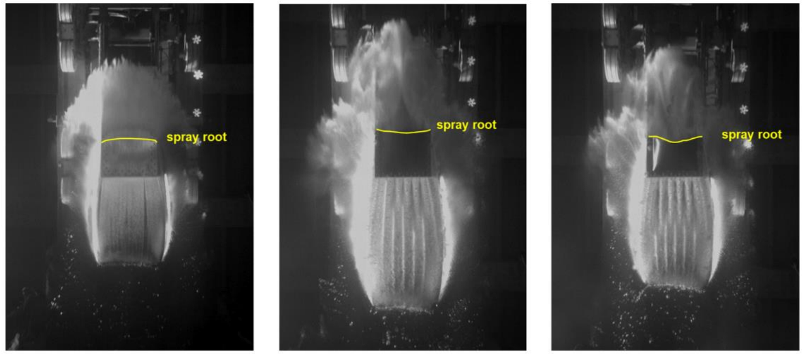

(a) 15_10_30 (thickness 15 mm) (b) 3_10_30 (thickness 3 mm) (c) 08_10_30 (thickness 0.8 mm)

Spinosa, Emanuele, and Alessandro Iafrati. "Experimental investigation of the fluid-structure interaction during the water impact of thin aluminium plates at high horizontal speed." *International Journal of Impact Engineering* 147 (2021): 103673.

Introduction - Objective and Approach

Objective

- Development of numerical methods for
  - Resolving complex FSI problem with large impacts and deformations
  - Understanding the physics of complex FSI phenomena
  - Assessing/investigating new advanced concepts, designs, and materials
  - Building capabilities for optimizing/controlling the response of ship structures with the aim of reducing the weight, increasing the structural payload, and personnel safety
- Development of effective analysis methods and approaches
  - Extended Bernoulli equation for spray root dynamic analysis
  - Energy conservation applied to FSI
- Analysis and multidisciplinary optimization of anisotropic structures
- Collaboration with UMD for investigation of elastic flat plate slamming

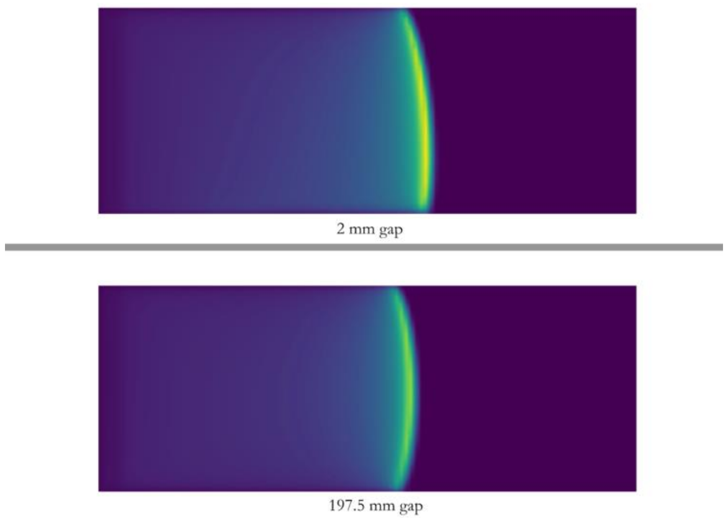

Spray root analysis, effect of the gap width

Approach

- Identification of a general and effective approach to model geometric nonlinearities
- Lagrangian and Eulerian approaches for the investigation of the physics of slamming
- Machine learning for MDO of anisotropic structures
- Comparison with UMD data from elastic plate slamming experiments

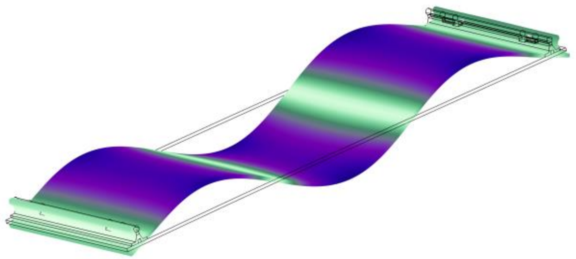

Prestressed modal analysis for nonlinear modal expansion setup

Experimental setup, conditions, and validation variables

- UMD test matrix covers 24 combinations of vertical and horizontal velocities for 3 plate thicknesses
- Selected cases are investigated with and without symmetry wall
- Validation variables are
  - Normal force and transverse moment
  - Pressure
  - Spray root position
  - Strains
  - Centerplate deflection

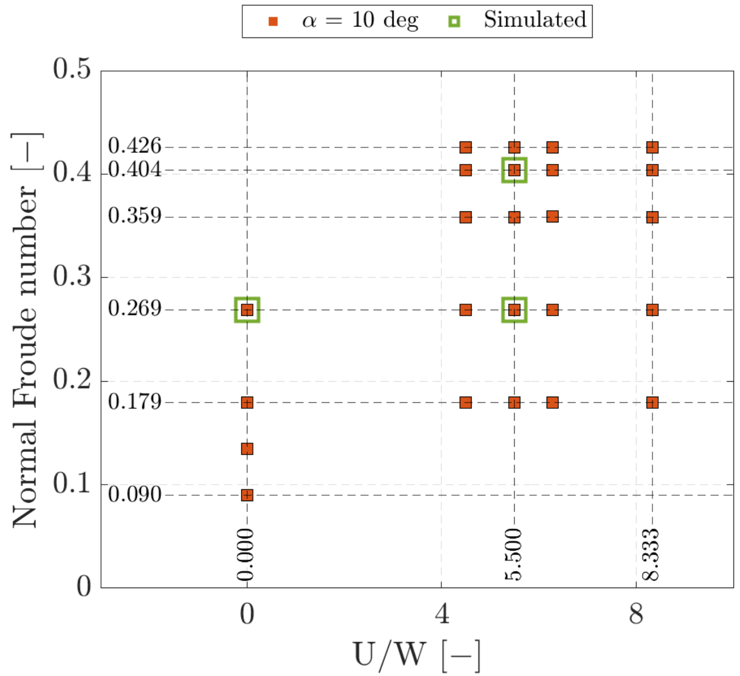

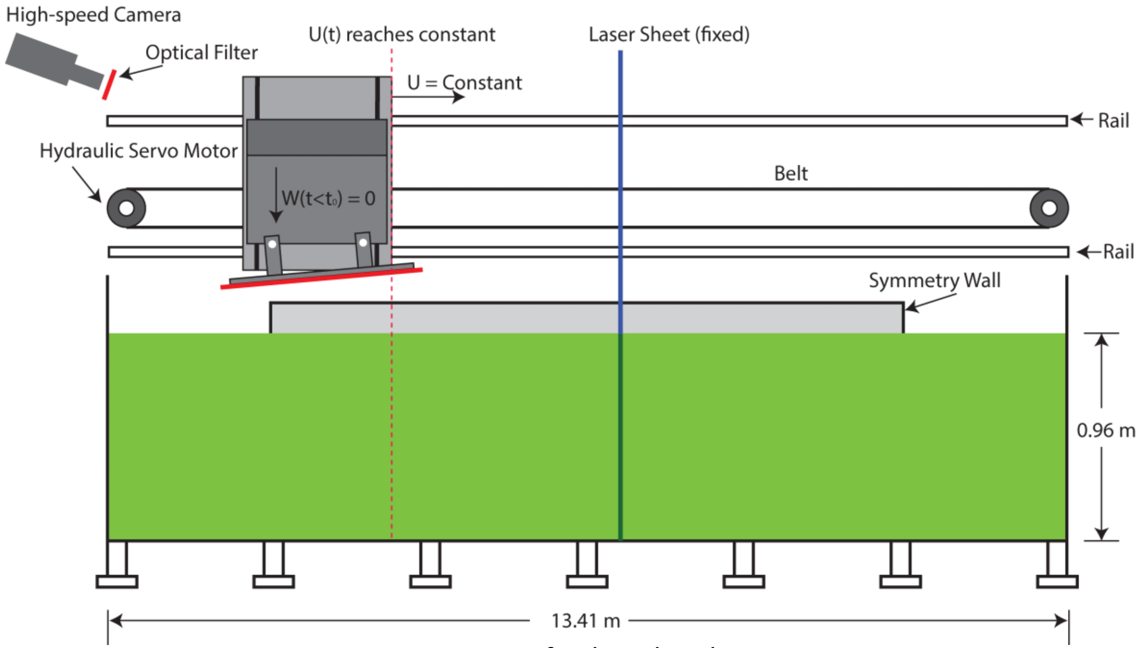

UMD facility sketch

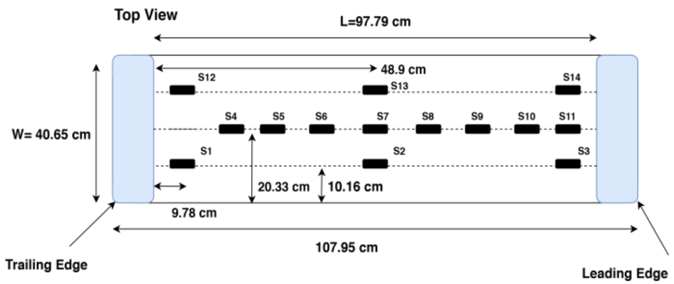

Strain sensors location for the h_3 plate

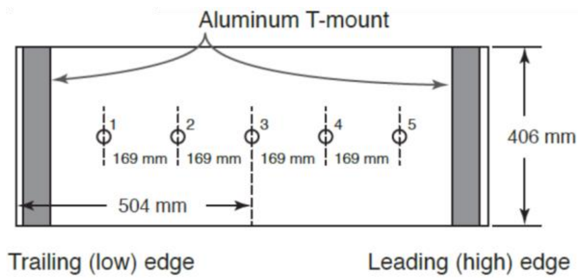

Deflection gauges location

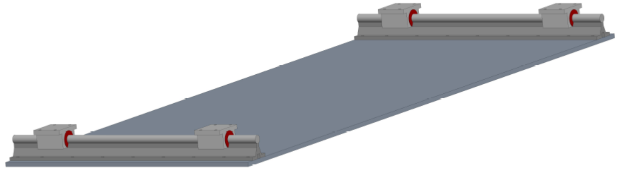
Plate with rails and rail's bearings (red)

Experimental setup, conditions, and validation variables

- Videos of the EFD, from the YouTube channel of An Wang from the University of Maryland.
  - U = 4 m/s, W = 0.8 m/s
  - Pitch angle = 10 deg

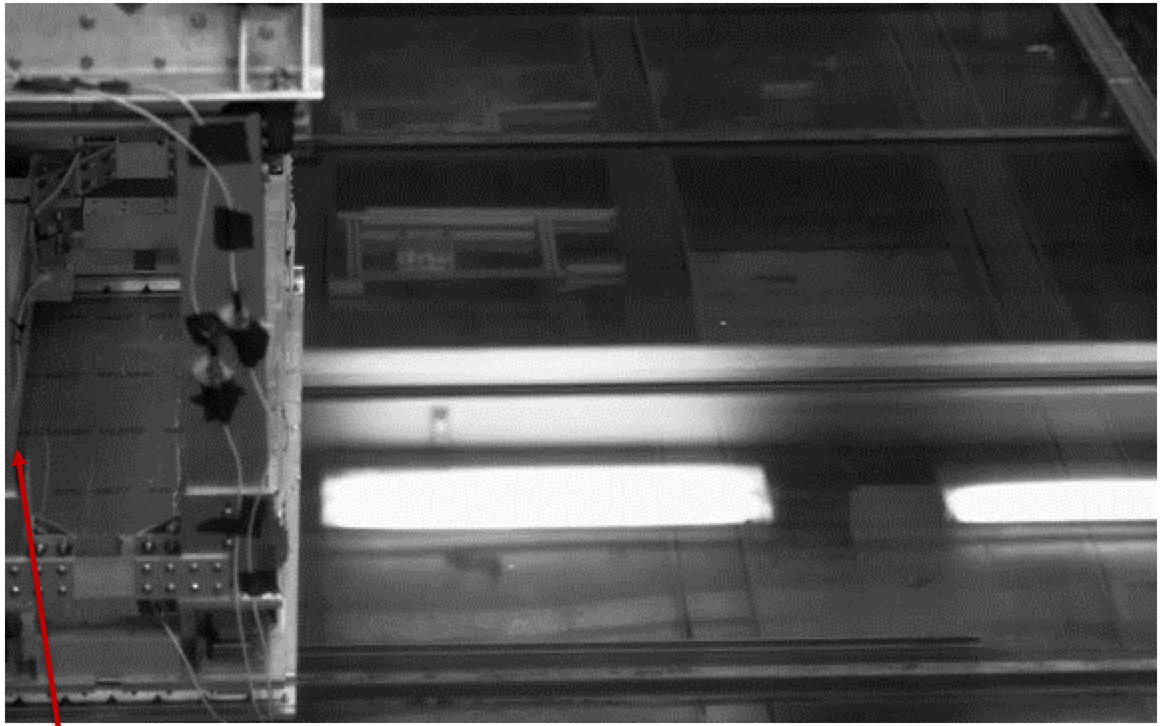

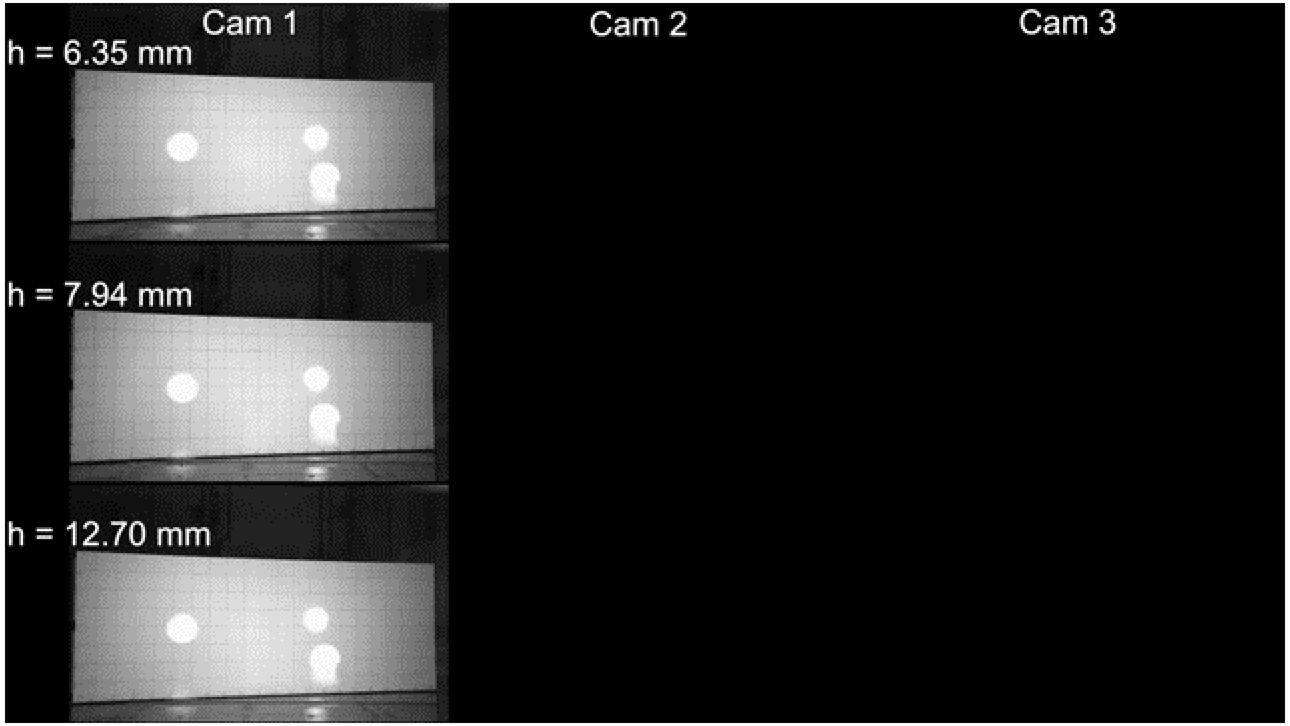

https://www.youtube.com/watch?v=_p7n1u-HewI

https://www.youtube.com/watch?v=eyU-HeDn52Y

Can you see the spray?

The hydroelastic parameter R – Literature review

Reference	Slam type	Structure	R definition	R interpretation	R threshold	Scaling
1999 Faltinsen **Water Entry of a Wedge**	Vertical	Plate reinforced with stiffeners	$\frac{\tan\beta}{V}\sqrt{\frac{EI}{\rho_w L^3}}$	Ratio between the wetting time of the rigid wedge and the first natural wet period of the stiffener	R<2 hydroelasticity matters	Maximum strain is scaled following a quasi-steady approach (with V_n^2) and a hydroeastic approach (with V_n)
2001 Bereznitski **Slamming: the role of hydroelasticity**	Vertical	Beam (as the lower part of a wedge)	$\frac{\text{duration of the slam}}{\text{structural dry } period}$	As per definition	R<2 hydroelasticity matters	The hydroelastic deflection is scaled with the equivalent quasi-steady deflection
2007 Bogaert and Kaminski **Hydro-elastic criterion for practical design**	Vertical	2D cone (wedge)	$\frac{force\ rise\ time}{\text{structura dry } period}$	As per definition	R<2 hydroelasticity matters	The hydroelastic deflection is scaled with the equivalent quasi-steady deflection
2007 Stenius et al. **Explicit FE-modelling of hydroelasticity in panel-water impacts**	Vertical	Beam	$\boldsymbol{R_1 = 4\left(\frac{\mu_{NP}}{\pi}\right)^2 \frac{1}{\sqrt{\pi}} \frac{\tan\beta}{V}\sqrt{\frac{D}{\rho_w L^3}}}$	Ratio between two times the wetting time of the panel and the first natural wet period	R<4 hydroelasticity matters	The hydroelastic deflection and strain are scaled with the equivalent quasi-steady deflection and strains
2010 Stenius et al. **Hydroelastic Interaction in Panel-Water Impacts of High-Speed Craft**	Vertical	Plate	$\boldsymbol{R_1 = 4\left(\frac{\mu_{NP}}{\pi}\right)^2 \frac{1}{\sqrt{\pi}} \frac{\tan\beta}{V}\sqrt{\frac{D}{\rho_w L^3}}}$	Ratio between two times the wetting time of the panel and the first natural wet period	R<4 hydroelasticity matters	The hydroelastic deflection and strain are scaled with the equivalent quasi-steady deflection and strains
2015 Panciroli, Porfiri **Analysis of hydroelastic slamming through particle image velocimetry**	Vertical	Plate	$\frac{\tan\beta}{V}\sqrt{\frac{D}{\rho_w L^3}}$	Not discussed	R<2 hydroelasticity matters	Not discussed

The hydroelastic parameter R – Literature review

Reference	Slam type	Structure	R definition	R interpretation	R threshold	Scaling
1999 Faltinsen **Water Entry of a Wedge**	Vertical	Plate reinforced with stiffeners	$\frac{\tan\beta}{V}\sqrt{\frac{EI}{\rho_w L^3}}$	Ratio between the wetting time of the rigid wedge and the first natural wet period of the stiffener	R<2 hydroelasticity matters	Maximum strain is scaled following a quasi-steady approach (with V_n^2) and a hydroeastic approach (with V_n) Quasi-steady scaling $\frac{\varepsilon_{max}}{z_a V^2}\frac{EI}{\rho_w L^2}\tan\beta$ Hydroelastic scaling $\frac{\varepsilon_{max}}{z_a V}\sqrt{\frac{EI}{\rho_w L}}$
2015 Panciroli, Porfiri **Analysis of hydroelastic slamming through particle image velocimetry**	Vertical	Plate	$\frac{\tan\beta}{V}\sqrt{\frac{D}{\rho_w L^3}}$		R<2 hydroelasticity matters	

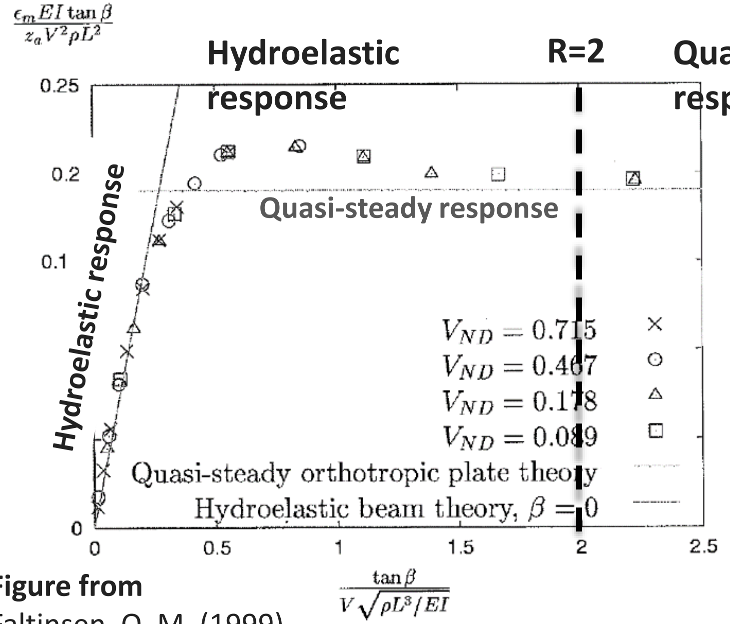

Figure from
Faltinsen, O. M. (1999)

- β is the deadrise angle
- L is the stiffener length
- V is the vertical velocity comprehensive of the ship motions contributions
- D is the bending stiffness of the plate

- Ongoing studies focus on the scaling of deflections and strains. Faltinsen, 1999 suggested two scaling for the maximum strains
- Quasi-steady response better use V_n^2: this results from the solution of a boundary value problem for quasi-steady response (Faltinsen, 1999)
- Hydroelastic response better use V_n : this results from the solution of a boundary value problem of a free-vibrating beam slamming on water (Faltinsen 1997, Kvalsvold and Faltinsen 1995)

The hydroelastic parameter R – Literature review

Reference	Slam type	Structure	R definition	R interpretation	R threshold	Scaling
2007 Stenius et al. **Explicit FE-modelling of hydroelasticity in panel-water impacts**	Vertical	Beam	$$R_1 = \underbrace{4\left(\frac{\mu_{NP}}{\pi}\right)^2 \frac{1}{\sqrt{\pi}}}_{\text{Boundary conditions contribution}} \frac{\tan\beta}{V}\sqrt{\frac{D}{\rho_w L^3}}$$	Ratio between two times the wetting time of the panel and the first natural wet period	R<4 hydroelasticity matters	The hydroelastic deflection and strain are scaled with the equivalent quasi-steady deflection and strains
2010 Stenius et al. **Hydroelastic Interaction in Panel-Water Impacts of High-Speed Craft**	Vertical	Plate				

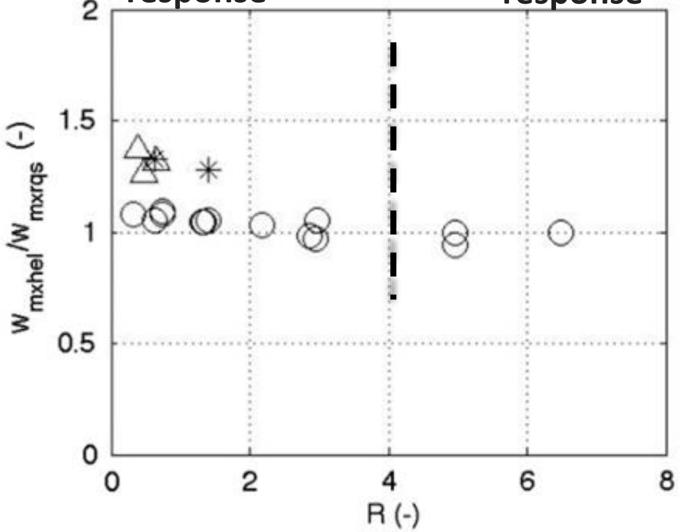

Results of numerical simulations

Figures from
Stenius et al. 2010

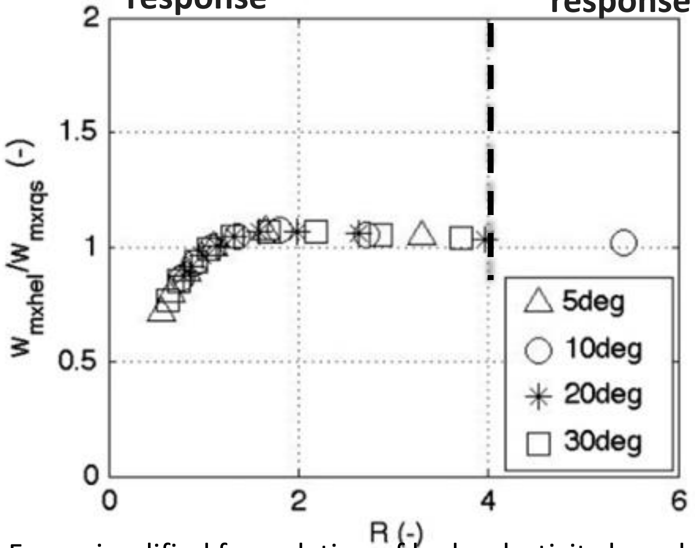

From simplified formulation of hydroelasticity based on engineering beam theory and potential theory
Similar to Faltinsen

- This formulation considers the boundary conditions of the structure
- The range of R is significantly different as the threshold for hydroelastic response
- Deflections are nondimensionalized with respect to the quasi-steady response
- There is a significant difference between simulations and the analytical model
- Many analytical models consider the slam until the spray root exits the structure thus not considering that the deformation of the structure may increase after

Hydroelastic parameter R for case selection

- Two definitions for the hydroelasticity parameter are used
  - R_3 is effective in identifying slamming conditions that have similar structural responses in terms of deflection
  - R_4 is effective to distinguish the different slam conditions and supports the choice of selecting only three slamming conditions to completely investigate the validation variables variability as per the experiments
- Hydroelasticity parameter (R) effectively to scale the maximum deflection (from EFD)
  - R is a reliable metric for the hydroelastic effects
- The V.269 and O.403 are characterized by significant hydroelastic effects
- The O.269 case shows limited hydroelastic effects
- The analysis based on the hydroelasticity parameter shows that the three cases selected for CFD and CFD/FSI numerical investigations are adequate to investigate the EFD trends

R_3

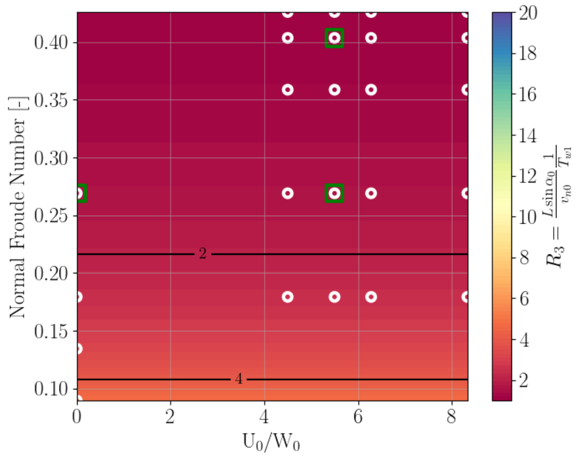

UMD test matrix with contour plot based on R_3 for 6.35 mm thick plate

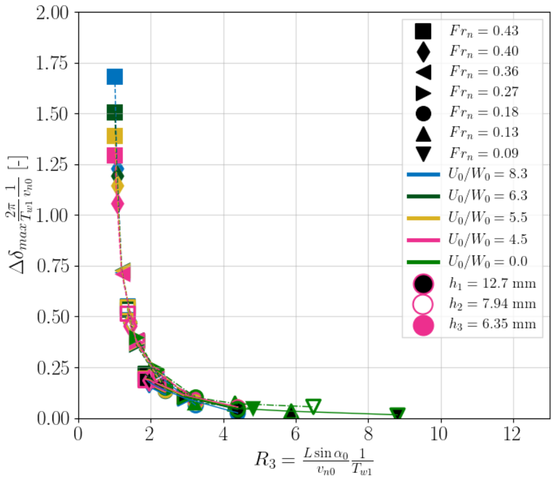

R_3, hydrodynamic scaling of the differential deflection

R_4

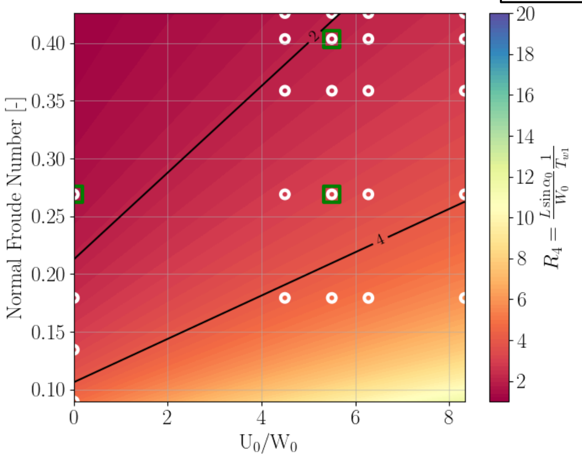

UMD test matrix with contour plot based on R_4 for 6.35 mm thick plate

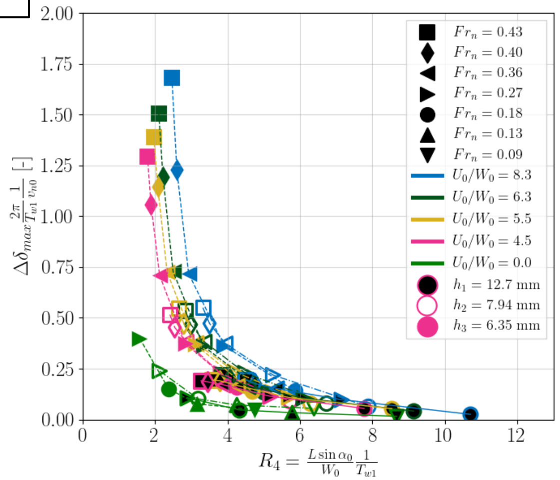

R_4, hydrodynamic scaling of the differential deflection

Simulated cases - Vertical slam

- This is the reference case.
- All the analysis will be performed in the direction normal to the plate (normal forces, normal velocity, etc…)

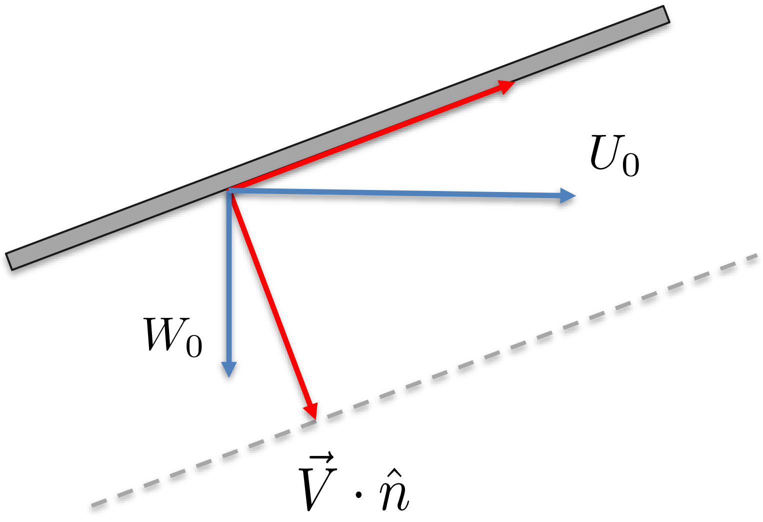

- V.269 – Vertical impact:

- W = 0.889 m/s
- U = 0
- U/W = 0

- Normal impact Fr = 0.269

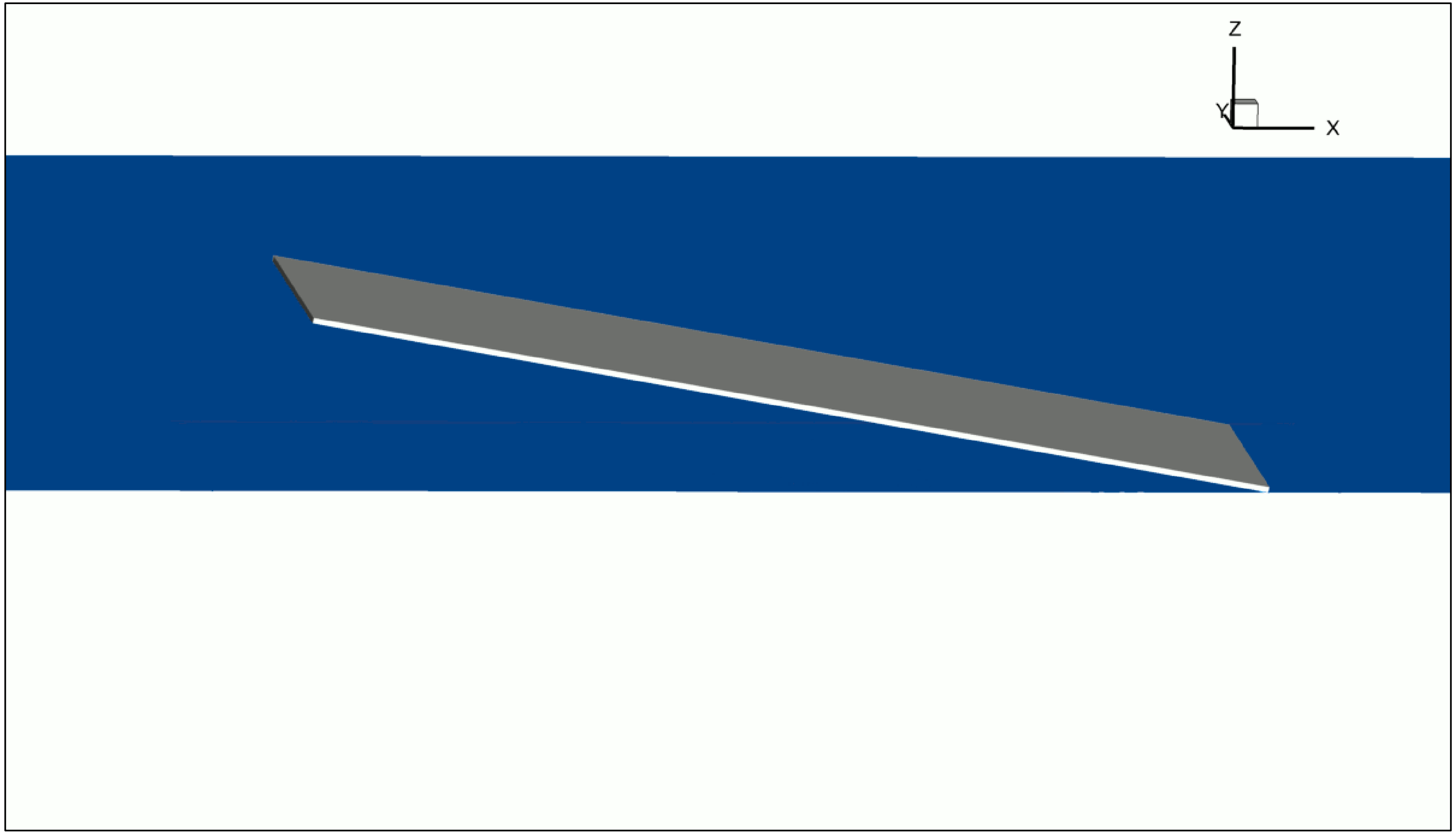

Simulated cases - Slow oblique slam

- What happen if a horizontal component of the velocity is considered without changing the normal impact Fr ?

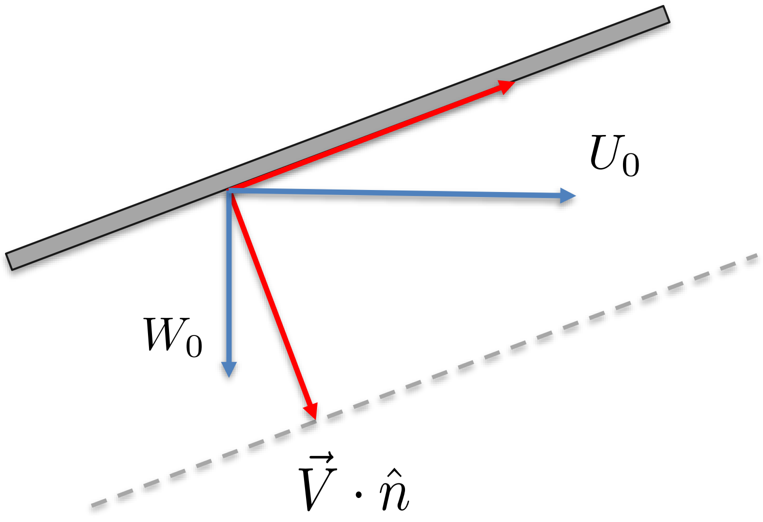

- O.269 – Slow oblique impact:

- W=0.451 m/s
- U=2.482 m/s
- U/W = 5.5

- Normal impact Fr = 0.269

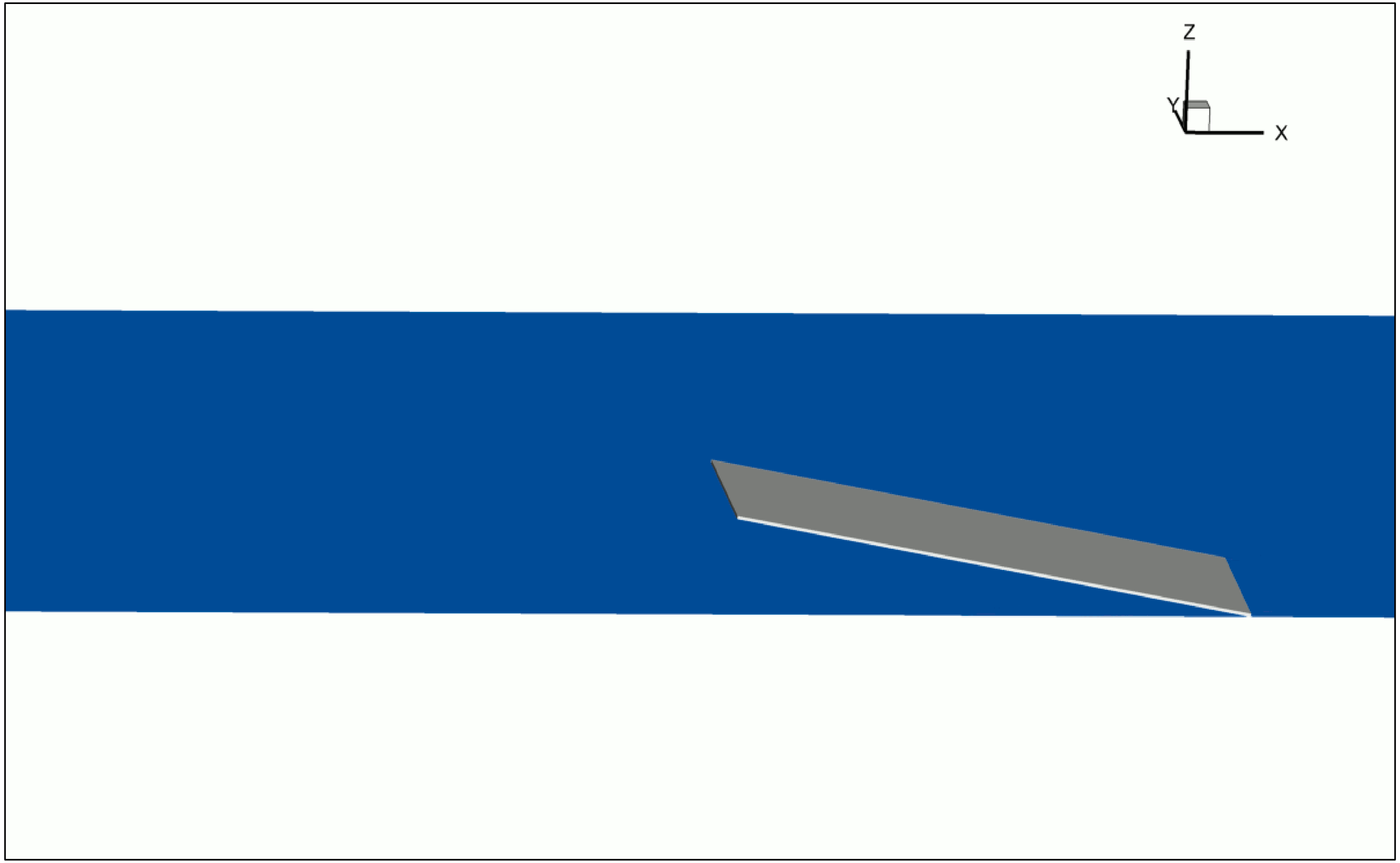

Simulated cases - Fast oblique slam

- What happen if the normal impact Fr is increased without changing the ratio of the velocity components?

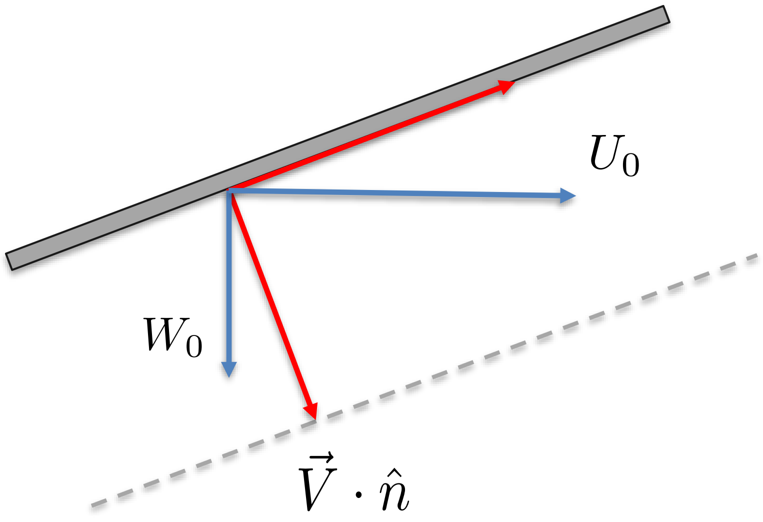

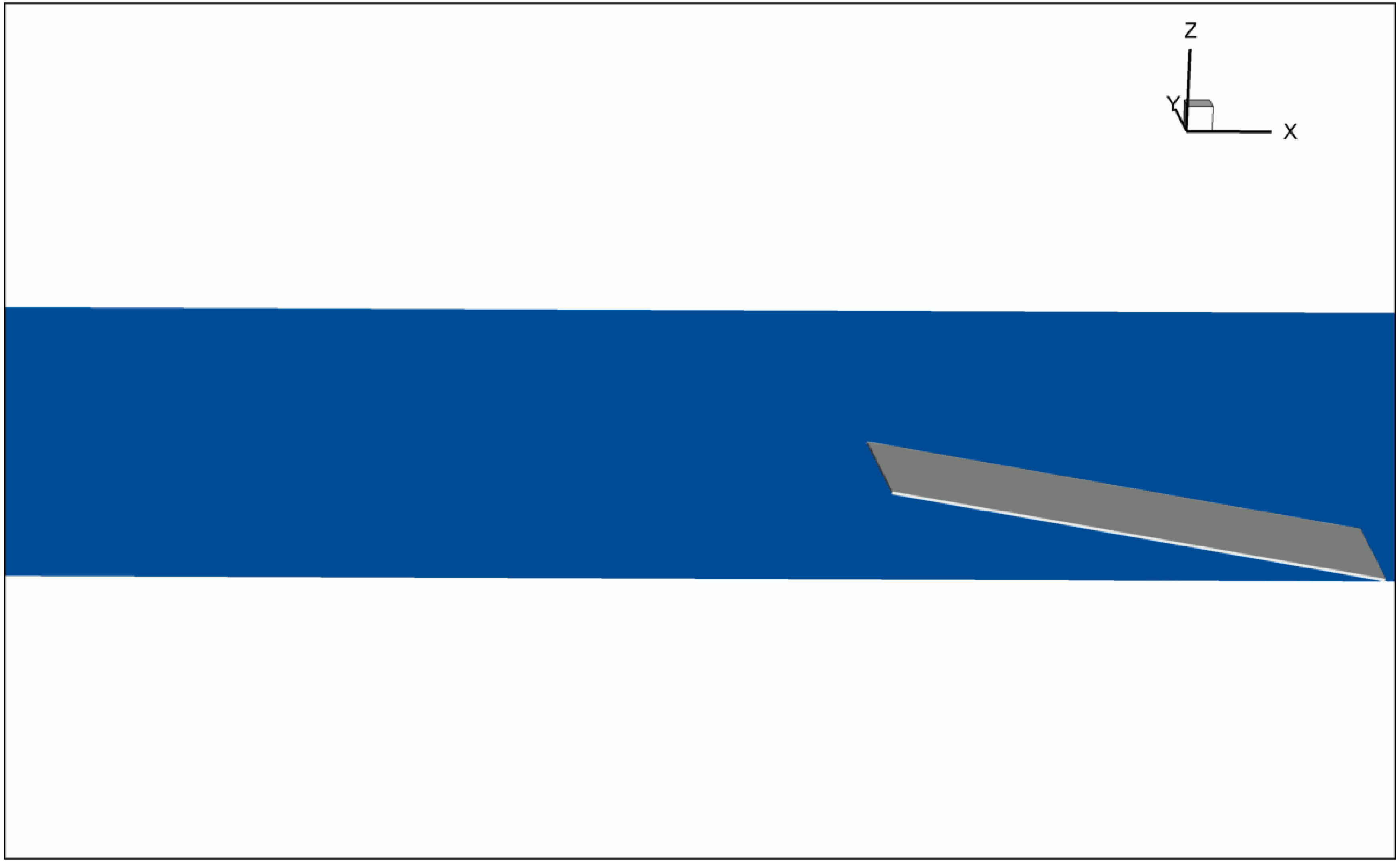

- O.403 – Fast oblique impact:

- W=0.677 m/s
- U=3.723 m/s
- U/W = 5.5

- Normal impact Fr = 0.403

CFD method

- CFDShip Iowa V4.5
- Simulation conditions selected to investigate the effects of Δh, U/W and Fr_n
- One and two-way FSI simulations are performed using both single and two-phase CFD models
- The 1-way results are compared with those for the thickest plate h_1 = 12.7 mm
- The grid is designed to investigate the fluid-structure interaction during the slamming and not yet refined for splash studies
- Width and depth of the domain are the same of the tank used for the experiments, including the gap between the plate and the inner “symmetry” wall
- For all the simulations, the crossing of the plate through the still water level is discretized with 334 time steps.
- FSI simulations are performed using 25 dry natural modes for the modal expansion with Rayleigh damping. The stiffness dumping coefficient is β = 0.0001

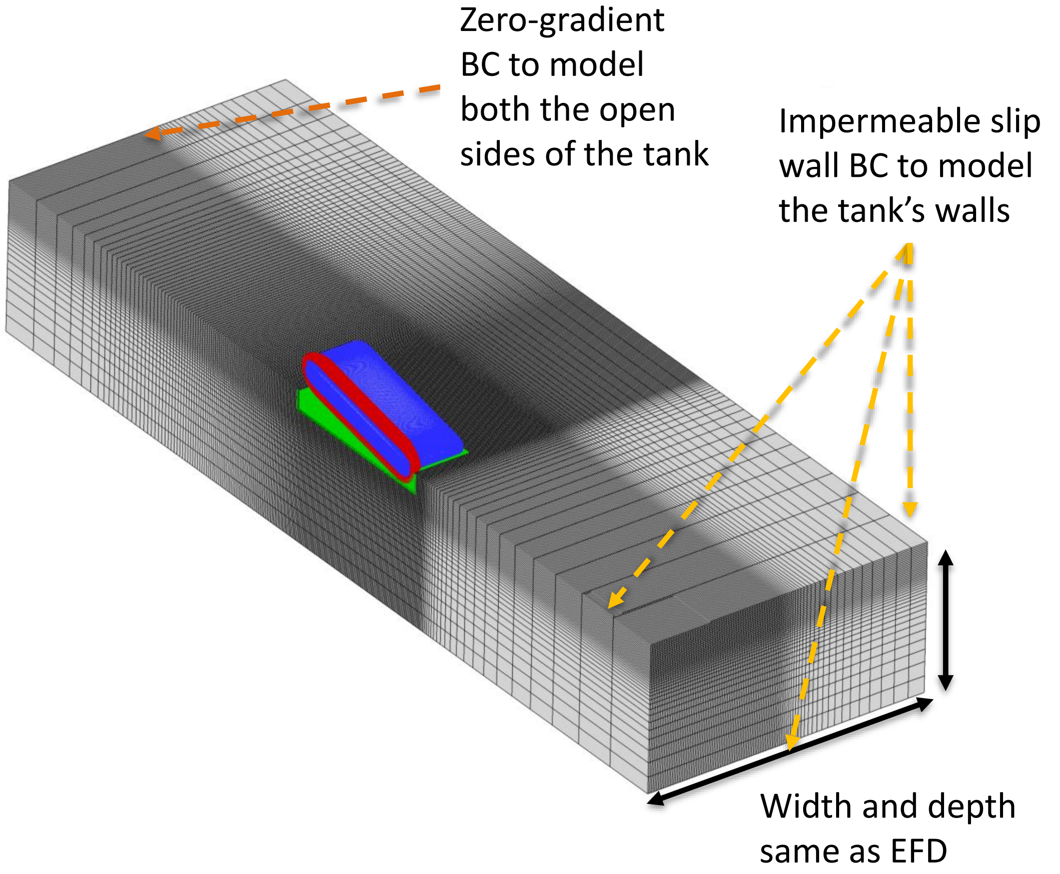

Block	Numbers of grid points [M]
Background (grey)	3.7
Plate’s body fitted (blue)	28.4
Gap (red)	1.5
Refinement (green)	2.7

CSD method

- COMSOL is used to model the plate by FEM
  - Spring foundations are used to calibrate the model
- Elastic constant of the springs is defined to match the first eigenfrequency of the pinned plate

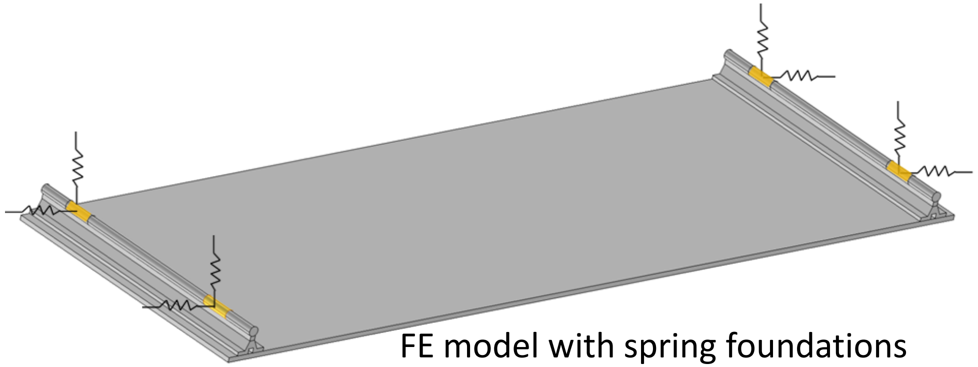

FE model with spring foundations

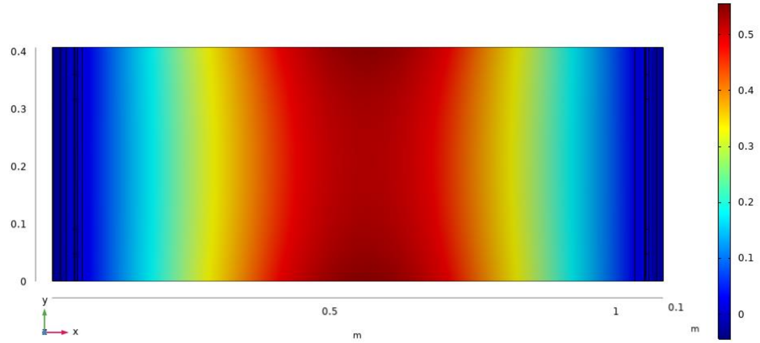

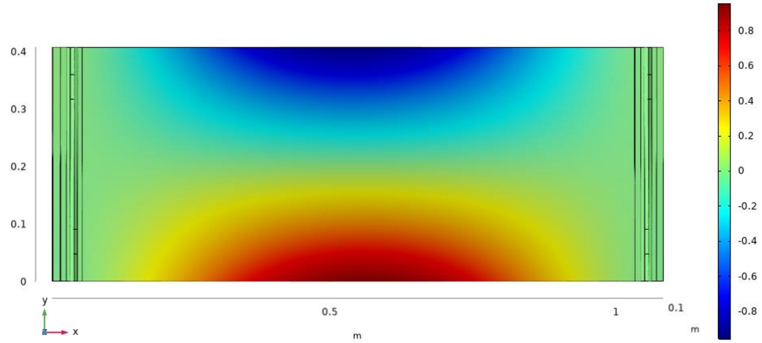

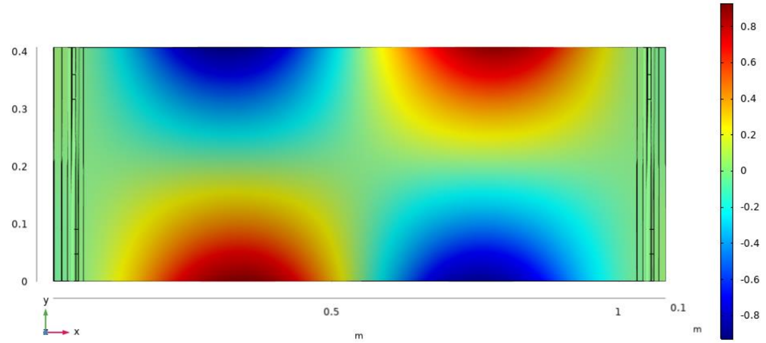

Structural nonlinearities

- Non-intrusive reduced order methods (ROM of discretized PDEs)
  - Any structure
  - Low computational cost
  - Easy to couple with other solvers for multidisciplinary analysis
- CFDShip-Iowa now uses a nonlinear modal expansion approach
  - The basis is computed as eigenvectors in vacuum
    - Water added mass effects are provided by direct computation of the fluid
  - Stiffness coefficients are determined by pre-stressed eigenfrequency analysis
  - **A polynomial model of the stiffness coefficient as a function of the modal coordinates is then realized**

$$\overline{\overline{M}}\ddot{\overline{u}} + \overline{\overline{K}}(\overline{u})\overline{u} = \overline{f_e} \xrightarrow[\textbf{expansion}]{\textbf{Modal}} \Delta\ddot{q}_i + 2\omega_i^2(\overline{q}_i)\xi\Delta\dot{q}_i + \omega_i^2(\overline{q}_i)\Delta q_i = \Delta f_i$$

The stiffness operator is nonlinear since is dependent from the displacement

Deflection, nonlinear versus linear evaluation

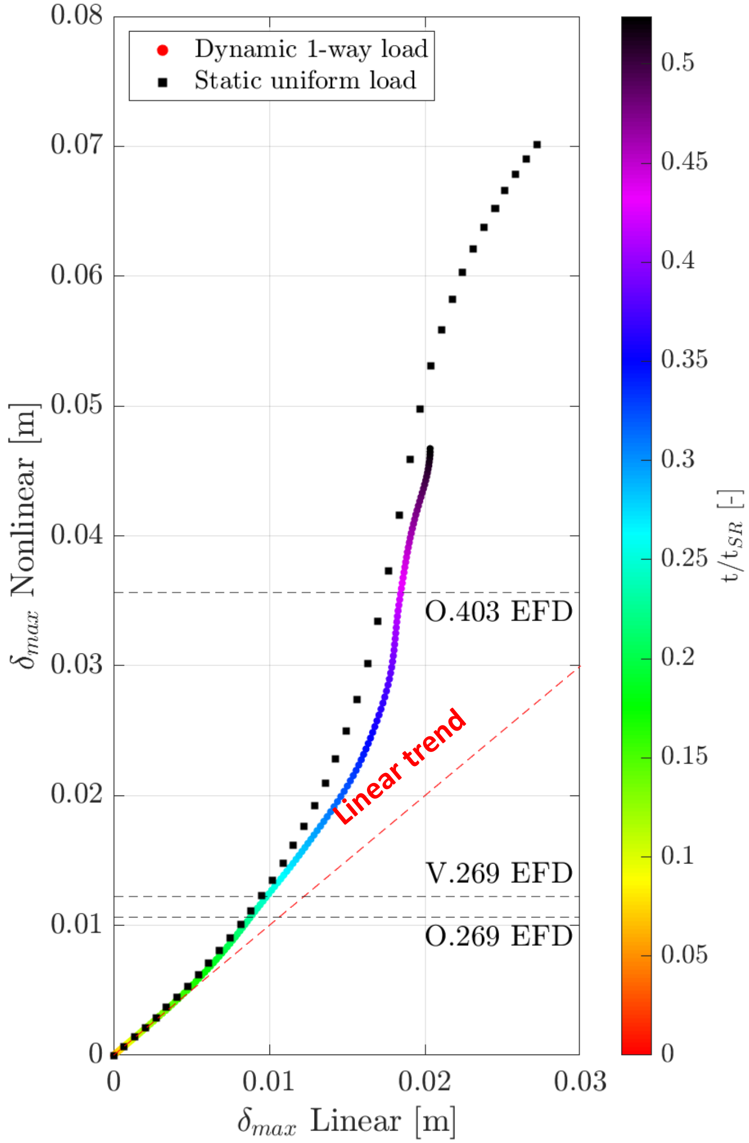

FSI method

- CFDShip-Iowa V4.5
  - Single phase
- Non-intrusive reduced order methods (ROM of discretized PDEs)
  - Any structure
  - Low computational cost
  - Easy to couple with other solvers for multidisciplinary analysis
- Any CSD software can be used
- The ROM can be easily trained for the specific FSI phenomena with a limited computational cost

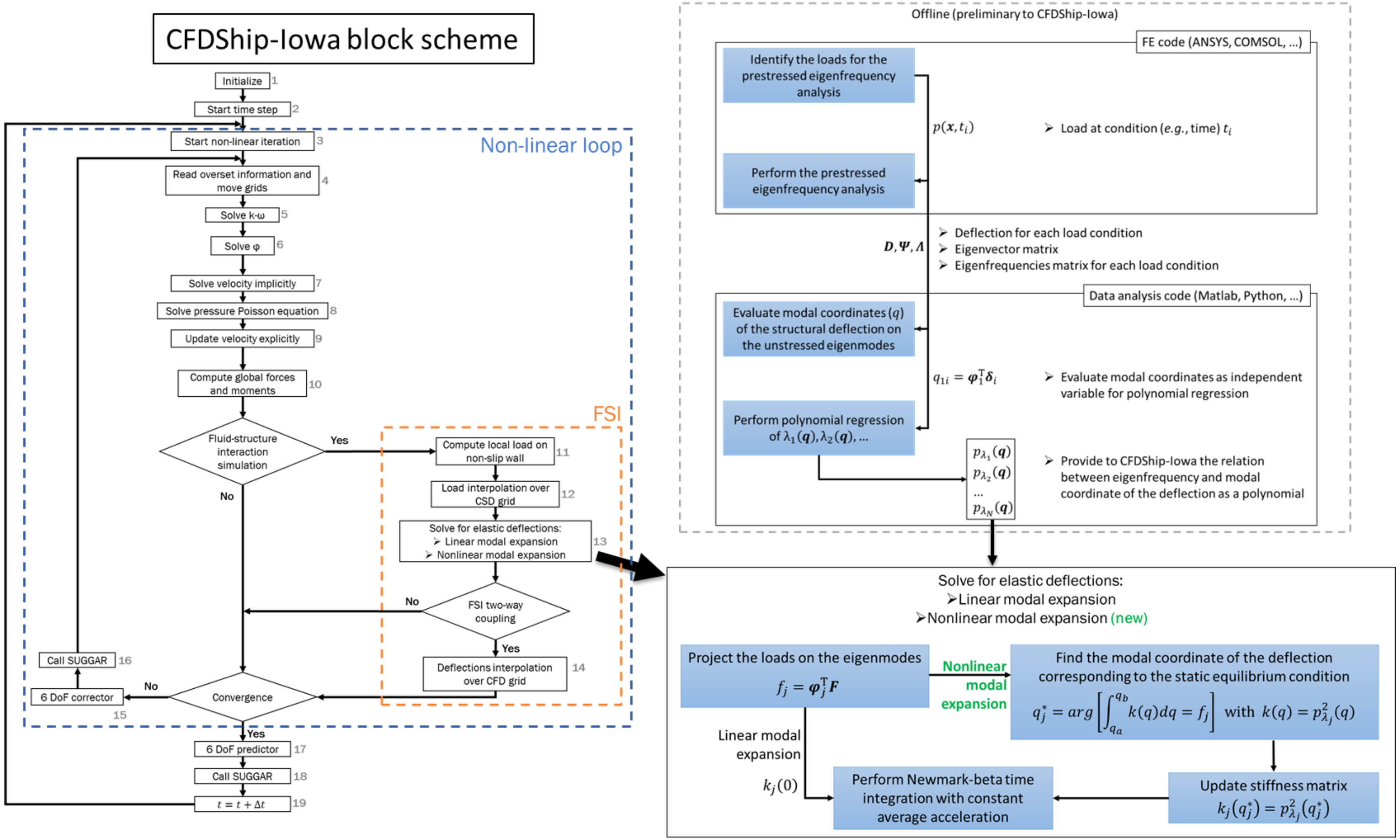

Overview validation – Force and moment

- Vertical slam
- Flexible plate shows initially a reduced load that significantly grows greater than with the rigid plate in the second part of the slam
- The peak values for the flexible plate are also postponed w.r.t. the rigid plate
- For the flexible plate the force grows concave whereas it is linear for the rigid plate
- The predictions are reasonably accurate, especially in the concave growth phase

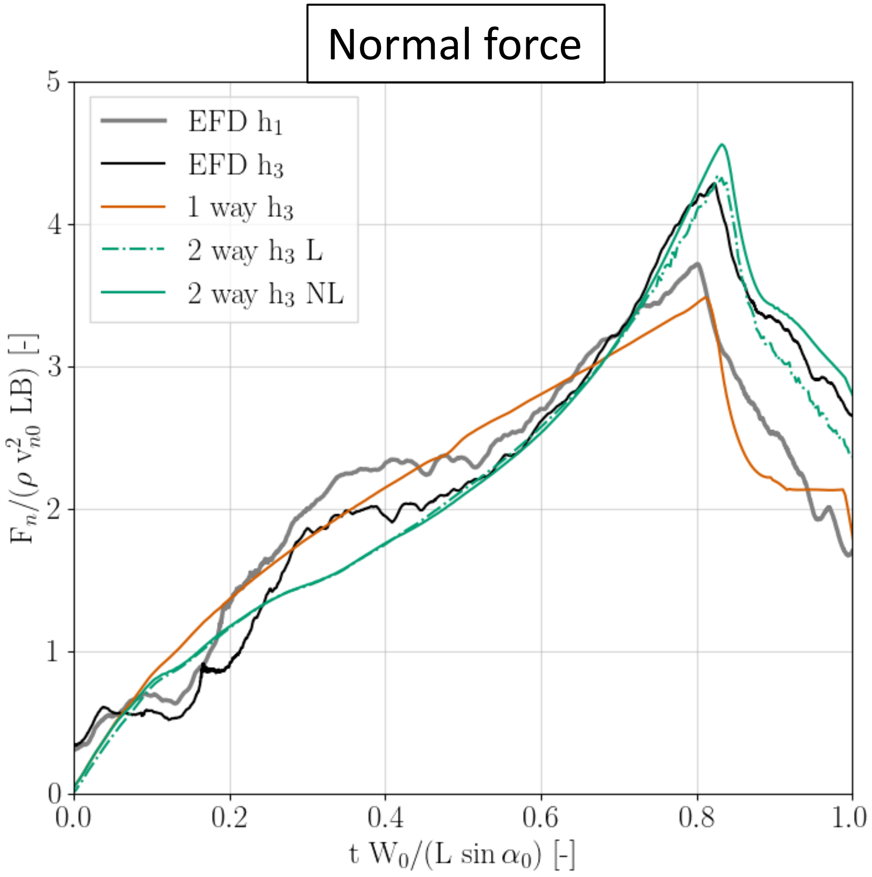

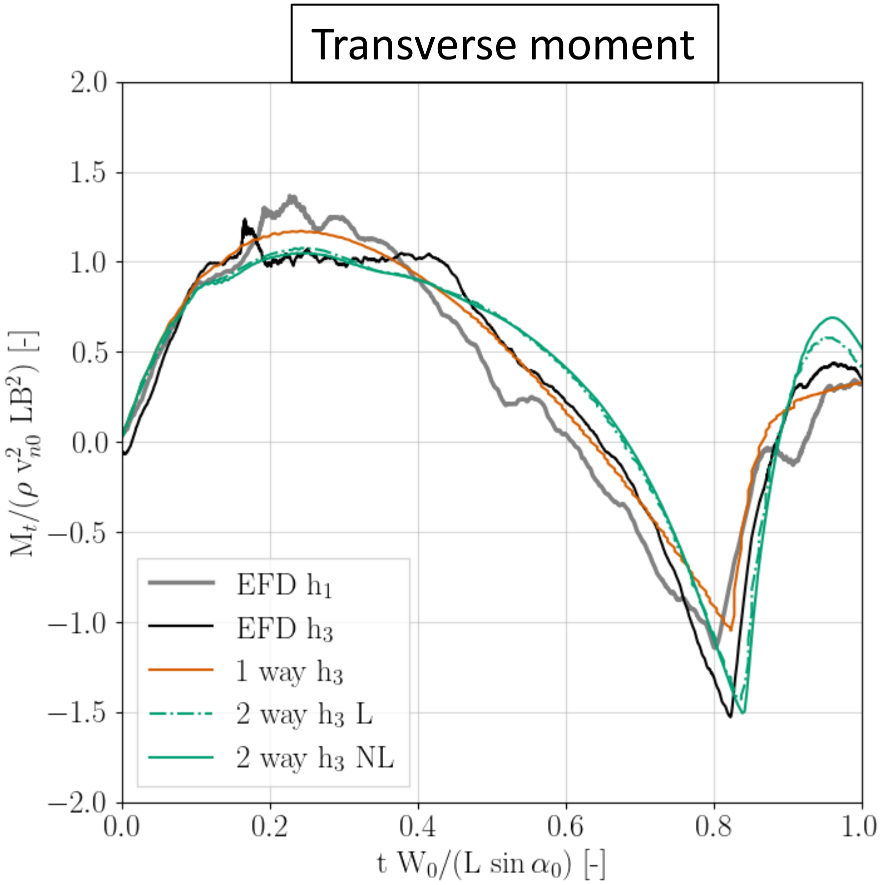

Overview validation – Pressure

- Vertical slam
- Significant differences exists between the rigid and flexible plates
- Qualitative analysis suggests an interaction of the high pressure ridge with the plate deformation

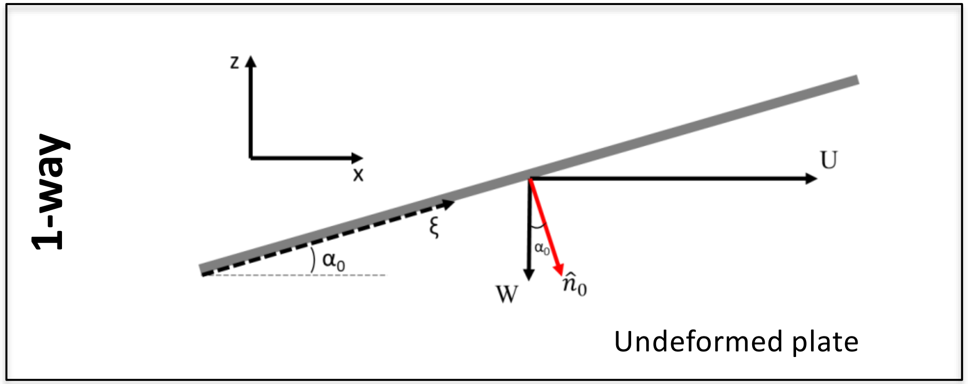

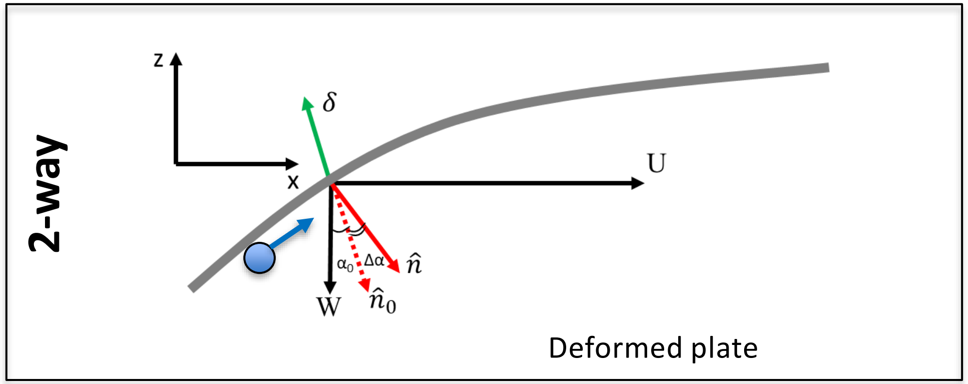

Rigid plate

Pressure

Flexible plate

Pressure

Displacement

Local variation of the impact angle

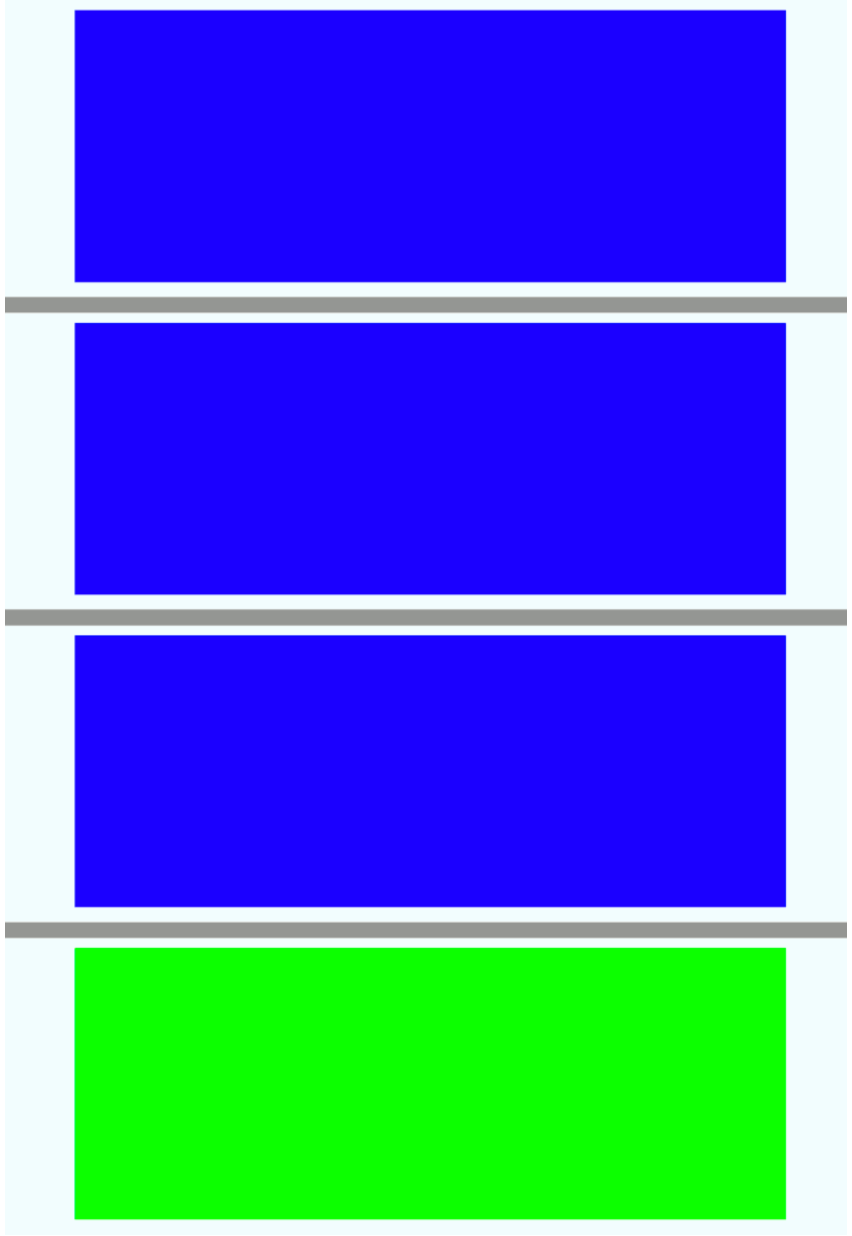

Overview validation – Spray root

- Vertical slam
- EFD and one- and two-way FSI simulations lies between the geometrical intersection and 2D Wagner prediction
- FSI predictions are reasonably accurate
- Rigid plate show a monotonic decrease of the spray root speed
- Flexible plate show a decrease and then increase of the spray root speed
- The spray root moves slower for the flexible plate in the fist part of the slam and then accelerates in the final part, when enters the region with a smaller pitch angle

Spray root position

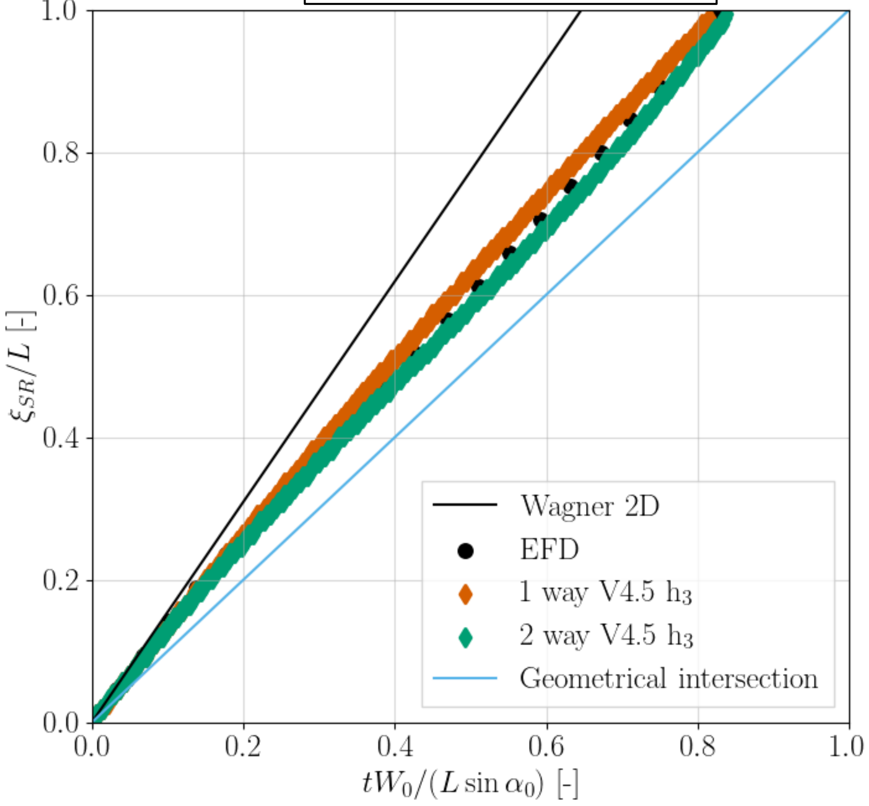

Spray root velocity

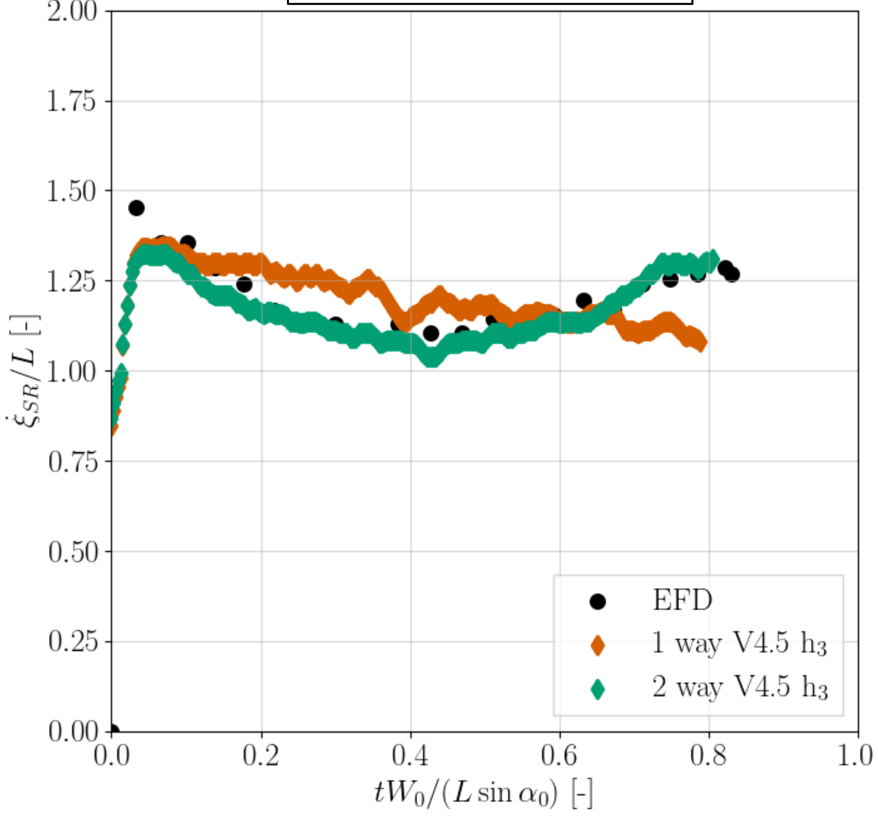

Overview validation – Strain

- Vertical slam
- Prediction accuracy is probe dependent, better agreement with EFD for probes on the edges of the plate
- Overall, the deflection distribution of the plate is well captured

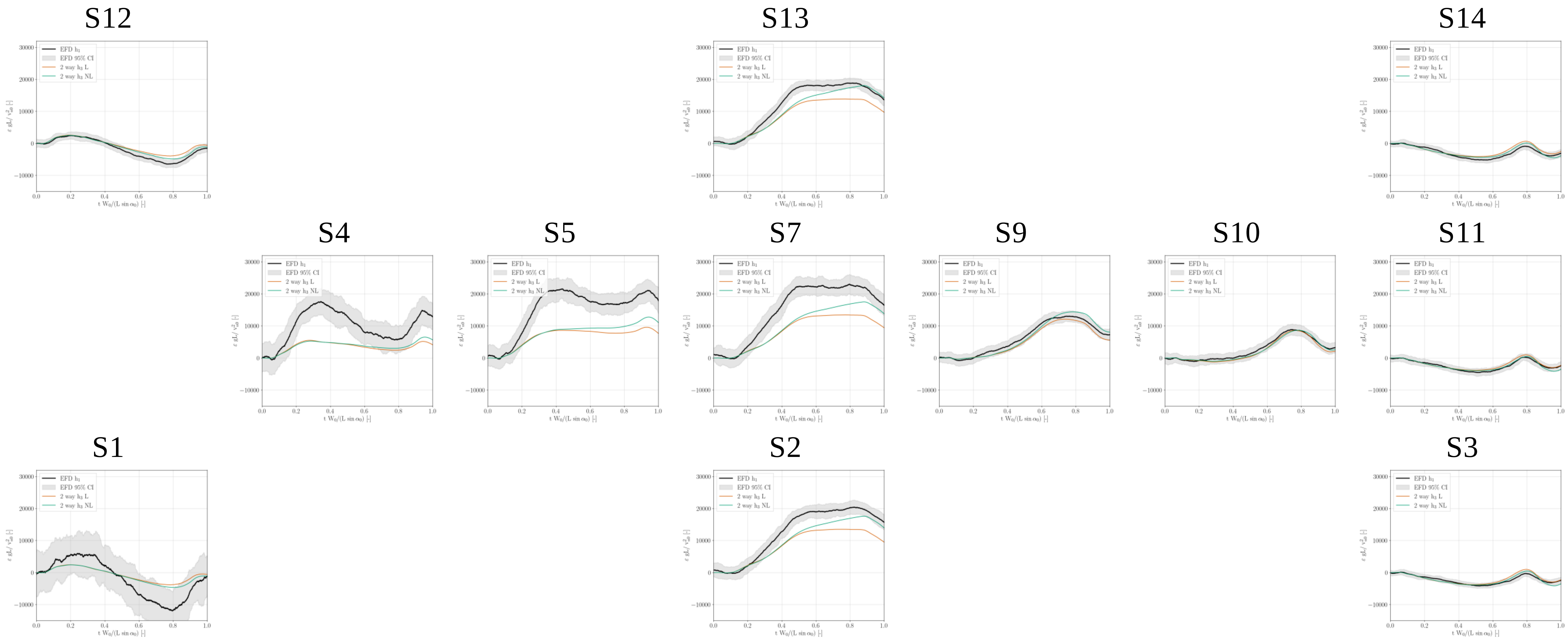

Figure 7.2: V.269 – h3, strain comparison between experimental and numerical results at probes location from the trailing (left) to the leading edge (right).

Overview validation – Centerplate deflection

- Vertical slam
- Normal deflection prediction with nonlinear solver is accurate, especially in predicting the peak value
- The linear solver can predict the time when the peak value occurs but underpredict the peak value
- For small deformations the linear and nonlinear solvers predict the same values

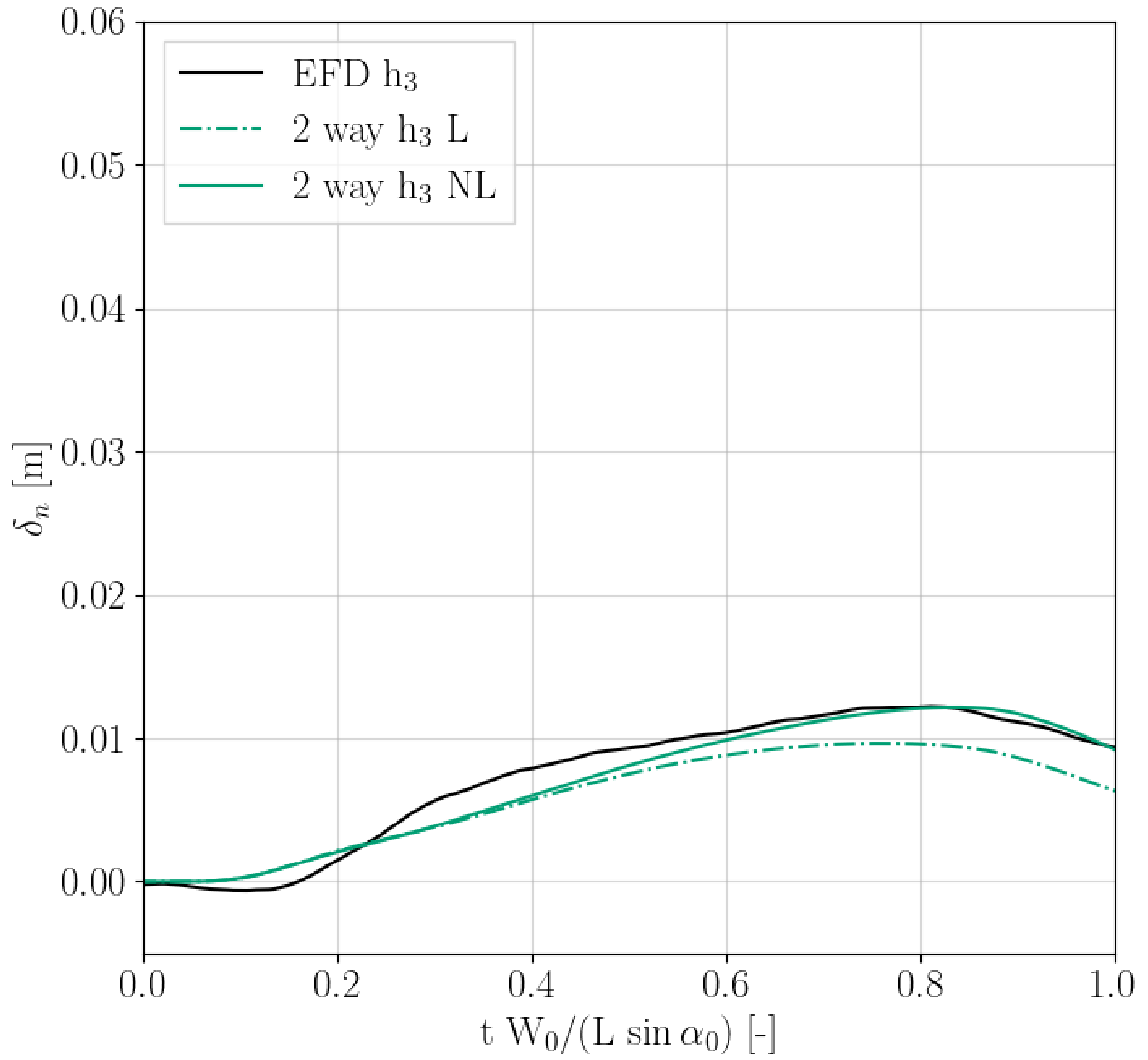

Stagnation Flow Model: Extended Bernoulli Equation Analysis (1)

- To investigate the role of the plate kinematics on the resulting forces an investigation of the spray root along the centerplate is performed
- The fluid is modeled as an inner wall jet boundary layer embedded in an outer stagnation flow
- The outer flow spray root physics can be modeled as an inviscid quasi-steady stagnation flow with a constant normal acceleration

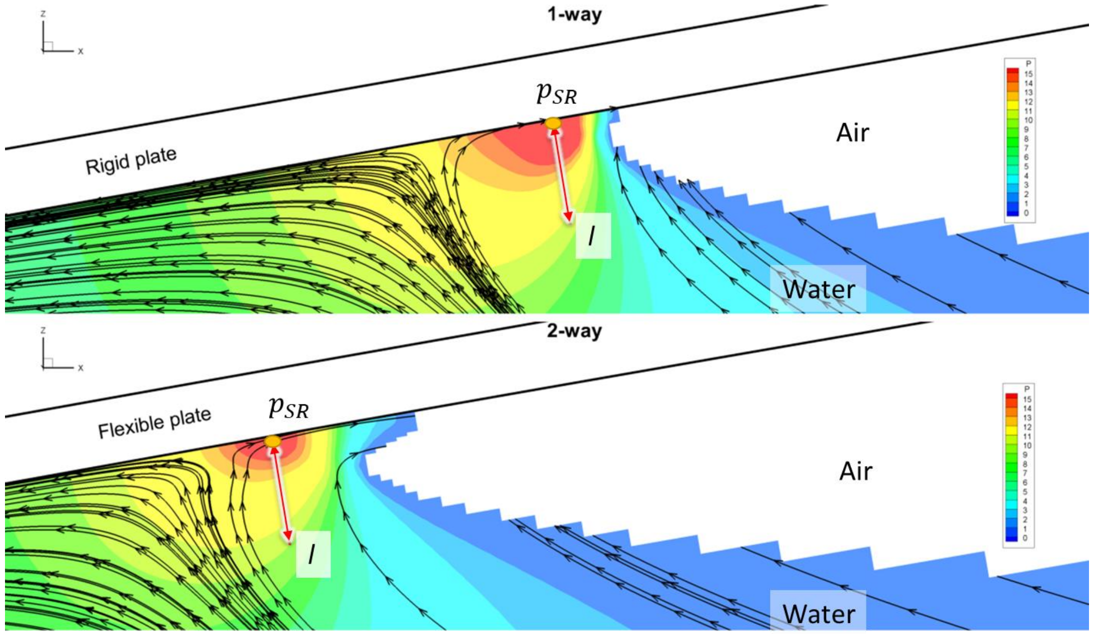

The fluid velocity components are in the moving plate reference system

Streamlines evaluated w.r.t. the spray root velocity

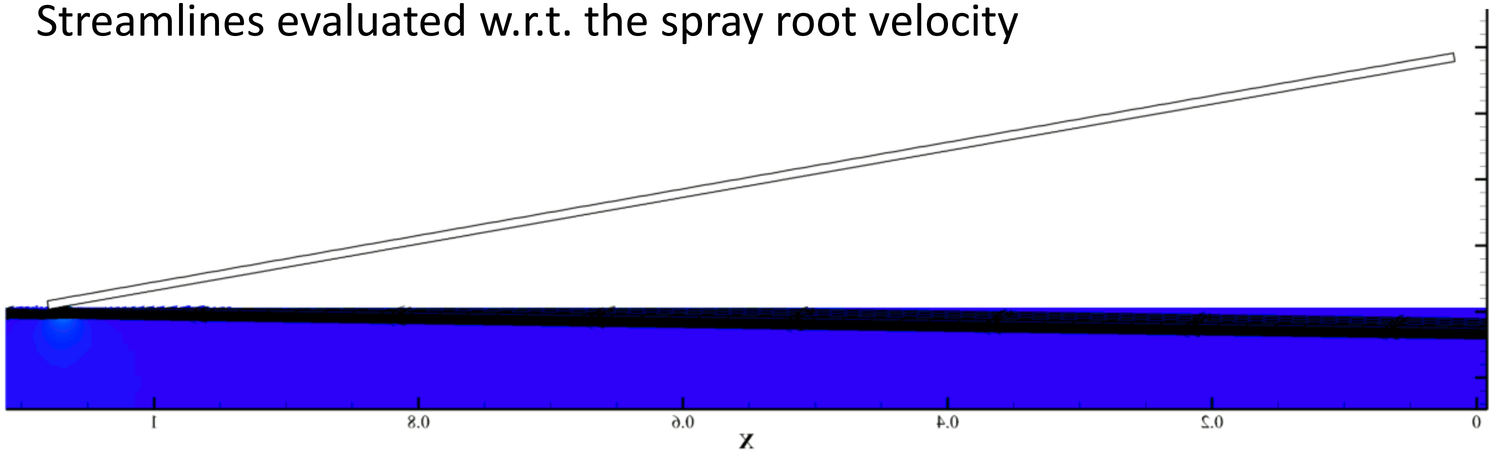

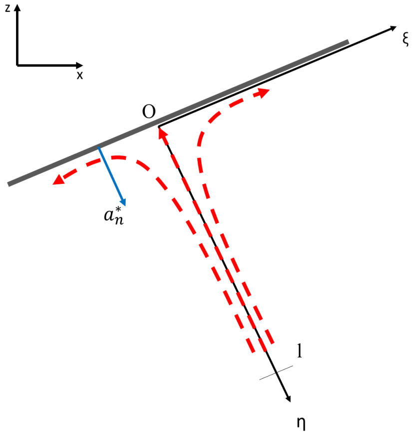

Moving reference system

Stagnation Flow Model: Extended Bernoulli Equation Analysis (2)

- The mono dimensional (along n, direction normal to the plate surface) Euler equations, in a moving reference frame with origin at the spray root point, with body force constant normal acceleration a_n^* with potential $\psi(n)$ are

$$\bar{u} \cdot \frac{\partial \bar{u}}{\partial \eta} = -\frac{1}{\rho}\frac{\partial p}{\partial \eta} + \bar{a}$$

$\bar{a} = \nabla\psi$, with $\psi(\eta) = a_n^* \eta$

$$\frac{\partial}{\partial \eta}\left(\frac{u^2}{2} + \frac{1}{\rho}p + \psi\right) = 0$$

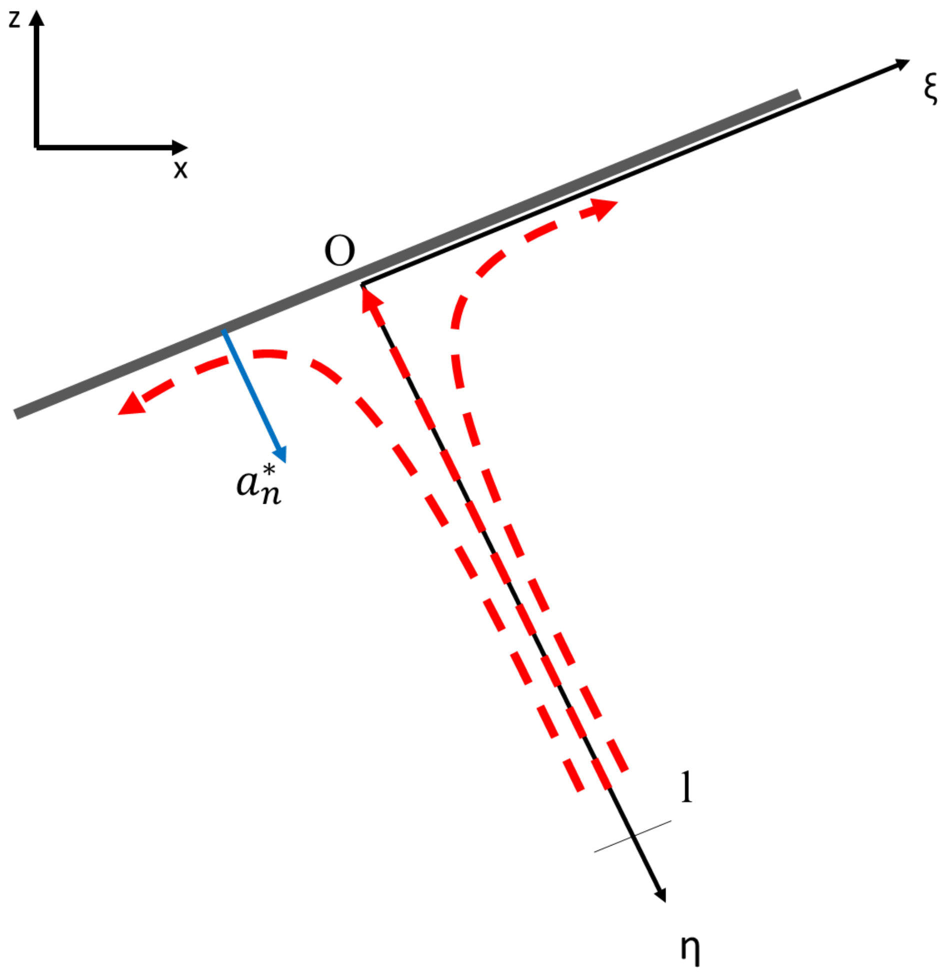

Integrating between η=0 and η=*l* with the following boundary conditions:

$$\eta = 0 \rightarrow \begin{cases} u(0) = 0 \\ \psi(0) = 0 \\ p(0) = p_{SR} \end{cases} \quad \eta = l \rightarrow \begin{cases} u(l) = -v_n \\ \psi(l) = a_n^* l \\ p(l) = 0 \end{cases}$$

Yields:

$$p_{SR} = \rho\left(\frac{{v_n}^2}{2} - a_n^* l\right)$$

Stagnation Flow Model: Extended Bernoulli Equation Analysis (3)

- The resulting pressure difference between a case with acceleration (flexible plate) and without acceleration (rigid plate) can be approximated with the following formula
- In this work the proportional sign is used because the current problem is not a stagnation point but an impact flow with free surface
- The analogy with a stagnation-point flow is used only as a model to explain the trends of rigid versus flexible plates

$$\Delta p_{SR} = \rho\left(\frac{{\Delta v_n}^2}{2} - a_n^* l\right) = p_{SR}\Big|_{2\mathrm{way}} - p_{SR}\Big|_{1\mathrm{way}} \propto \rho\left(\frac{\Delta v_n^2}{2} - l a_n^*\right)$$

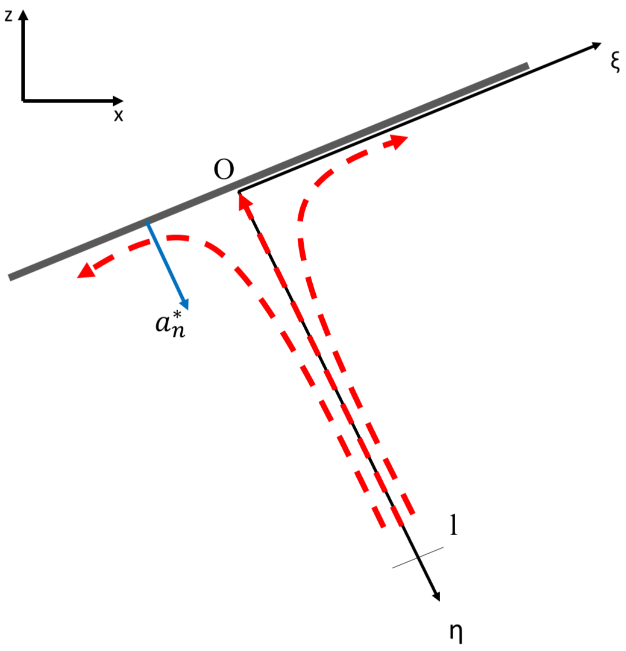

Stagnation Flow Model: Extended Bernoulli Equation Analysis (4)

- Differences in rigid versus flexible deformation, loads, and spray root velocity explain how the interplay of global/local loads and deformation is an important factor in the physics of the hydroelastic response
- Δp_{SR} shows a good correlation with ΔF_n
- All three slams cases can be divided into five phases based on Δp_{SR}
  - I. $\Delta p_{SR} \approx 0$
  - II. Δp_{SR} decreases to its minimum
  - III. Δp_{SR} increases to zero
  - IV. Δp_{SR} increases to its maximum
  - V. the spray root exits the plate, i.e. $t = t_{SR}$
- For phases II-III Δp_{SR} is negative, therefore the deformation reduces the load, whereas for phase IV Δp_{SR} is positive, meaning the deformation dynamics increases the load

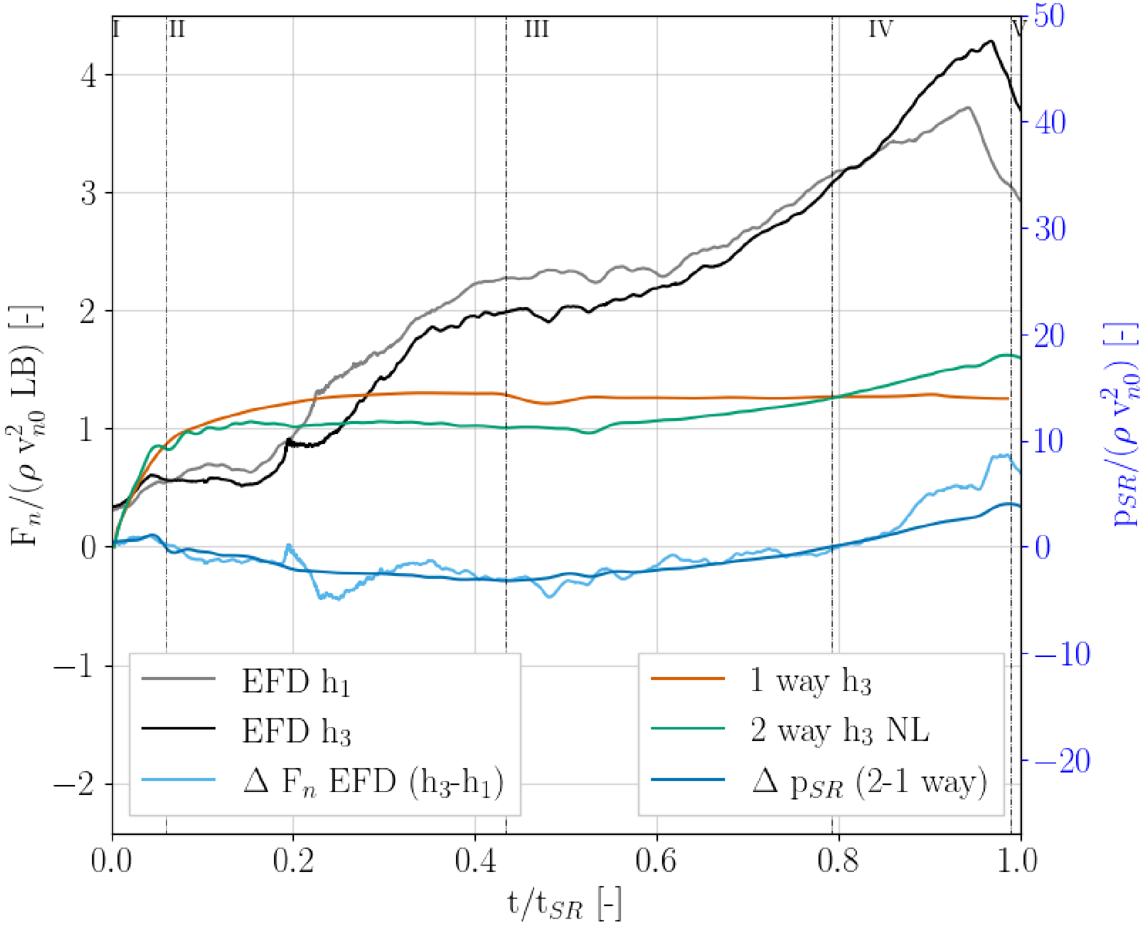

Stagnation Flow Model: Extended Bernoulli Equation Analysis (5)

$$\Delta p_{SR} = \left. p_{SR}\right|_{2\text{way}} - \left. p_{SR}\right|_{1\text{way}} \propto \rho\left(\frac{\Delta v_n^2}{2} - l a_n^*\right), l = 0.01$$

- The proportional terms of the extended Bernoulli equation model reproduce quite well Δp_{SR} trend, although it overpredicts Δp_{SR}
- The simplified model can explain the physics and the dynamics associated to the peak value of the pressure:
  I. Δv_n^2 is almost zero and decreases, the acceleration decreases reaching its minimum, normal impact velocity and acceleration have opposite effects on Δp_{SR}
  II. Δv_n^2 is negative and minimum, the acceleration is negative and increases to zero; in this phase velocity and acceleration have opposite effects
  III. Δv_n^2 goes from negative to positive reaching its maximum, the acceleration increases and achieves its maximum, the two terms both contribute to the load reduction in the first part of this phase; the 2-way FSI load is larger than the 1-way and reaches its maximum along with (positive) Δp_{SR}
  IV. Δv_n^2 is positive, and the acceleration significantly decreases, both terms contribute to the load increase, especially the acceleration in the very last part where the pressure peak occurs
  V. both velocity and acceleration terms go to zero
- The load-reduction phase corresponds to minimum impact velocity and positive acceleration
- The load-increase phase corresponds to an increase of the impact velocity along with a significant negative minimum value for the deformation acceleration

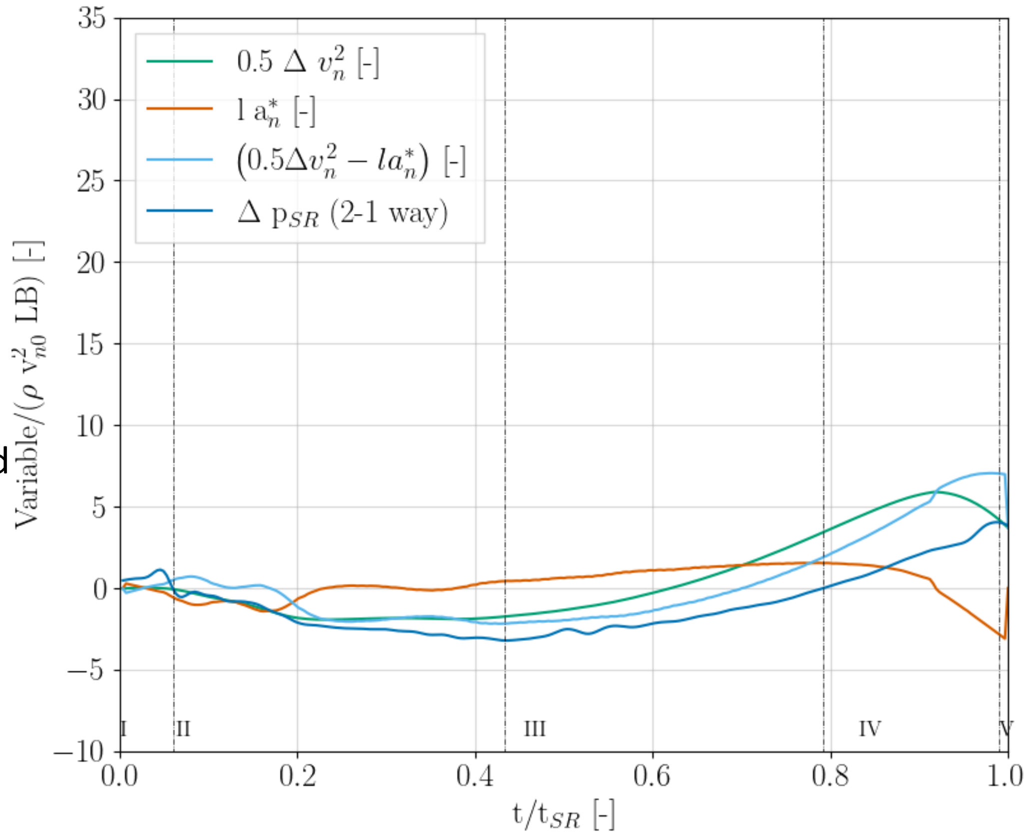

Stagnation Flow Model: Extended Bernoulli Equation Analysis (6)

- To understand the role of the plate kinematics on the impact force differences between the rigid and flexible plate the quantities that concur to the evaluation of the extended Bernoulli equation are investigated

1. $\Delta v_n^2 = v_n^{*2} - v_{n0}^2$ — **The difference of the normal impact velocity due to the plate deformation**
2. $v_{n0} = (W \cos \alpha_0 + U \sin \alpha_0)$ — **The normal impact velocity of the undeformed plate**
3. $v_n^* = \frac{D\delta_n}{Dt} + v_n$ — **The normal impact velocity at the spray root considering the local impact angle and deformation velocity**
4. $\frac{D\delta_n}{Dt} = \frac{\partial \delta_n}{\partial t} + v_{SR} \frac{\partial \delta_n}{\partial x}$ — **The material derivative of the plate deformation**
5. $v_n = (W \cos \alpha + U \sin \alpha)$ — **The normal impact velocity at the spray root considering only the local impact angle**
6. $\alpha = \alpha_0 + \Delta\alpha$ — **The impact angle**
7. $\Delta\alpha = -\frac{\partial \delta_n}{\partial x}$ — **The local variation of the impact angle at the spray root**
8. $a_n^* = \frac{Dv_n^*}{Dt} = \frac{D}{Dt}\left(\frac{D\delta_n}{Dt} + v_n\right) = \frac{D^2\delta_n}{Dt^2} + \frac{Dv_n}{Dt}$ — **The acceleration at the spray root**
9. $\frac{D^2\delta_n}{Dt^2} = \left(\frac{\partial^2 \delta_n}{\partial t^2} + \frac{\partial V_{SR}}{\partial t}\frac{\partial \delta_n}{\partial x} + V_{SR}\frac{\partial^2 \delta_n}{\partial t \partial x}\right) + \left(V_{SR}\frac{\partial^2 \delta_n}{\partial t \partial x} + V_{SR}^2 \frac{\partial^2 \delta_n}{\partial x^2} + V_{SR}\frac{\partial V_{SR}}{\partial x}\frac{\partial \delta_n}{\partial x}\right)$
10. $\frac{Dv_n}{Dt} = \left(-W\frac{\partial \alpha}{\partial t}\sin \alpha + U\frac{\partial \alpha}{\partial t}\cos \alpha\right) + \left(-W\, V_{SR}\frac{\partial \alpha}{\partial x}\sin \alpha + U\, V_{SR}\frac{\partial \alpha}{\partial x}\cos \alpha\right)$

Stagnation Flow Model: Extended Bernoulli Equation Analysis (7)

- Δv_n^2 is first negative and then positive meaning that the impact velocity is first reduced and then increased
- The time derivative of the deflection ($\partial\delta_n/\partial t$) provides the reduction of the impact velocity in the first part of the slam, the plate is moving away from the spray root
- In the second part $v_{SR}\partial\delta_n/\partial x$ provides the greater contribution meaning that the curvature of the plate plays a significant role in this phase in increasing the impact velocity and thus the pressure
- The local pitch angle changes significantly during the slam, achieving its minimum when the normal force is at its maximum

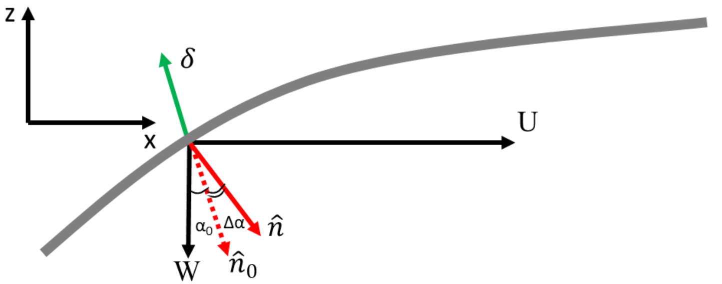

$$\Delta v_n^2 = v_n^{*2} - v_{n0}^2$$

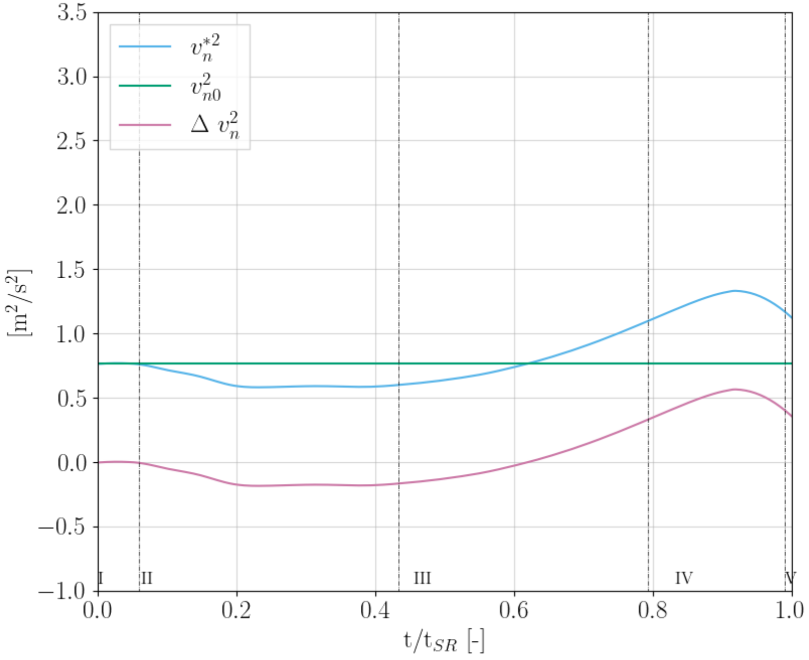

$$v_n^* = \frac{D\delta_n}{Dt} + v_n$$

$$\frac{D\delta_n}{Dt} = \frac{\partial\delta_n}{\partial t} + v_{SR}\frac{\partial\delta_n}{\partial x}$$

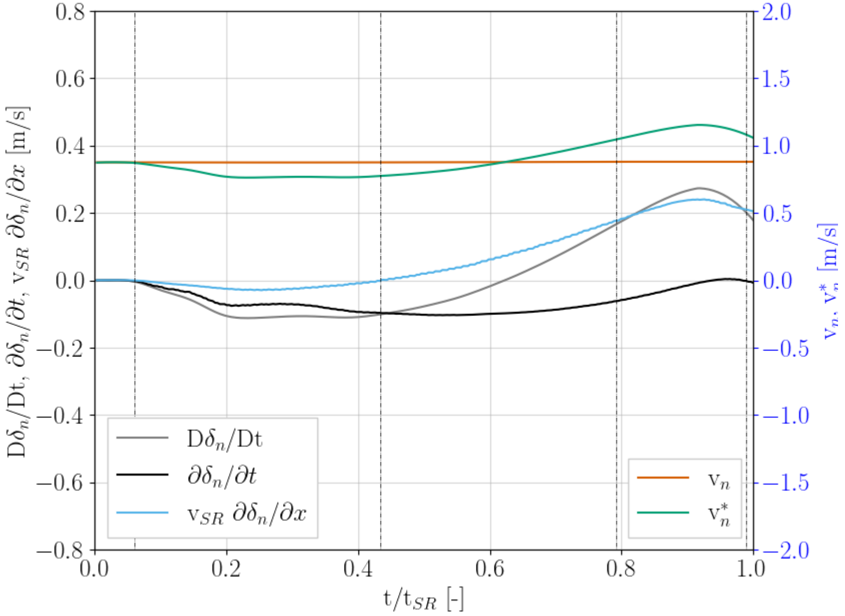

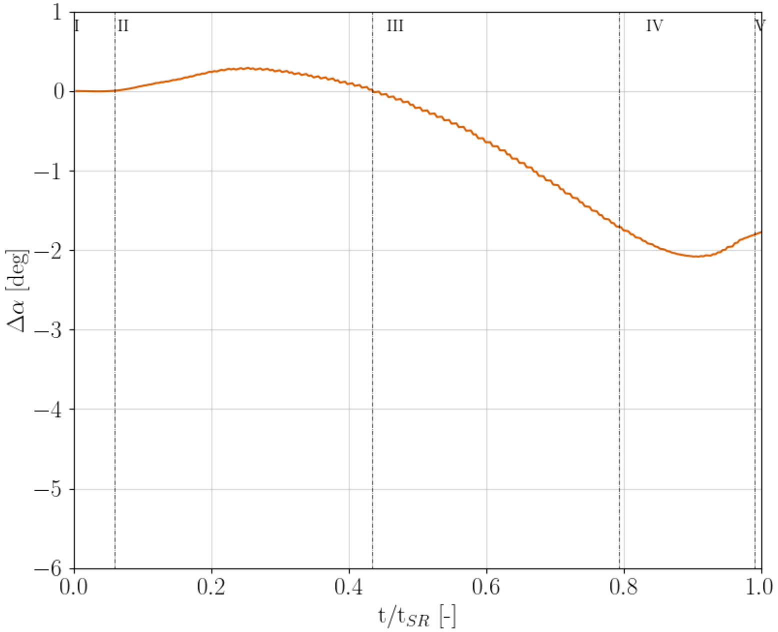

Stagnation Flow Model: Extended Bernoulli Equation Analysis (8)

- The term $\frac{D^2\delta_n}{Dt^2}$ provides the greatest contribution to a_n^* meaning that the geometric deflection provides a greater contribution to the acceleration than the local pitch angle variation
- The components of $\frac{D^2\delta_n}{Dt^2}$ have similar contribution to their resulting sum
- The convective term of $\frac{Dv_n}{Dt}$ have a greater influence than the time varying, confirming the significant role of the geometric deflection

$$a_n^* = \frac{D^2\delta_n}{Dt^2} + \frac{Dv_n}{Dt}$$

$$\frac{D^2\delta_n}{Dt^2} = \left(\frac{\partial^2\delta_n}{\partial t^2} + \frac{\partial V_{SR}}{\partial t}\frac{\partial \delta_n}{\partial x} + V_{SR}\frac{\partial^2\delta_n}{\partial t\partial x}\right) + \left(V_{SR}\frac{\partial^2\delta_n}{\partial t\partial x} + V_{SR}^2\frac{\partial^2\delta_n}{\partial x^2} + V_{SR}\frac{\partial V_{SR}}{\partial x}\frac{\partial \delta_n}{\partial x}\right)$$

$$\frac{Dv_n}{Dt} = \left(-W\frac{\partial\alpha}{\partial t}\sin\alpha + U\frac{\partial\alpha}{\partial t}\cos\alpha\right) + \left(-W\,V_{SR}\frac{\partial\alpha}{\partial x}\sin\alpha + U\,V_{SR}\frac{\partial\alpha}{\partial x}\cos\alpha\right)$$

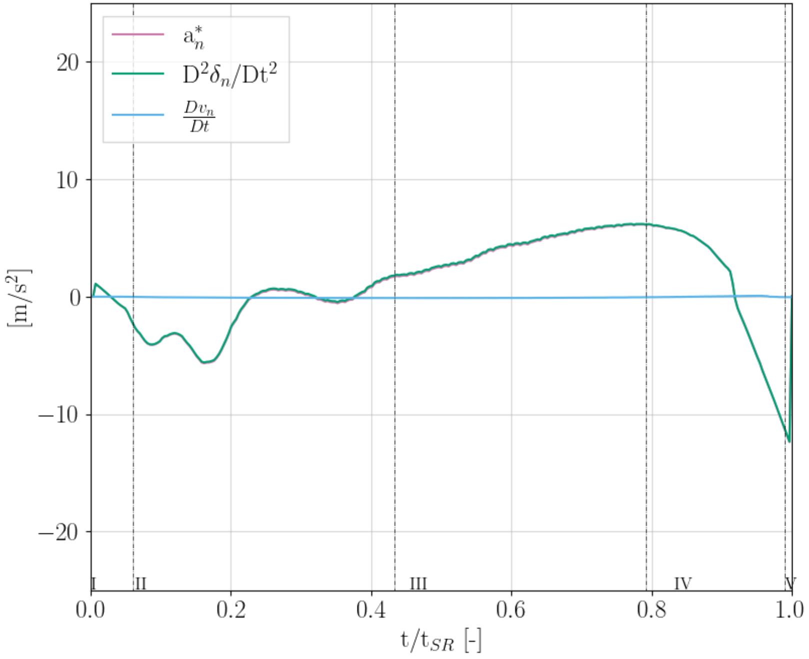

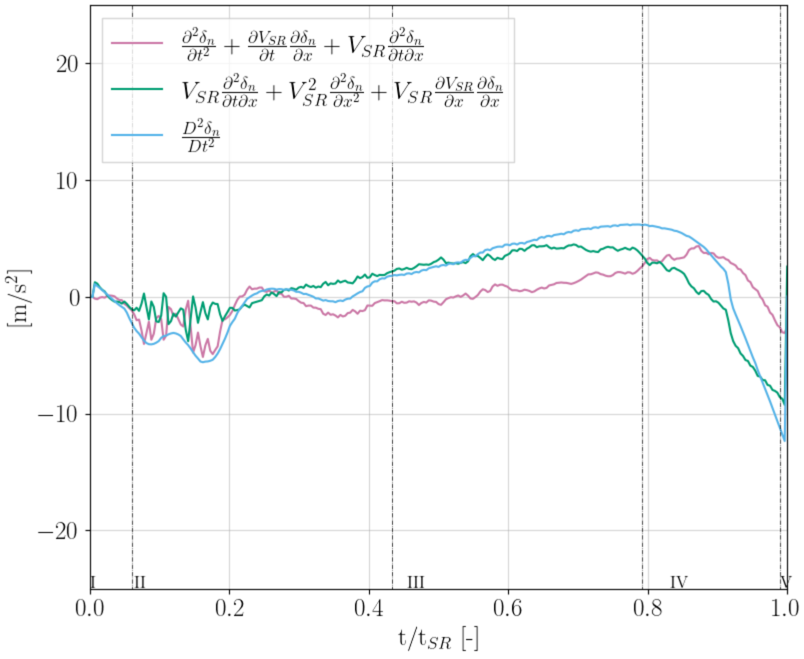

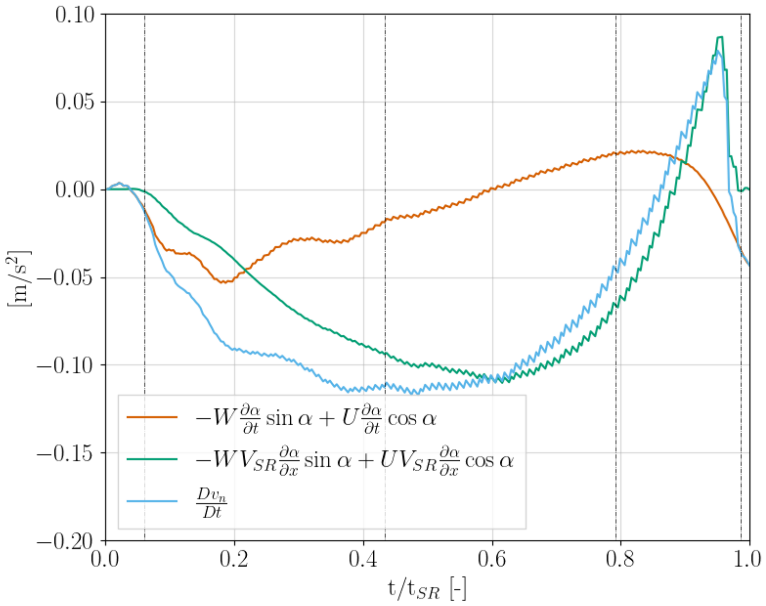

Stagnation Flow Model: Extended Bernoulli Equation Analysis (9)

- The correlation between Δp_{SR} and Δv_n^2 exists only phase wise in the first part of the slam
- The correlation of Δp_{SR} with Δv_n^2 cannot explain the peak phase (IV)
- The correlation of Δp_{SR} with $\left(\frac{\Delta v_n^2}{2} - \ l a_n^*\right)$ is significantly better than using Δv_n^2 only. The proportional terms correlate very well with phase IV of Δp_{SR}
- Although the extended Bernoulli equation is a simplified model, it predicts accurately Δp_{SR} during phase IV, explaining the contribution of the deformation velocity and acceleration to the increased pressure peak
- The acceleration experienced by the spray root is fundamental to the final pressure/force increase
- A reduction of the acceleration experienced by the spray root would lead to a smaller peak in the final part of the slam

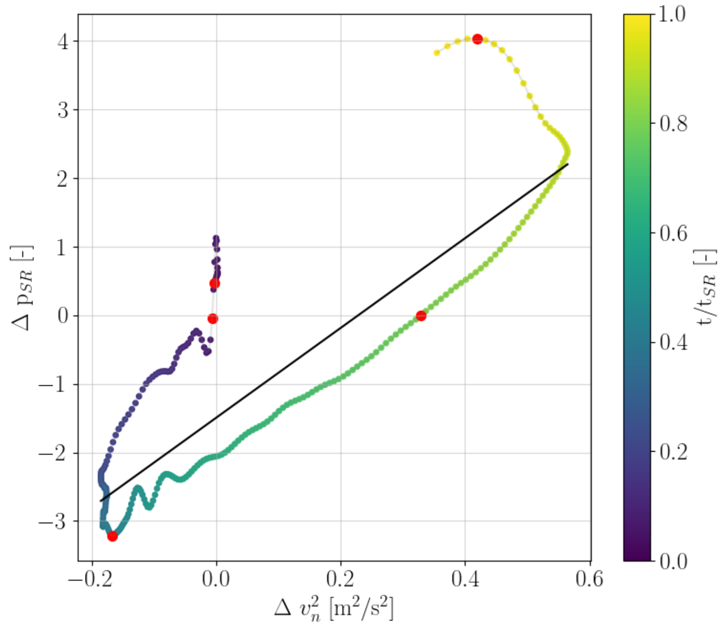

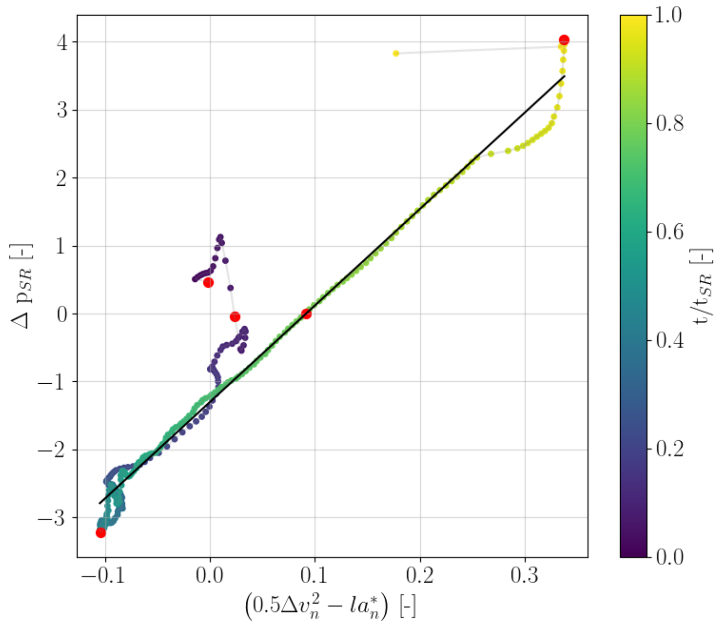

Conservation of Energy Analysis (1): Motivation

- During the slam the plate undergoes significant deformations that interact with the spray root
- The analysis of the energy conservation during the slam can help in understanding the role of the structure on the spray root dynamics and therefore on the pressure acting on the structure itself
- The energy equation for an adiabatic control volume in inertial coordinates is

$$-\frac{\delta W}{dt} = \frac{dE}{dt} = \frac{\partial}{\partial t}\iiint_{V(t)} e\rho\, dV + \iint_{S(t)} e\rho(\boldsymbol{u}\cdot\hat{n})dS$$

$$e = \underbrace{k_e}_{\text{Kinetic potential energy}} + \overbrace{p_{e\varepsilon}}^{\text{Elastic potential energy}} + \underbrace{p_{eg}}_{\text{Gravitational potential energy}}$$

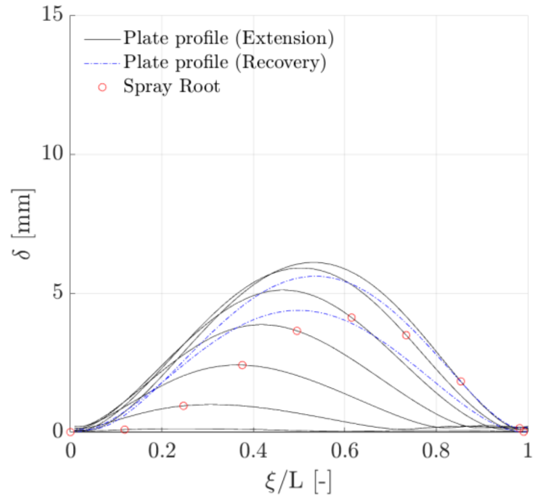

V.269 plate midline displacement and spray root position

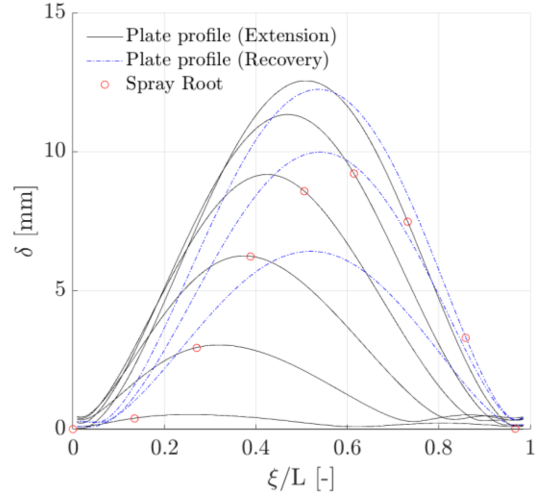

O.403 plate midline displacement and spray root position

Conservation of Energy Analysis (2): Water

Water (subscript w)

- the energy flux terms are zero due to the rigid wall and adiabatic boundary conditions
- neglecting air and considering only the rate of pressure work done across the wetted surface of the plate S_{wet}

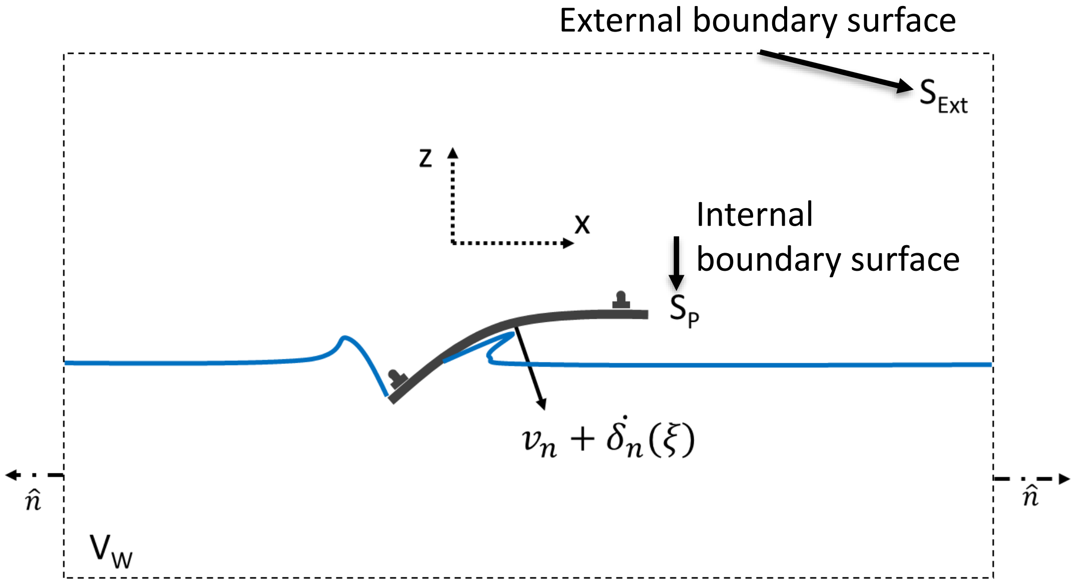

$\boldsymbol{u}_w$= the fluid velocity

$\dot{W}_{pR}$= power provided by the pressure due to rigid body motion

$\dot{W}_{p\dot{\delta}_n}$= power provided by the pressure due to the plate's flexibility

$$e = k_e + p_{eg}$$

$$v_n = \boldsymbol{v} \cdot \hat{n}$$
$$\delta_n = \boldsymbol{\delta} \cdot \hat{n}$$

$$\frac{dE}{dt} = \frac{\partial}{\partial t}\iiint_{V_w} \rho\left(gz + \frac{\|\boldsymbol{u}_w\|^2}{2}\right) dV_w = -\frac{\delta W}{dt} = \iint_{S_{Wet}} p[v_n + \dot{\delta}_n]dS = \dot{W}_{pR} + \dot{W}_{p\dot{\delta}_n}$$

Conservation of Energy Analysis (3): Structure

Structure (subscript s)

- the energy flux terms are zero due to the impermeability and adiabatic boundary conditions
- neglecting air and considering only the rate of pressure work done across the wetted surface of the plate S_{wet}

$$\frac{\partial}{\partial t}\iiint_{V_s} \rho e \, dV = -\iint_{S_{Wet}} p\left[\left(\boldsymbol{v}_n + \dot{\boldsymbol{\delta}}_n\right)\cdot\hat{n}\right] dS + \boldsymbol{F}_M \cdot \boldsymbol{v}_n$$

$$e = k_e + p_{e\varepsilon} + p_{eg} = \rho\frac{\left\|v_n + \dot{\delta}_n\right\|^2}{2} + \frac{1}{2}\sum_{i=1}^{3}\sum_{j=1}^{3}\sigma_{ij}\varepsilon_{ij} + g\left(z_{s0} + \boldsymbol{\delta}\cdot\hat{k}\right)$$

z-coordinate of the undeformed plate

$$v_n = \boldsymbol{v} \cdot \hat{n}$$
$$\delta_n = \boldsymbol{\delta} \cdot \hat{n}$$

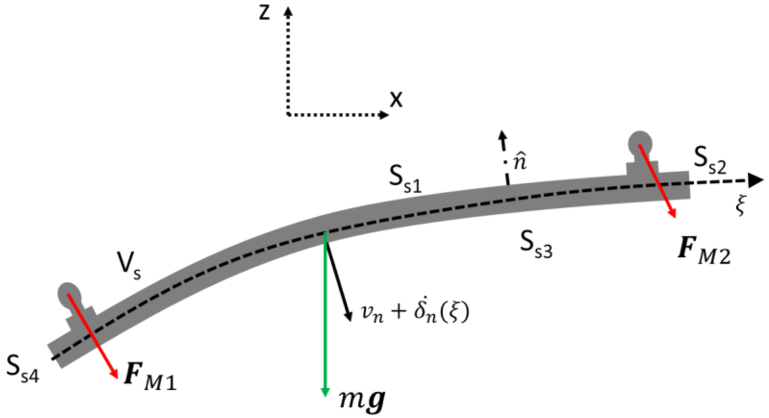

$$\dot{K}_{\dot{\delta}_n} + \dot{U}_{\varepsilon} + \dot{U}_{\delta_n z} = -\left(\dot{W}_{pR} + \dot{W}_{p\dot{\delta}_n}\right) + \dot{W}_M$$

$\dot{K}_{\dot{\delta}_n}$= time derivative of kinetic energy

$\dot{U}_{\varepsilon}$= time derivative of elastic potential energy

$\dot{U}_{\delta_n z}$= time derivative of gravitational potential energy

$\dot{W}_M$= power provided by the carriage through the mount

$\hat{n}$ is pointing outward for the structure but inward for the fluid

Conservation of Energy Analysis (4): Structure

Structure (subscript s)

- Considering an isotropic homogeneous material

$$\sigma_{ij} = \lambda k_{ij}\varepsilon_{kk} + \mu(2\varepsilon_{ij})$$

$$v_n = \boldsymbol{v} \cdot \hat{n}$$
$$\delta_n = \boldsymbol{\delta} \cdot \hat{n}$$

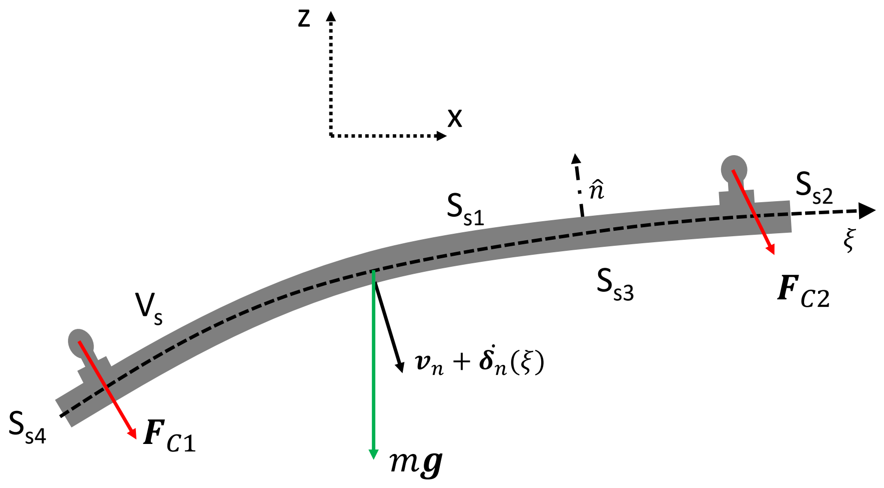

$$e = \rho\frac{\left\|v_n + \dot{\delta}_n\right\|^2}{2} + \frac{1}{2}\sum_{i=1}^{3}\sum_{j=1}^{3}\left[\lambda k_{ij}\varepsilon_{kk} + \mu(2\varepsilon_{ij})\right]\varepsilon_{ij} + g\left(z_{s0} + \boldsymbol{\delta} \cdot \hat{k}\right)$$

$$\lambda = \frac{E\upsilon}{(1+\upsilon)(1-2\upsilon)} \quad \text{and} \quad \mu = \frac{E}{2(1+\upsilon)}$$

$$p_{e\varepsilon} = \frac{1}{2}\sum_{i=1}^{3}\sum_{j=1}^{3}\left[\lambda k_{ij}\varepsilon_{kk} + \mu(2\varepsilon_{ij})\right]\varepsilon_{ij} = \frac{1}{2}(\lambda + 2\mu)(\varepsilon_{11}^2 + \varepsilon_{22}^2 + \varepsilon_{33}^2) + \lambda(\varepsilon_{11}\varepsilon_{22} + \varepsilon_{11}\varepsilon_{33} + \varepsilon_{22}\varepsilon_{33}) + \mu(\varepsilon_{12}^2 + \varepsilon_{13}^2 + \varepsilon_{23}^2)$$

1 is x-direction
2 is y-direction
3 is z-direction

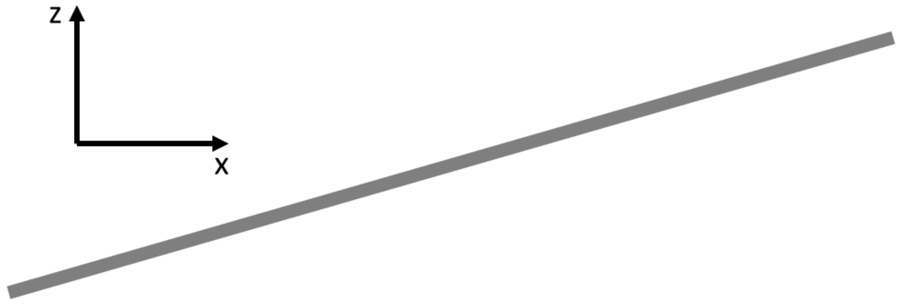

Conservation of Energy Analysis (5): Rigid and Flexible Plate

- Rigid plate
  - The mount transfers energy directly to the fluid since the plate is rigid

Water

$$\frac{\partial}{\partial t}\iiint_{V_w} \rho_w \left(\frac{\|\boldsymbol{u}_w\|^2}{2}\right) dV_w = \iint_{S_{Wet}(t)} p(v_n) dS = \dot{W}_{pR}$$

Structure

$$-\dot{W}_{pR} = \dot{W}_M$$

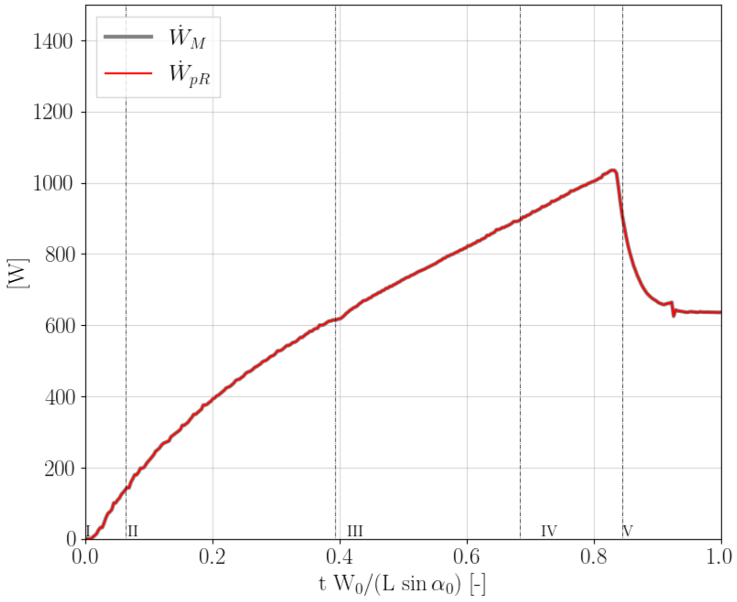

- Flexible plate
  - The mount transfers energy to the fluid and to the plate (kinetic and potential elastic energy) since the plate is deforming

Water

$$\frac{\partial}{\partial t}\iiint_{V_w} \rho \left(\frac{\|\boldsymbol{u}_w\|^2}{2}\right) dV_w = \iint_{S_{Wet}} p[v_n + \dot{\delta}_n] dS = W_{pR} + W_{p\delta_n}$$

Structure

$$\dot{K}_{\dot{\delta}_n} + \dot{U}_\varepsilon + \dot{U}_{\delta_n z} + \left(\dot{W}_{pR} + \dot{W}_{p\dot{\delta}_n}\right) = \dot{W}_M$$

$$v_n = \boldsymbol{v} \cdot \hat{n}$$
$$\delta_n = \boldsymbol{\delta} \cdot \hat{n}$$

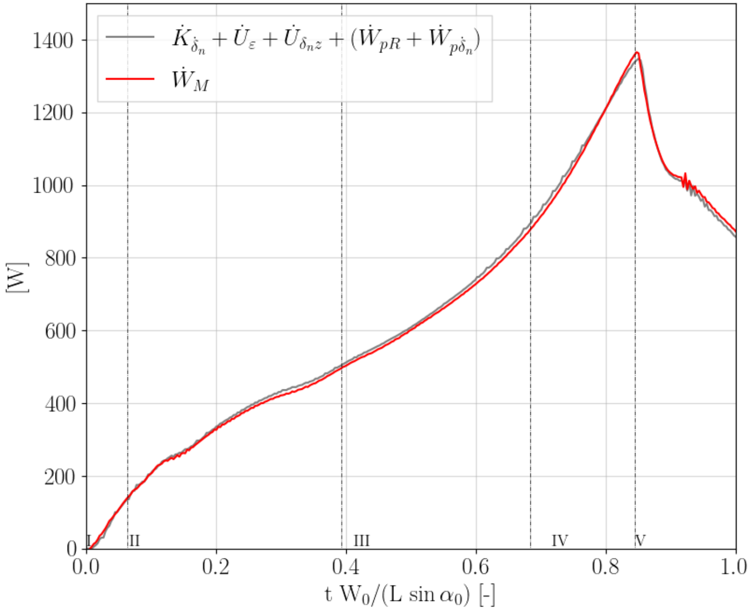

Conservation of Energy Analysis (6): Rigid versus Flexible Plate

- Subtracting the equation for the energy conservation for the flexible and the rigid cases allows to study the dynamics of the difference in the force acting on the plate between the flexible and the rigid case

Water

$$\left[\frac{\partial}{\partial t}\iiint_{V_w}\rho\left(\frac{\|\boldsymbol{u}_w\|^2}{2}\right)dV_w\right]_{Flexible}-\left[\frac{\partial}{\partial t}\iiint_{V_w}\rho\left(\frac{\|\boldsymbol{u}_w\|^2}{2}\right)dV_w\right]_{Rigid}=$$

$$=\left[-\iint_{S_{Wet}(t)}p(v_n)dS\right]_{Flexible}-\left[\iint_{S_{Wet}(t)}p(v_n)dS\right]_{Rigid}+\left[-\iint_{S_{Wet}(t)}p(\dot{\delta}_n)dS\right]_{Flexible}=$$

$$=\dot{W}_{p\dot{\delta}_n}+\Delta\dot{W}_{pR}$$

Structure

$$\dot{K}_{\dot{\delta}_n}+\dot{U}_{\varepsilon}+\dot{U}_{\delta_n z}+\dot{W}_{p\dot{\delta}_n}=\Delta\dot{W}_M-\Delta\dot{W}_{pR}$$

Conservation of Energy Analysis (8): Equation Difference

- The difference equation is satisfied
- The kinetic energy content is the smallest
- The elastic potential energy almost equals the power provided by the pressure due to the flexibility suggesting that most of the work done from the fluid to the plate goes into the plate's deformation

$$\dot{K}_{\dot{\delta}_n} + \dot{U}_{\varepsilon} + \dot{U}_{\delta_n z} + \dot{W}_{p\dot{\delta}_n} = \Delta\dot{W}_M - \Delta\dot{W}_{pR}$$

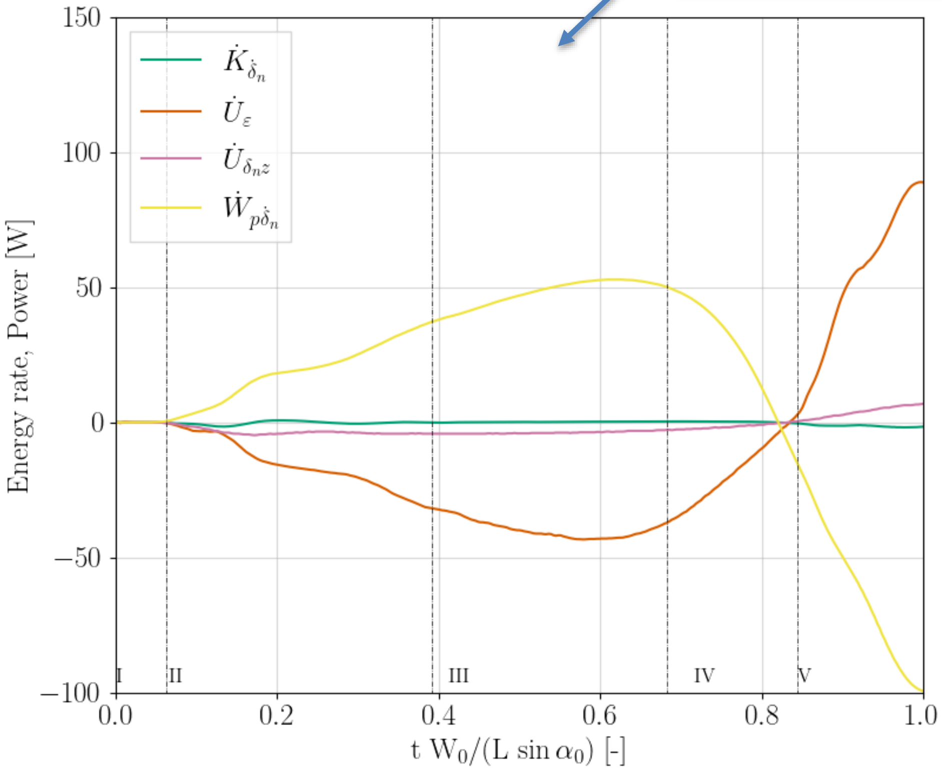

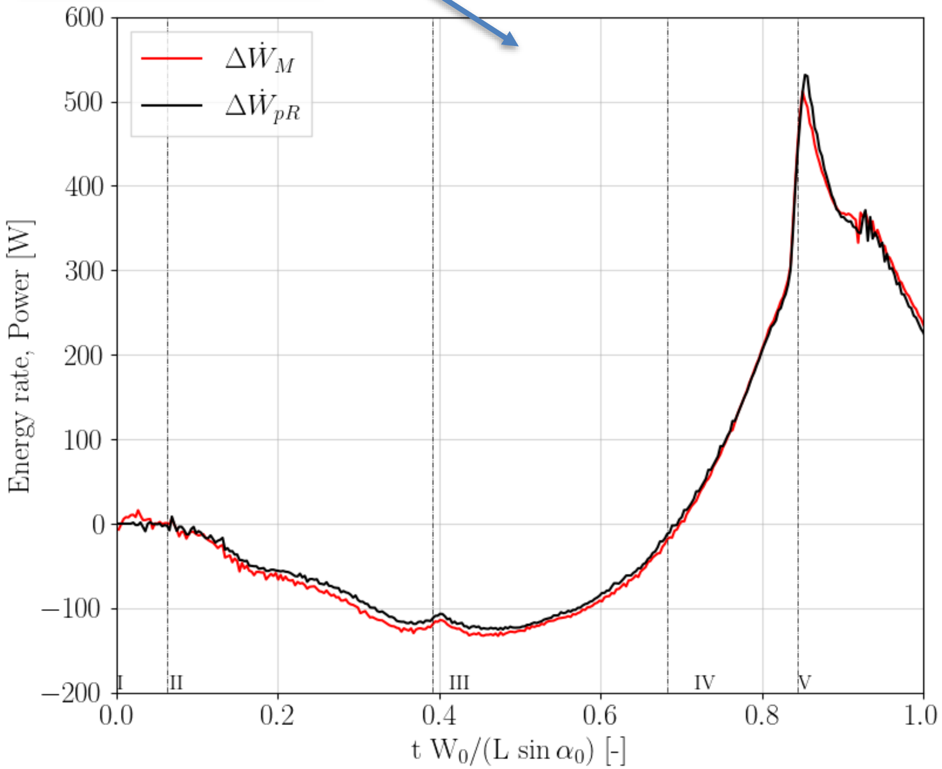

3. Conservation of Energy Analysis (10): Elastic Energy Components

- For all the cases the longitudinal (ε_{xx}^2) strain contribution is the most important
- This suggests that the plate rigidity should be increased in this direction to reduce the total deflection
- The other directions are less solicited during this specific slam and therefore their rigidity could be reduced in order to reduce the structural weight

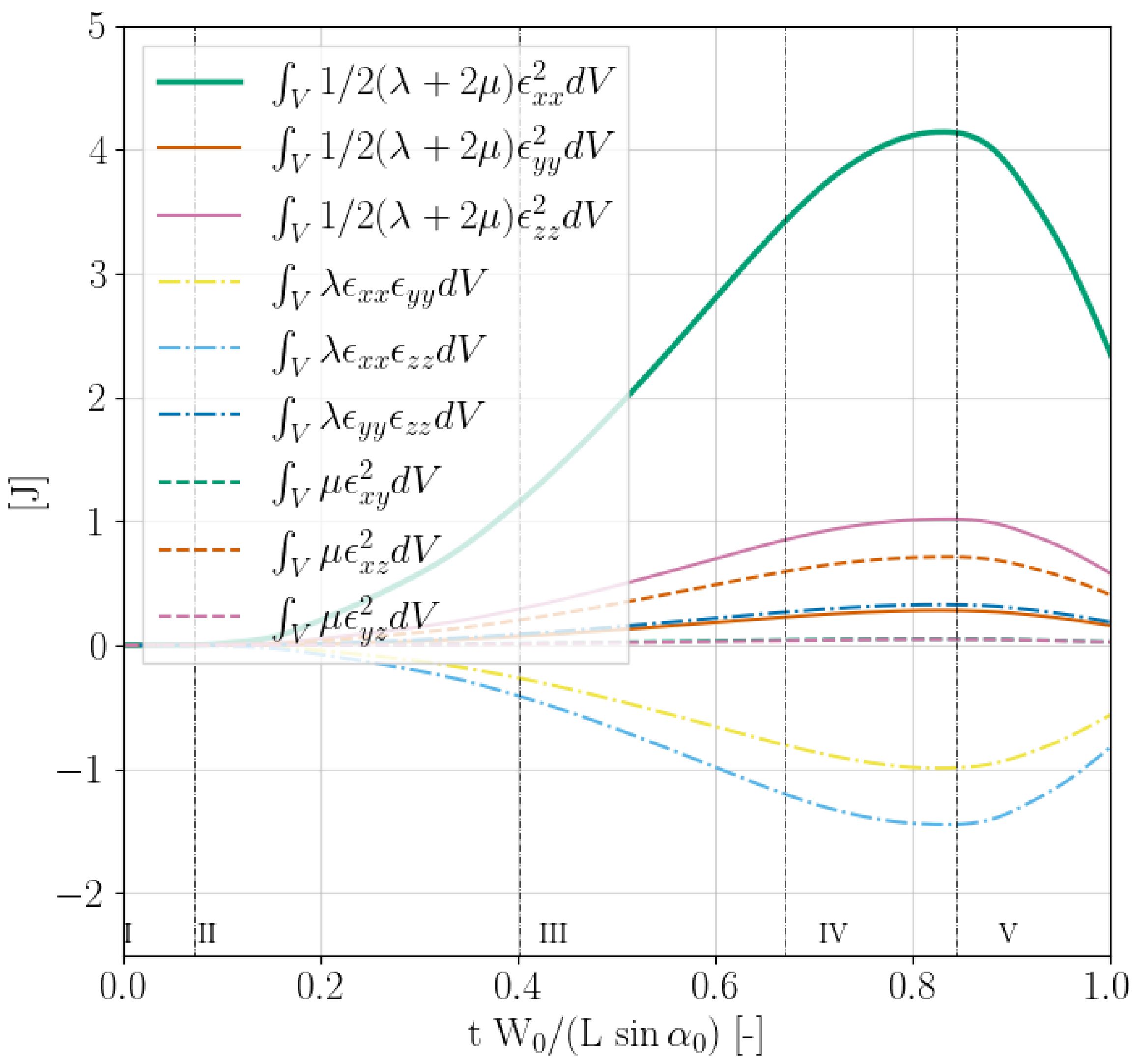

MDO for reduced slamming response

- Materials that exhibit macroscopically non-isotropic response are considered
  - Orthotropic material
    - Material properties are defined according to three principal (orthogonal) directions
    - **e.g.** Plates with stiffeners, single layer composites
  - Anisotropic material
    - Material properties changes with the direction
    - **e.g.** Laminated composites

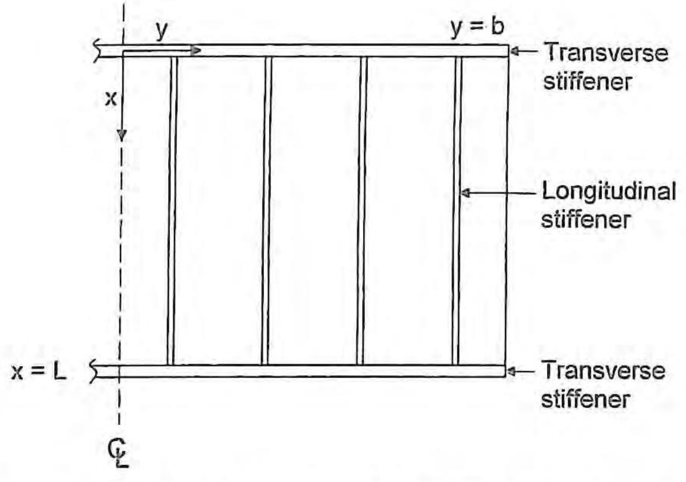

Orthotropic plate by reinforcing a simple plate with stiffeners.
Faltinsen, 1999, "Water Entry of a Wedge by Hydroelastic Orthotropic Plate Theory". Journal of Ship Research **49**: 180–193

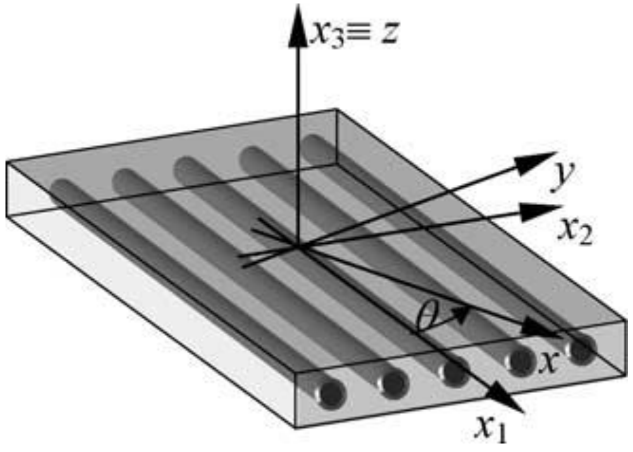

General sketch of an orthotropic layer: case of an isotropic matrix reinforced by fibres.
Vannucci, 2002, "A Special Planar Orthotropic Material". Journal of Elasticity **67**: 81–96

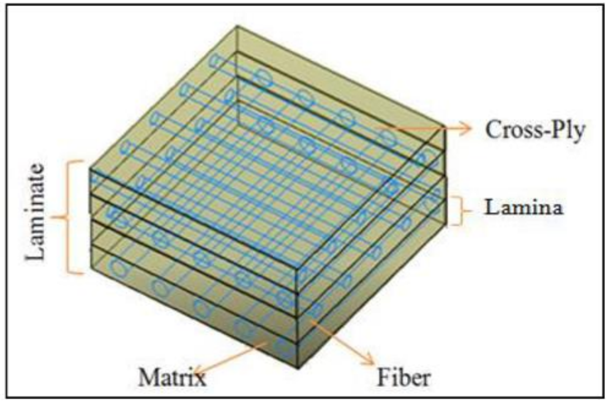

Schematic diagram of a [0/90/0/90] cross-ply laminate.
Saxena, M. and Sushen Kirtania. "Stiffness analysis of symmetric cross-ply laminated composite plates." ADBU Journal of Engineering Technology (AJET) 4 (2016)

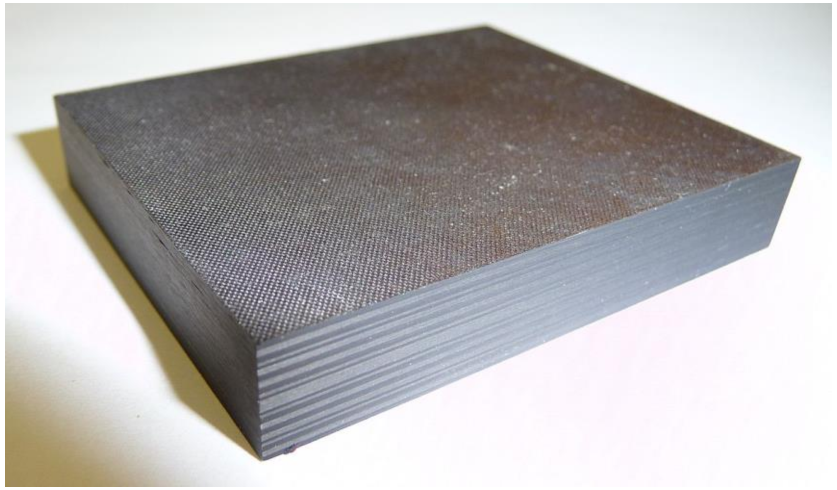

This is a photo of a small piece of laminated uni-directional Carbon Fibre. Simon.white.1000 (2012)

MDO for reduced slamming response

- MDO problem formulation using orthotropic materials
  - structural weight (W) and the strain/stress/normal force peak
  - industrial interest (weight/stress)
  - fundamental research perspective (strain/stress/normal force peak)
- Bernoulli analysis showed that the local pitch angle directly affects the spray root pressure and thus the normal force
- Controlling the plate deformation to control the local pitch angle can achieve the desired hydroelastic response
- Plate deformation can be controlled by changing the flexural rigidity along the longitudinal direction
- Use of grooves and non-uniform thickness allow to vary the longitudinal flexural rigidity

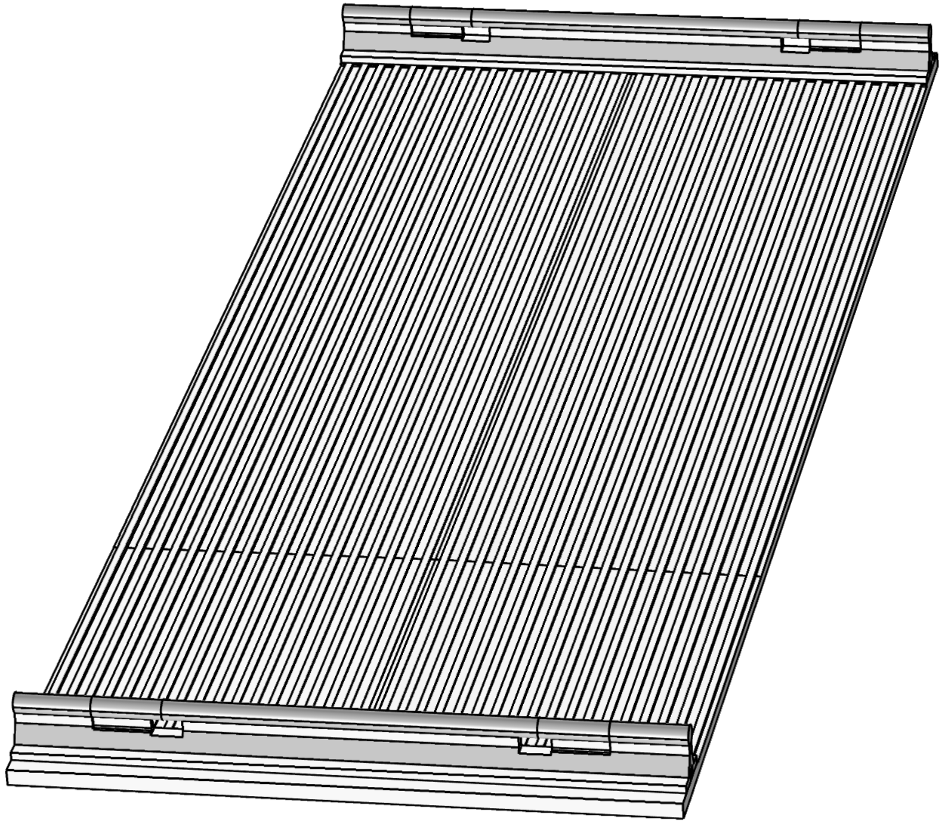

$$\text{minimize} \quad \boldsymbol{f}(\boldsymbol{x}) = \{W(\boldsymbol{x}), \max[\sigma_{Mises}(\boldsymbol{x}), \varepsilon_{Mises}(\boldsymbol{x}), \Delta F_n(\boldsymbol{x}), \delta_n(\boldsymbol{x})]\}$$

$$\text{subject to} \begin{cases} \max(\boldsymbol{\sigma}) < \boldsymbol{\sigma}_{max} \\ \max(\boldsymbol{\tau}) < \boldsymbol{\tau}_{max} \end{cases}$$

MDO - Design space 1, structural model

- Longitudinal thickness variations of the stiffeners is initially not allowed to obtain a plate that is equivalent to the original rectangular isotropic plate
- Domain center is defined to have a weight close to the original
- Variable ranges are defined in order to provide large design variability while maintaining a certain degree of manufacturability

Variable	Description
1	Thickness variation of the plate along x-direction (γ_1)
2	Thickness variation of the plate along y-direction (γ_2)
3	Minimum plate thickness at centerline, at $x_{h,min}$ ($h_{M,in}$)
4	Longitudinal position of the minimum thickness ($x_{h,min}$)
5	Maximum groove thickness (h)
6	Width of the grooves (w_g)
7	Number of grooves (N_g)

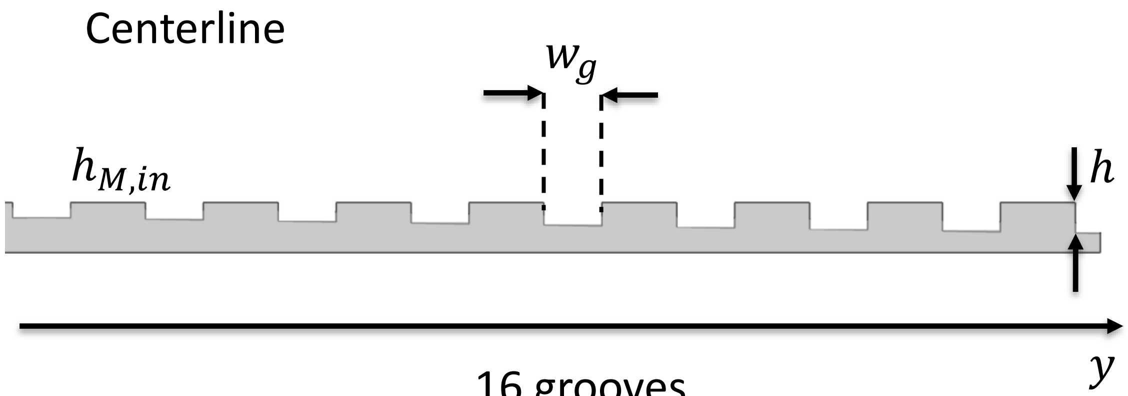

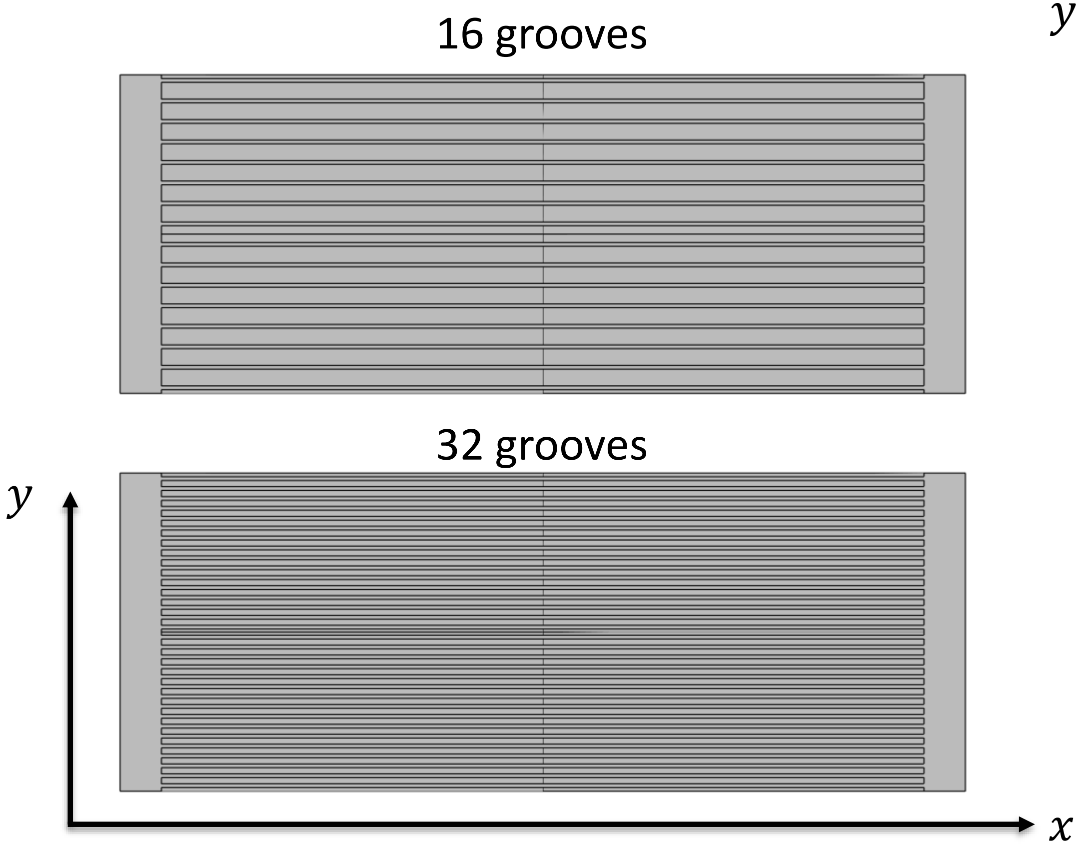

MDO - Design space 2, structural model

- Stiffeners thickness variations in the longitudinal direction are allowed
- Domain center is defined to have a weight close to the original

Variable	Description
1	Plate thickness – midline - xMinThick
2	Plate thickness – edge - xMinThick
3	Plate thickness – midline – TE
4	Plate thickness – edge – TE
5	Plate thickness – midline – LE
6	Plate thickness – edge – LE
7	Stiffeners thickness – midline - xMinThick
8	Stiffeners thickness – edge – xMinThick
9	Stiffeners thickness – midline – TE
10	Stiffeners thickness – edge – TE
11	Stiffeners thickness – midline – LE
12	Stiffeners thickness – edge – LE

Variable	Description
13	Longitudinal position of the minimum plate thickness (xMinThick)
14	Stiffeners width
15	Overall plate thickness
16	Number of stiffeners

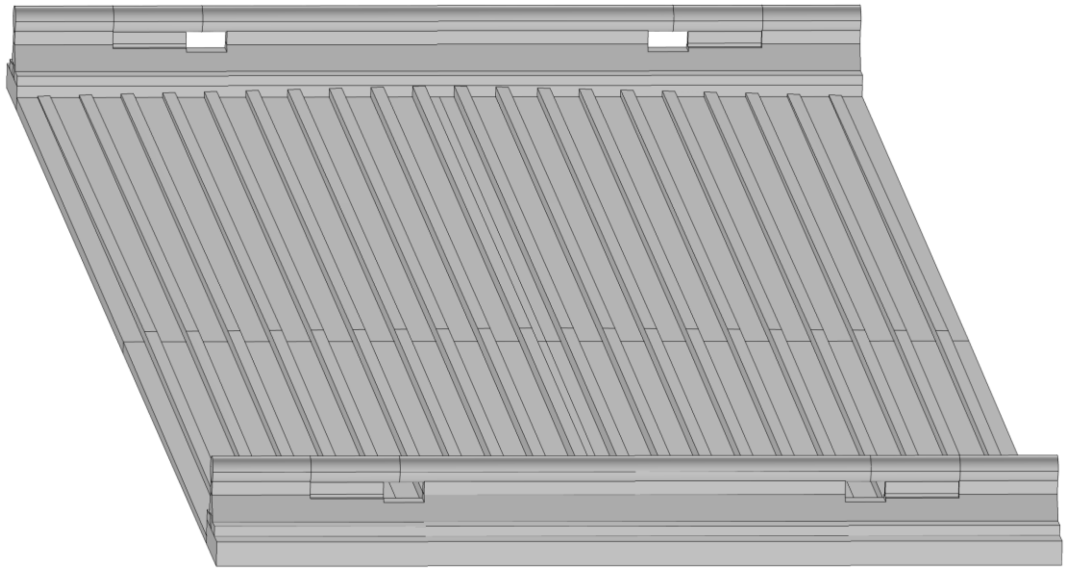

MDO - Design space 2, active learning for MDO

- The optimization on Design Space 2 achieve better optimal results than Design Space 1
  - 489 one-way simulations have been performed
  - Using a larger design space allowed a significant improvement of the plate performance
  - The entire Pareto set has been improved

Aggregated results

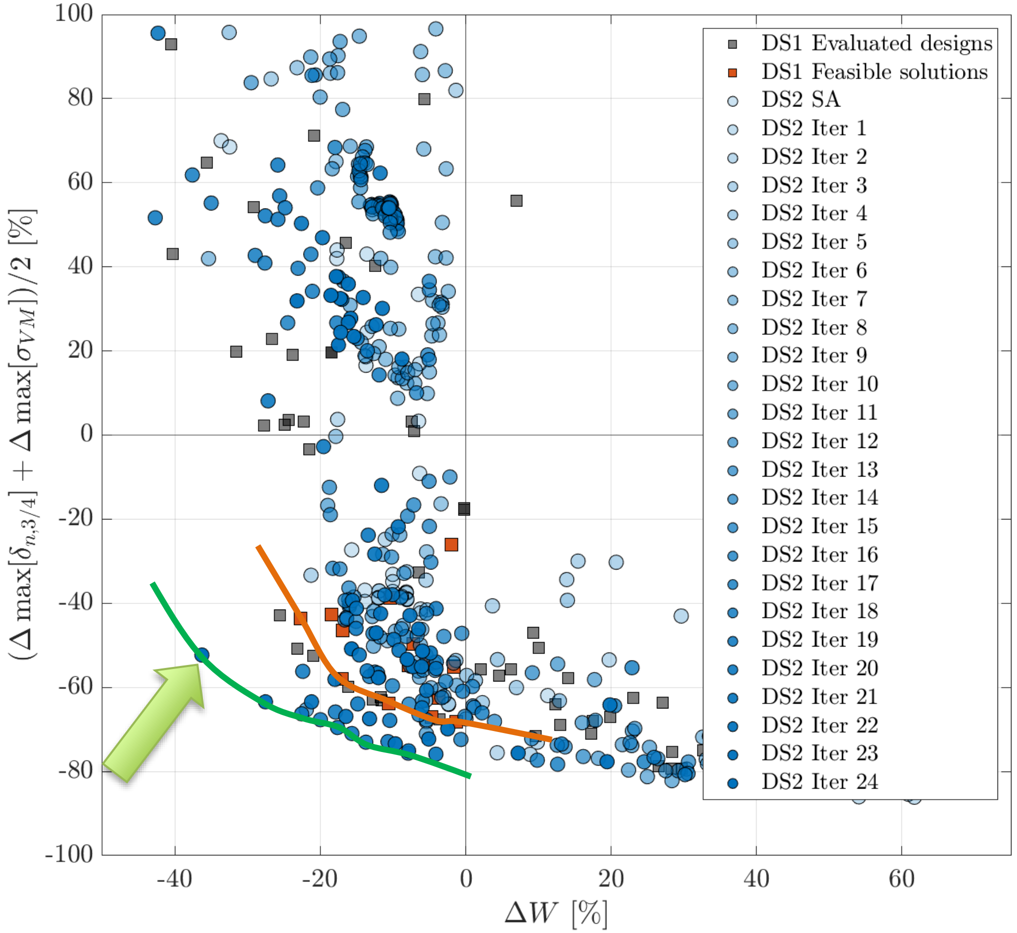

Maximum normal deflection

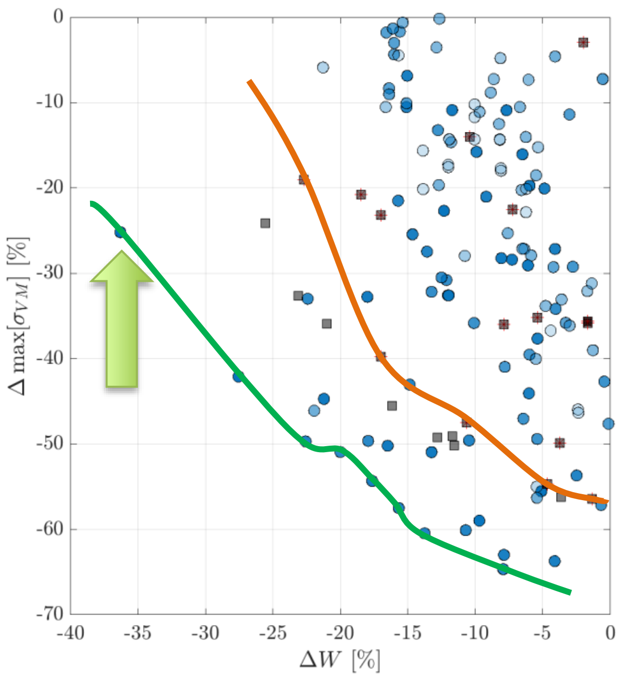

Maximum Von Mises stress

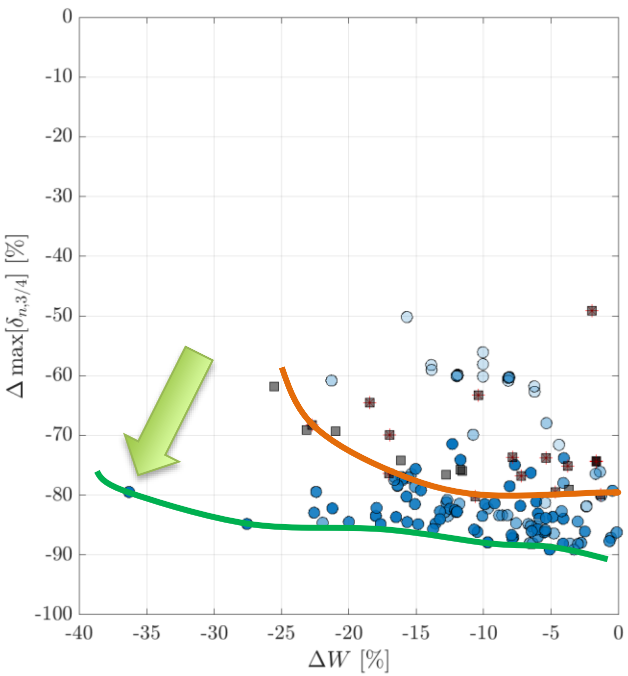

MDO - Design space 2, candidate solution

- The use of the O.403 case loads guarantees that the maximum stress will remain below yielding also for the other cases
- All the objectives have been improved with respect to the candidate solution found with Design Space 1

Variations with respect to the original plate

	ΔW	$\delta_{n3/4}$	$\max[\sigma_{VM}]$
DS1 candidate	-22%	-66%	-19%
DS2 candidate	-36%	-79%	-25%

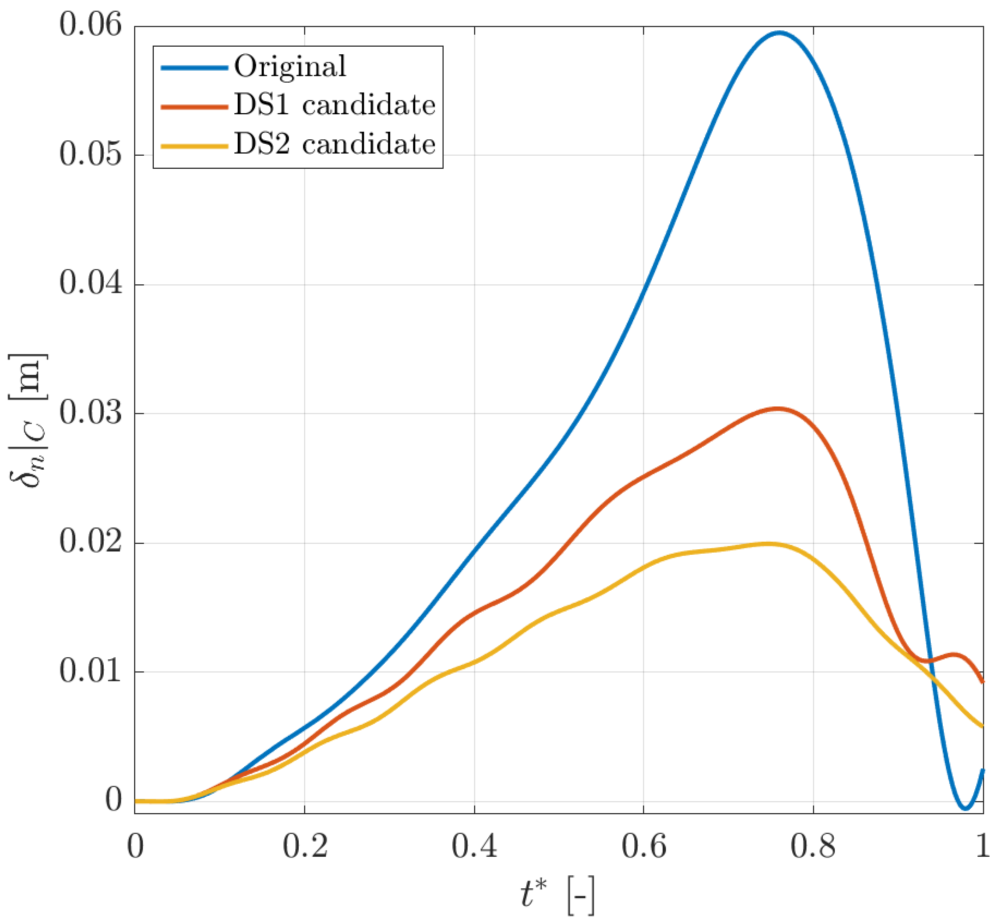

MDO - Design space 2, candidate solution

- Current candidate solution
  - Eight stiffeners
  - Minimum plate thickness: 1.7 mm
  - Maximum plate thickness: 2 mm
- The thickness of the optimized plate grows from the external sides towards the midline
- The stiffeners thickness grows from the trailing edge to the leading edge

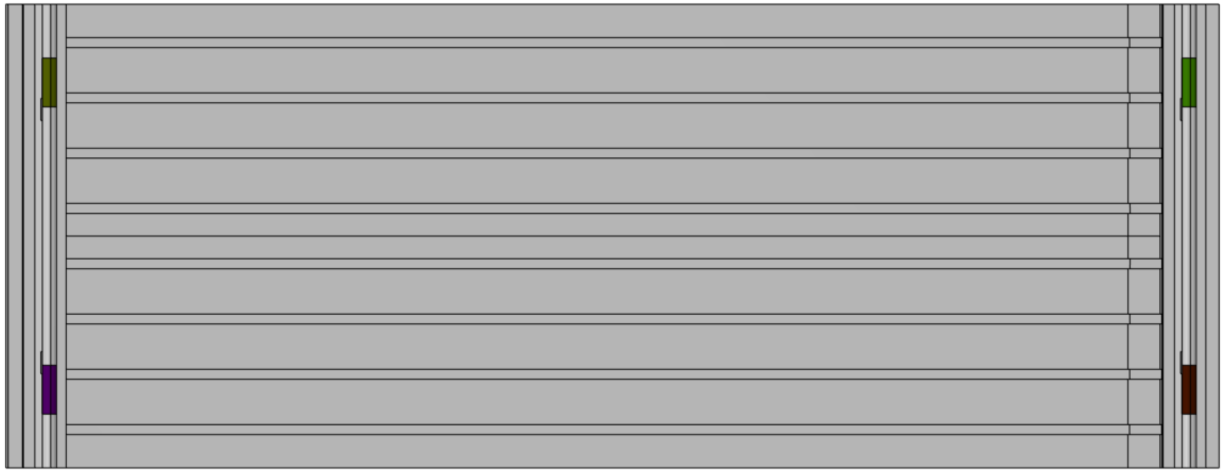

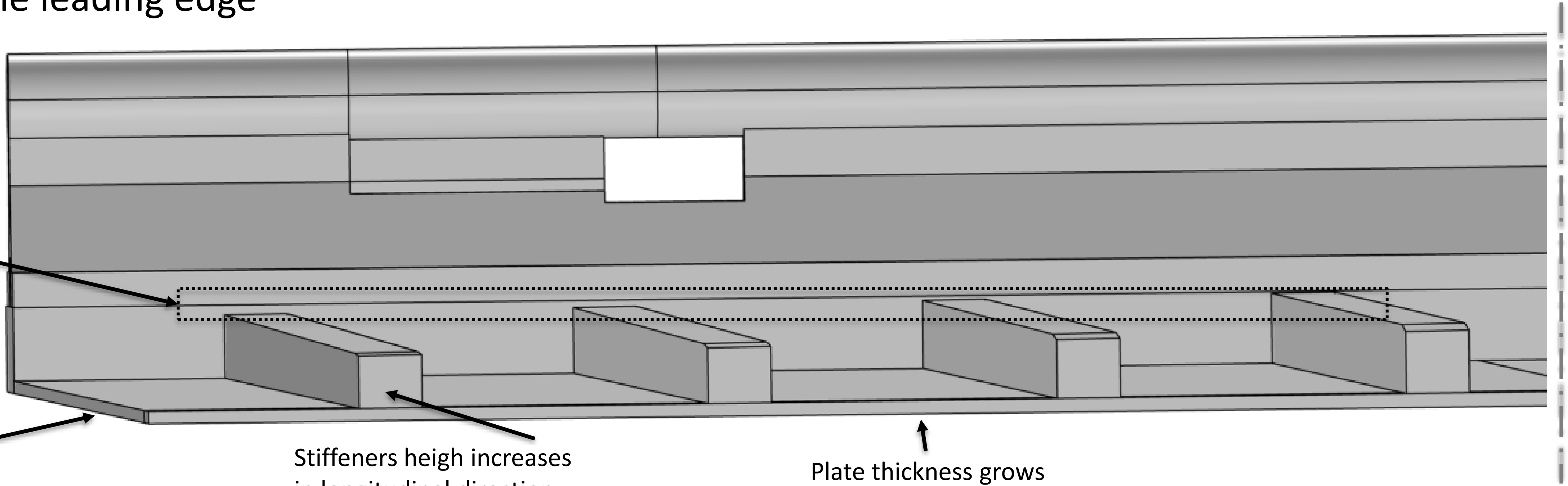

Conclusions and future research

Conclusions

- Available numerical and experimental data have been exploited to investigate several aspects of the slamming of elastic plates on quiescent water
  - Methods required for the effective analysis of the slamming of elastic solids (two-way FSI with nonlinear structural solver)
  - The role of hydroelasticity and its use to select relevant cases for the effective investigation of the slamming physics
  - The use of a stagnation flow model to investigate the role of the plate kinematics on the impact force
  - The analysis of the conservation of energy to identify an effective strategy for the multidisciplinary optimization for weight reduction and safety increase
  - The effect of the plate aspect ratio on the slamming physics
- The MDO of a macroscopically orthotropic plate has been performed

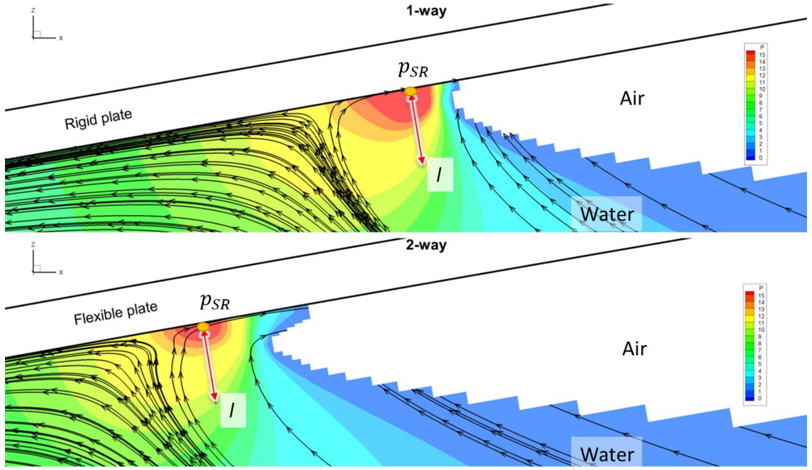

Future research

- Collaborate with UMD for MDO (EFD on new geometry)
- Flexible plate slamming with waves, study to be planned with UMD
- High-fidelity CFD/CSD FSI multi-phase flow simulation
  - Perform a simulation with CFDShip-Iowa V5.5 for the 7.5 deg pitch angle, Vn = 1.39 m/s, and U/W = 17.27 case with a nonlinear structural solver

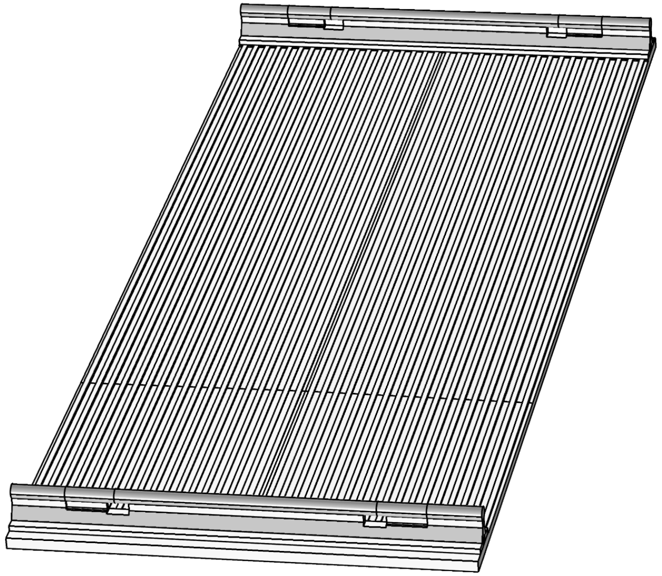

Bibliography

- Faltinsen, Odd M. "The effect of hydroelasticity on ship slamming." Philosophical Transactions of the Royal Society of London. Series A: Mathematical, Physical and Engineering Sciences 355, no. 1724 (1997): 575-591.
- Faltinsen, Odd M. "Water entry of a wedge by hydroelastic orthotropic plate theory." *Journal of ship research* 43, no. 03 (1999): 180-193.
- Faltinsen, Odd M., Jan Kvålsvold, and Jan V. Aarsnes. "Wave impact on a horizontal elastic plate." Journal of Marine Science and Technology 2, no. 2 (1997): 87-100.
- Huang, J., Carrica, P.M., and Stern, F, 2008. "Semi-coupled air/water immersed boundary approach for curvilinear dynamic overset grids with application to ship hydrodynamics". International Journal for Numerical Methods in Fluids, 58(6): 591-624.
- Iafrati, A. "Experimental investigation of the water entry of a rectangular plate at high horizontal velocity." Journal of Fluid Mechanics 799 (2016): 637-672.
- Panciroli, Riccardo, and M. Porfiri. "Analysis of hydroelastic slamming through particle image velocimetry." *Journal of Sound and Vibration* 347 (2015): 63-78.
- Segletes, S.B., Walters, W.P., "A note on the application of the extended Bernoulli equation", International Journal of Impact Engineering, 27 (2002) 561–576.
- Stenius, Ivan, Anders Rosén, and Jacob Kuttenkeuler. "Explicit FE-modelling of hydroelasticity in panel-water impacts." *International Shipbuilding Progress* 54, no. 2-3 (2007): 111-127.
- Stenius, Ivan, Anders Rosén, and Jakob Kuttenkeuler. "Hydroelastic interaction in panel-water impacts of high-speed craft." *Ocean Engineering* 38, no. 2-3 (2011): 371-381.
- Volpi, S., M. Diez, H. Sadat-Hosseini, D-H. Kim, F. Stern, R. S. Thodal, and J. L. Grenestedt. "Composite bottom panel slamming of a fast planing hull via tightly coupled fluid-structure interaction simulations and sea trials." *Ocean Engineering* 143 (2017): 240-258.
- Wang, A., Wong, K.P., Yu, M., Kiger, K.T. and Duncan, J.H., 2022. The controlled impact of elastic plates on a quiescent water surface. *Journal of Fluid Mechanics*, *939*, p.A4.
- Wang, A., Kim, H. T., Wong, K. P., Yu, M., Kiger, K. T., & Duncan, J. H. (2019). "Spray formation and structural deflection during the oblique impact of a flexible plate on a quiescent water surface". Journal of Ship Research, 63(3), 154-164.
- Zhao, R. and Faltinsen, O., 1993. Water entry of two-dimensional bodies. *Journal of fluid mechanics*, *246*, pp.593-612.
- Wu, G.X. and Sun, S.L., 2014. Similarity solution for oblique water entry of an expanding paraboloid. *Journal of fluid mechanics*, *745*, pp.398-408.
- Judge, C., Troesch, A. and Perlin, M., 2004. Initial water impact of a wedge at vertical and oblique angles. *Journal of Engineering Mathematics*, *48*, pp.279-303.
- Panciroli, R., 2013. Water entry of flexible wedges: Some issues on the FSI phenomena. *Applied Ocean Research*, *39*, pp.72-74.
- Khabakhpasheva, T.I. and Korobkin, A.A., 2013. Elastic wedge impact onto a liquid surface: Wagner's solution and approximate models. *Journal of Fluids and Structures*, *36*, pp.32-49.
- Korobkin, A.A. and Khabakhpasheva, T.I., 2006. Regular wave impact onto an elastic plate. *Journal of engineering mathematics*, *55*, pp.127-150.

Backup slides – Bernulli equation

Stagnation Flow Model: Extended Bernoulli Equation Analysis (4)

O.269

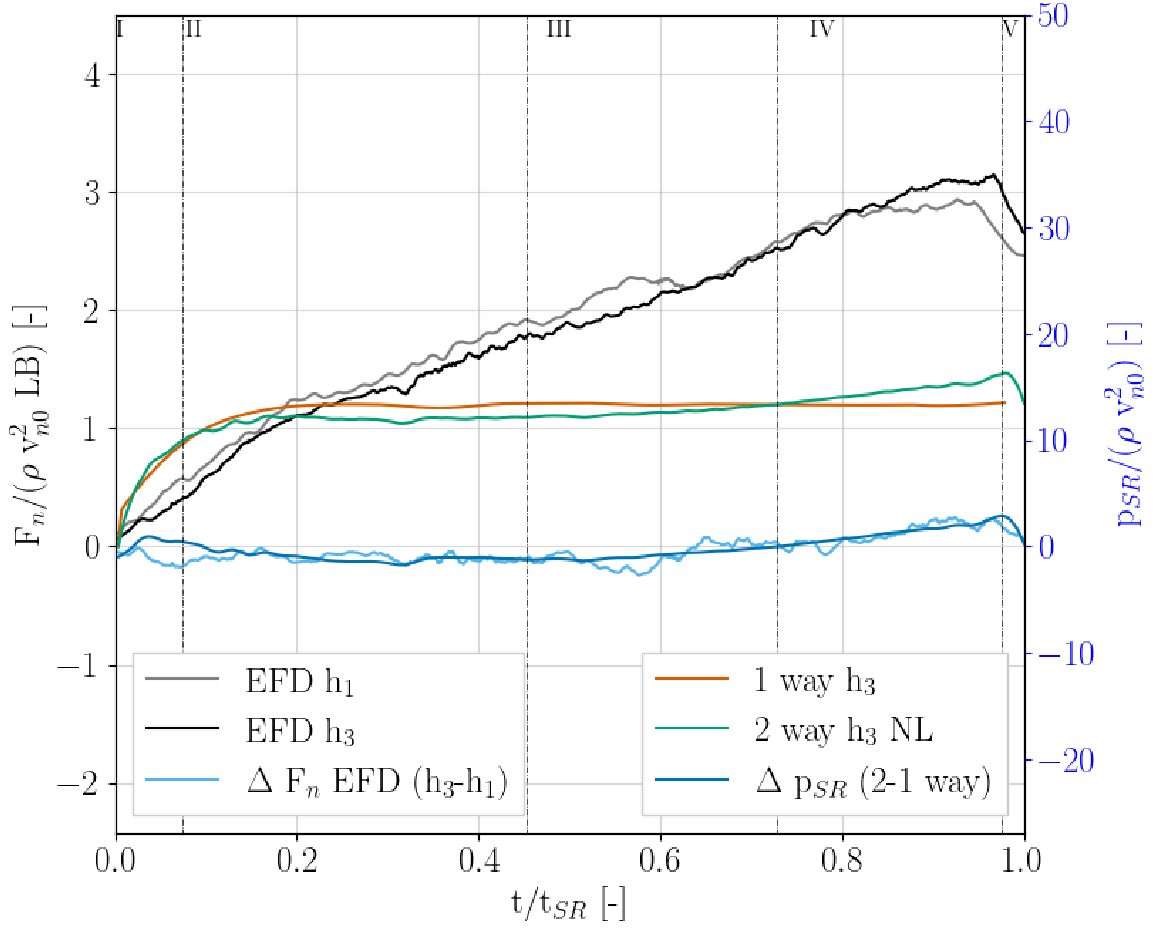

O.403

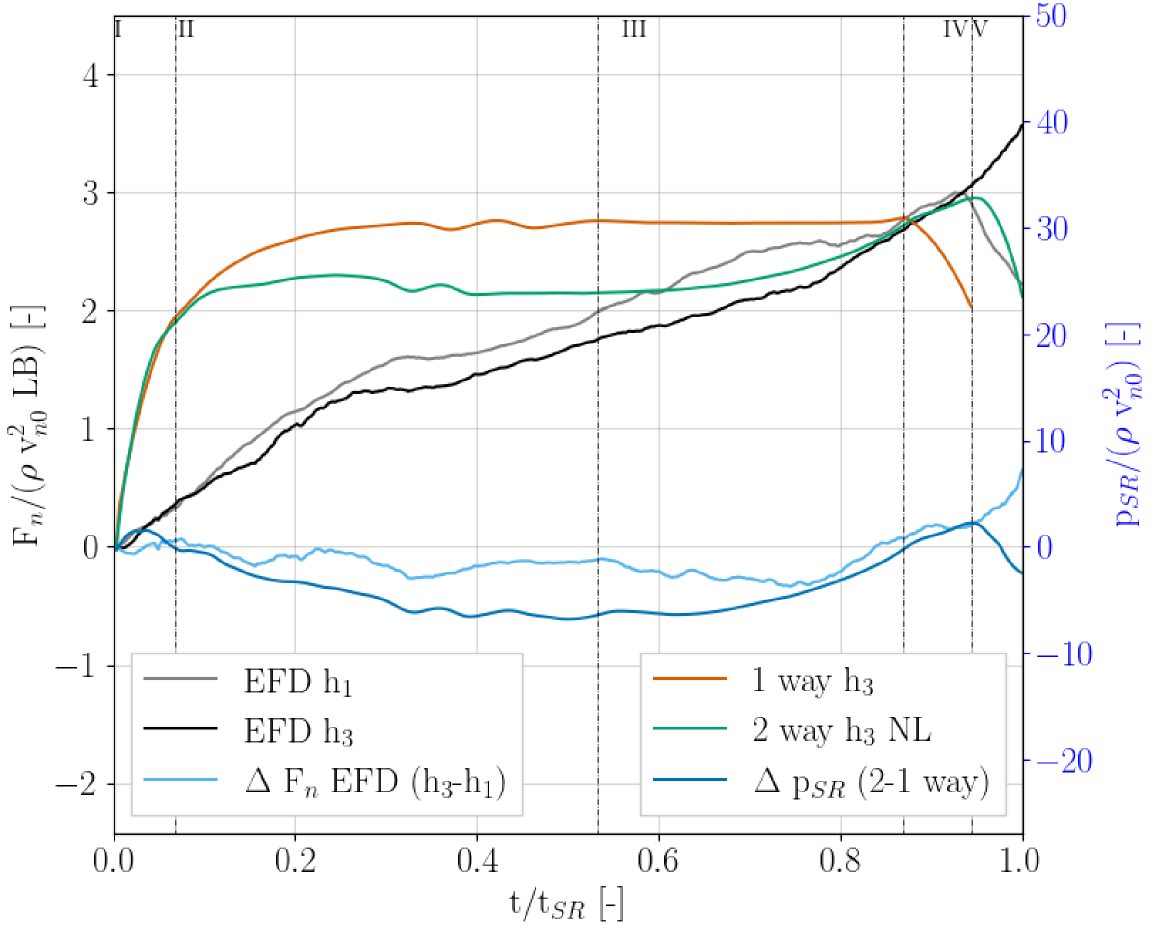

Stagnation Flow Model: Extended Bernoulli Equation Analysis (5)

O.269

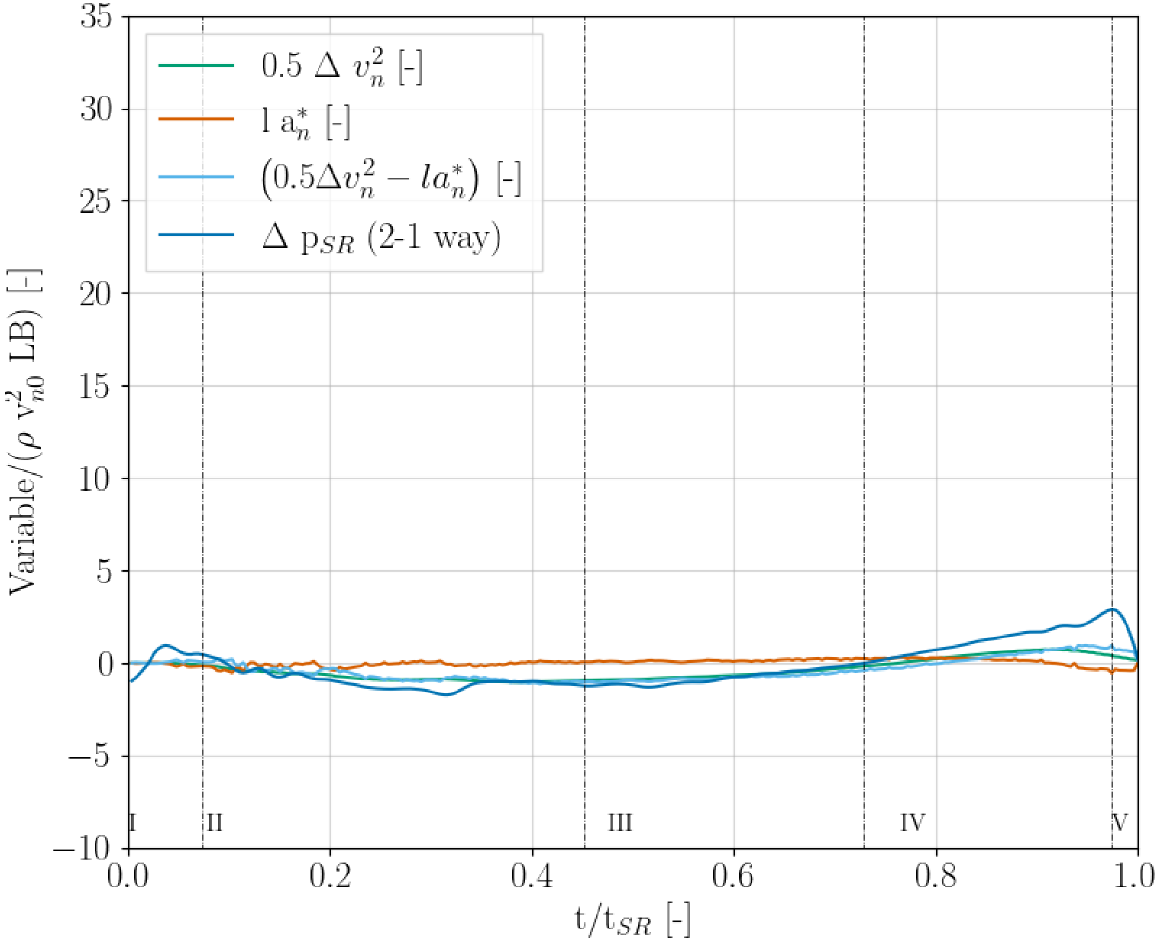

O.403

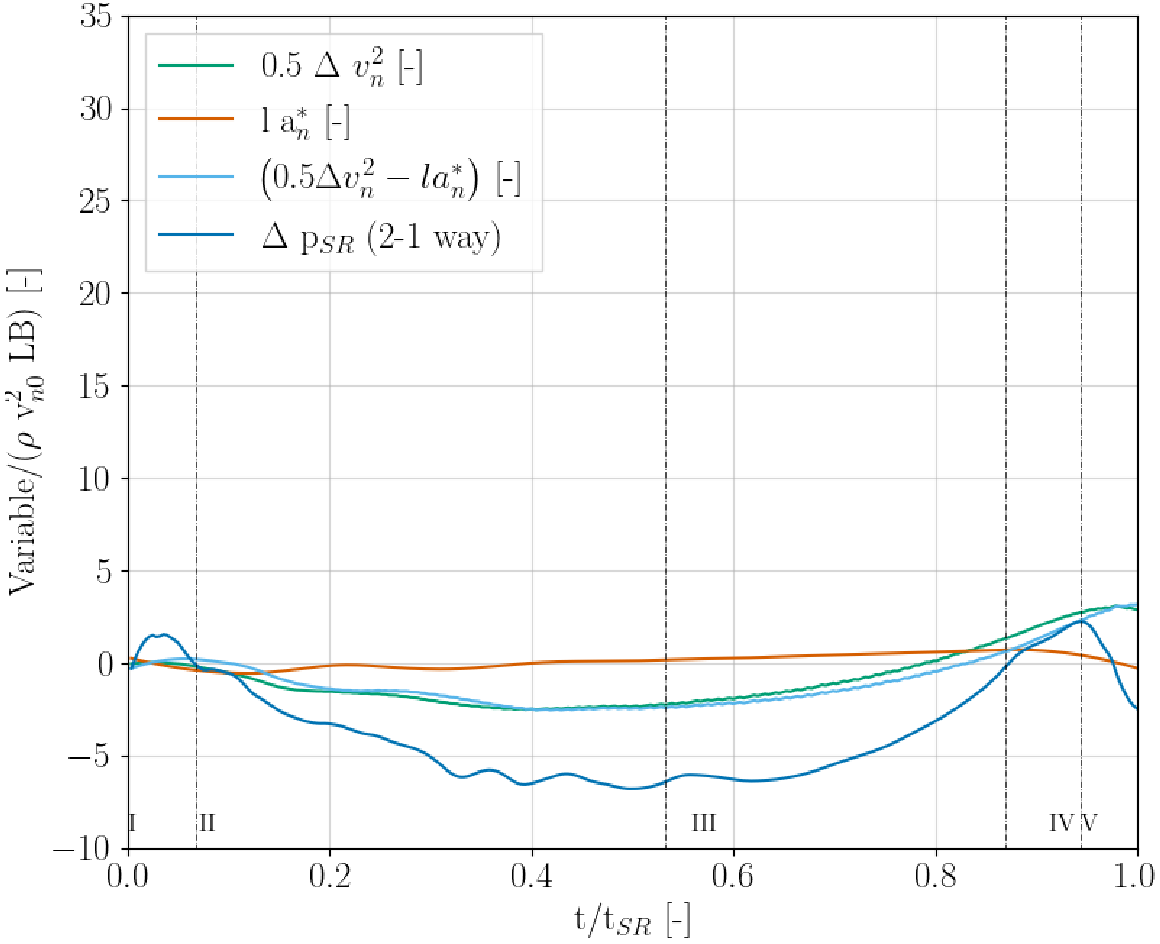

Stagnation Flow Model: Extended Bernoulli Equation Analysis (6)

0.269

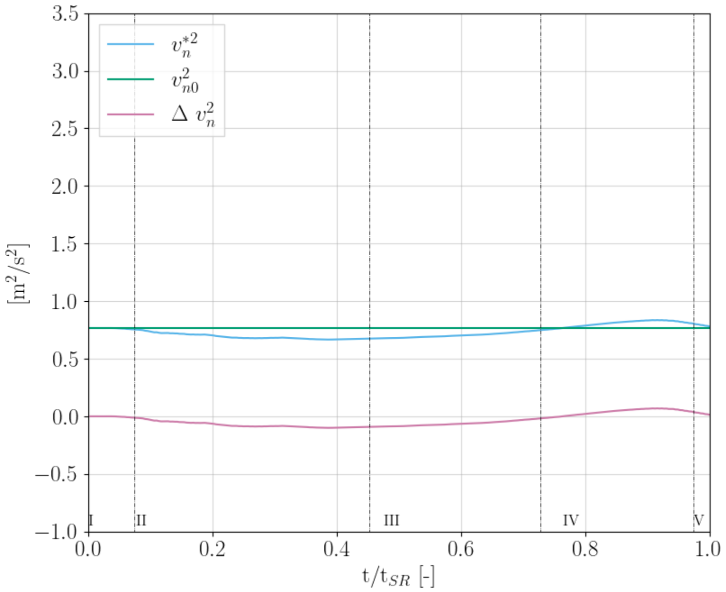

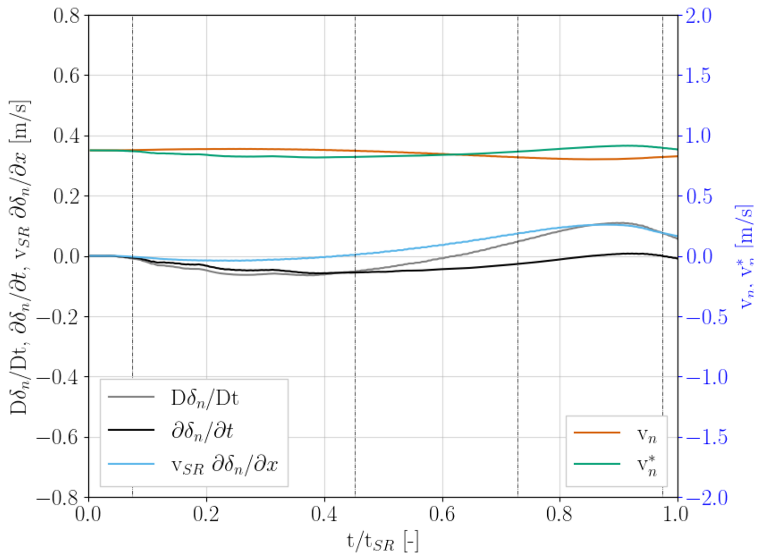

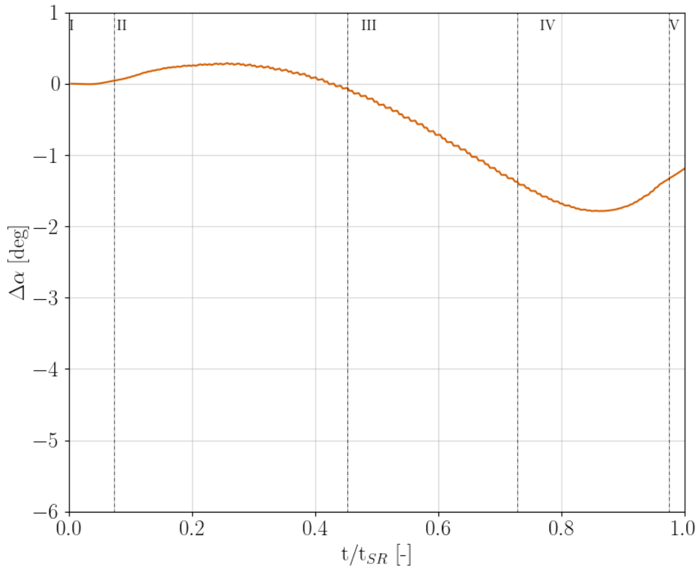

0.403

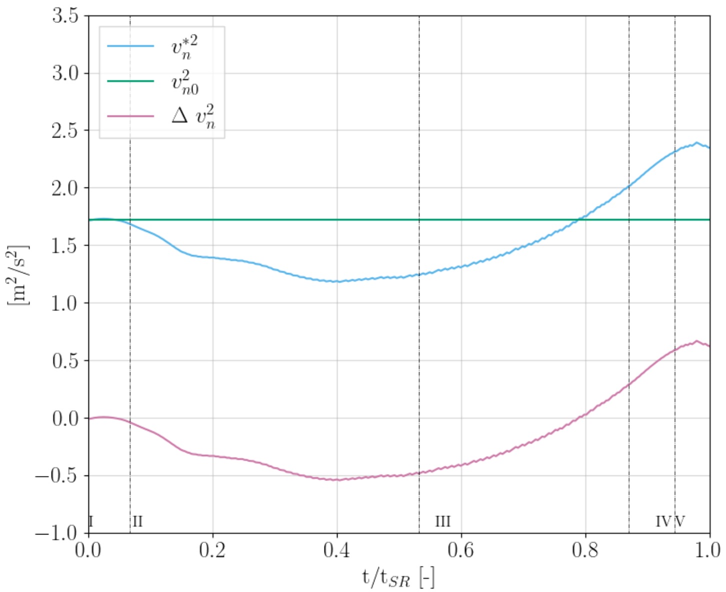

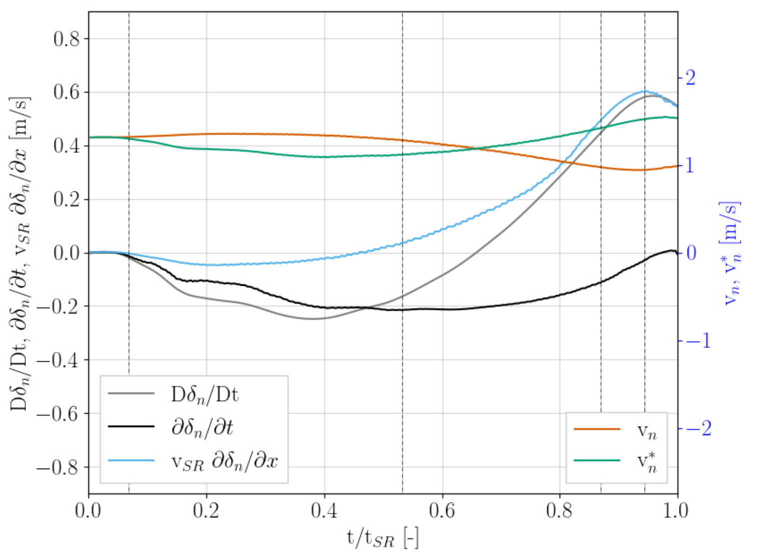

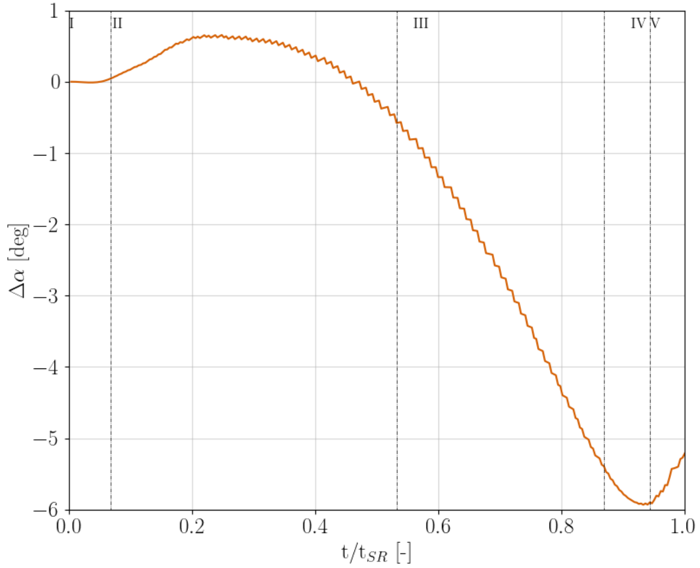

Stagnation Flow Model: Extended Bernoulli Equation Analysis (7)

0.269

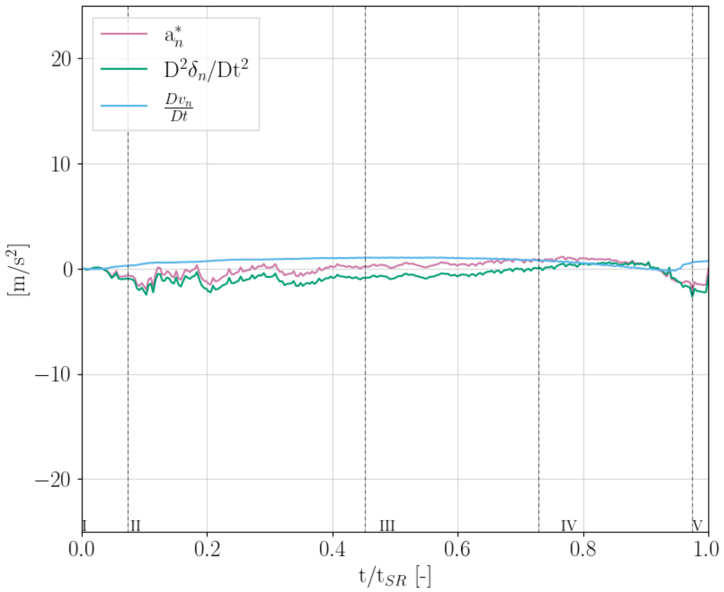

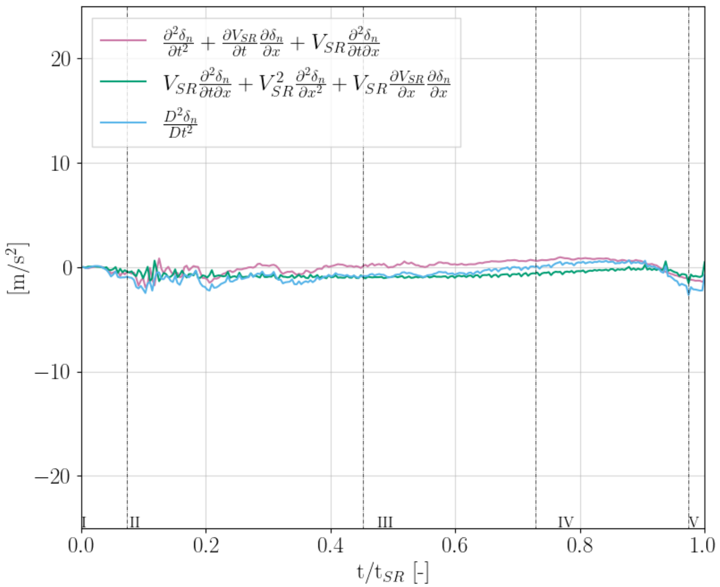

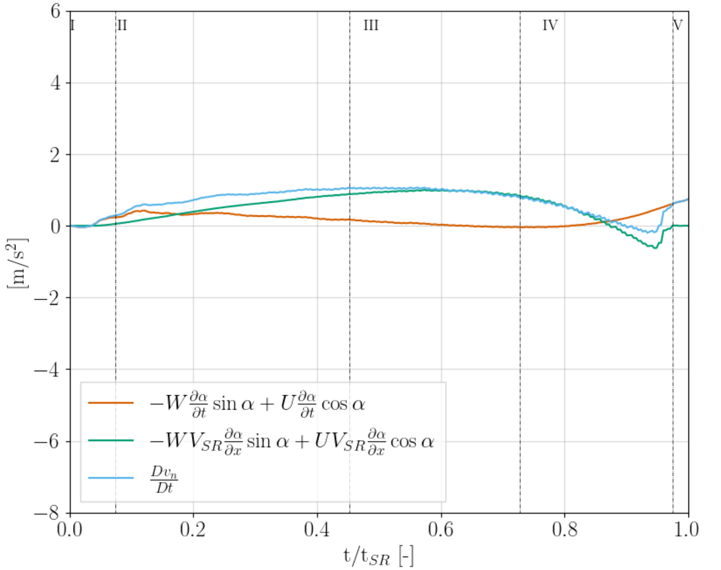

0.403

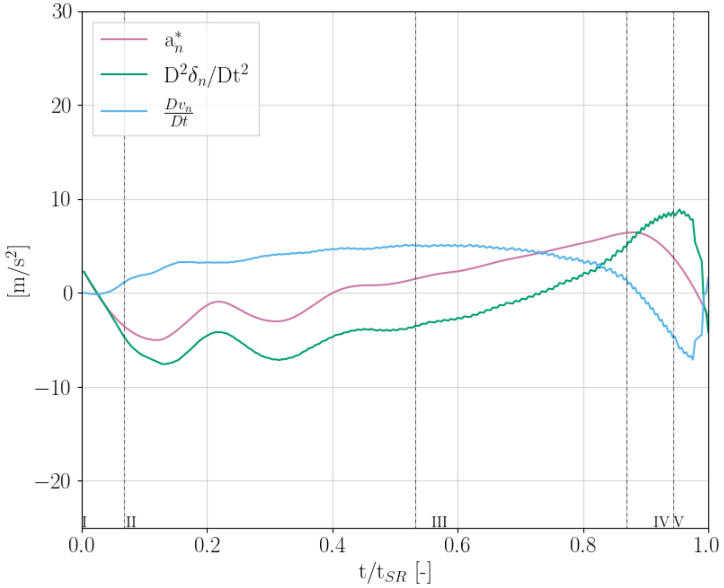

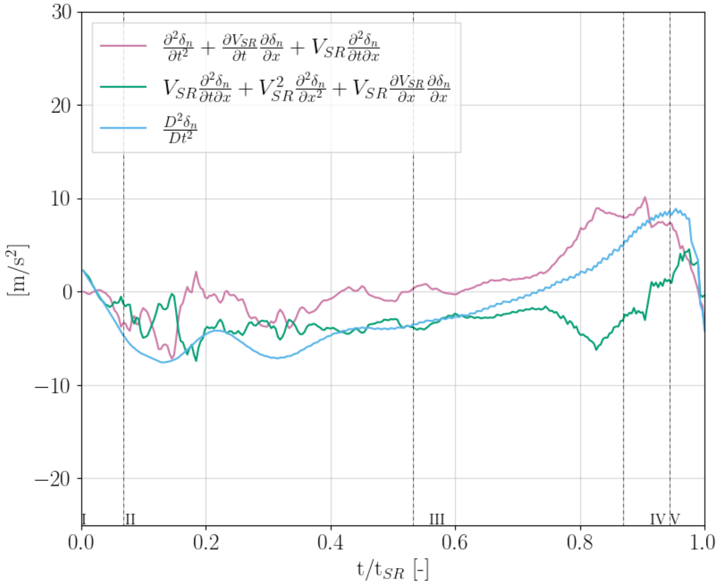

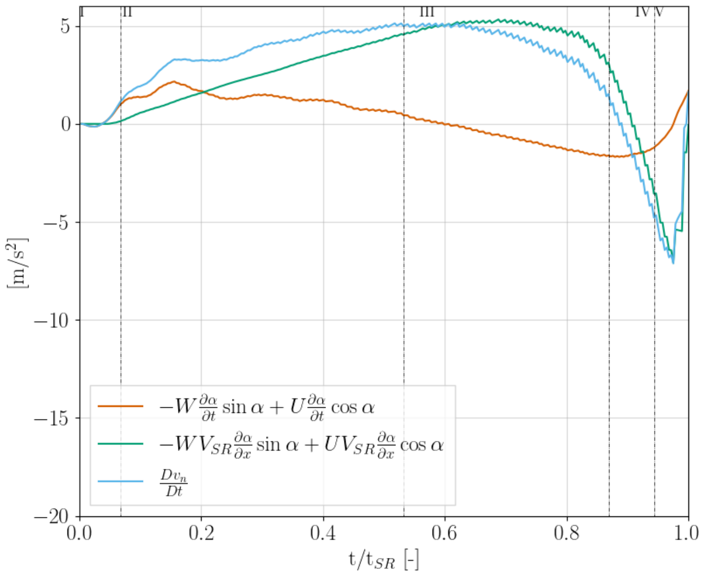

Stagnation Flow Model: Extended Bernoulli Equation Analysis (8)

0.269

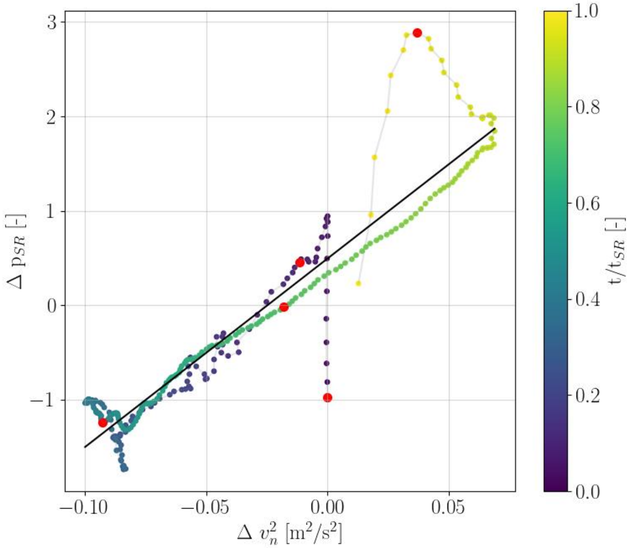

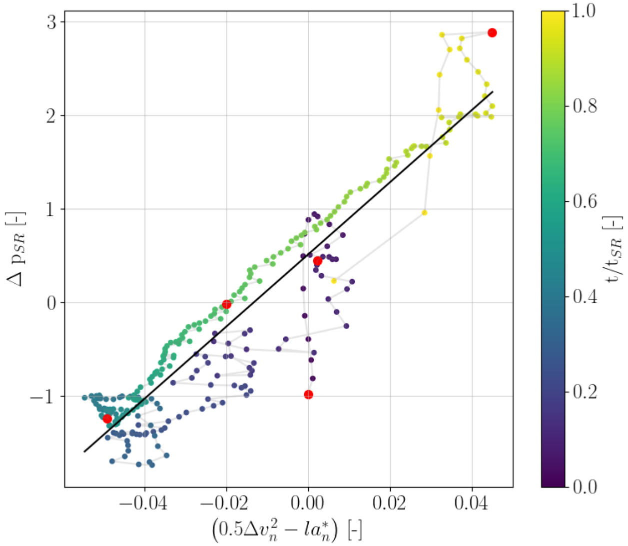

0.403

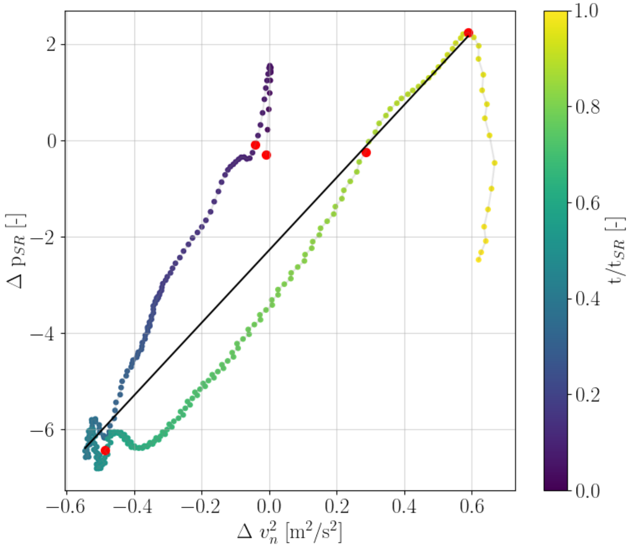

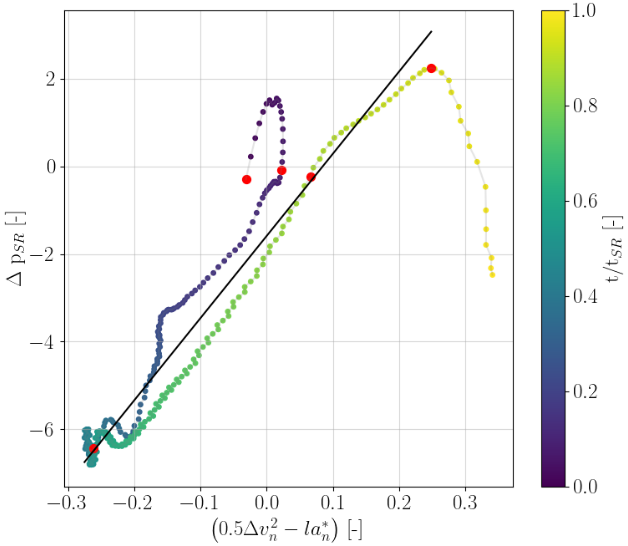

Backup slides – Energy conservation O.269

Conservation of Energy Analysis (5): Rigid and Flexible Plate

- Rigid plate
  - ➢ The mount transfers energy directly to the fluid since the plate is rigid

Water
$$\frac{\partial}{\partial t}\iiint_{V_w} \rho_w \left(\frac{\|\boldsymbol{u}_w\|^2}{2}\right) dV_w \;=\; \iint_{S_{Wet}(t)} p(v_n)dS \;=\; W_{pR}$$

Structure
$$-W_{pR} = W_M$$

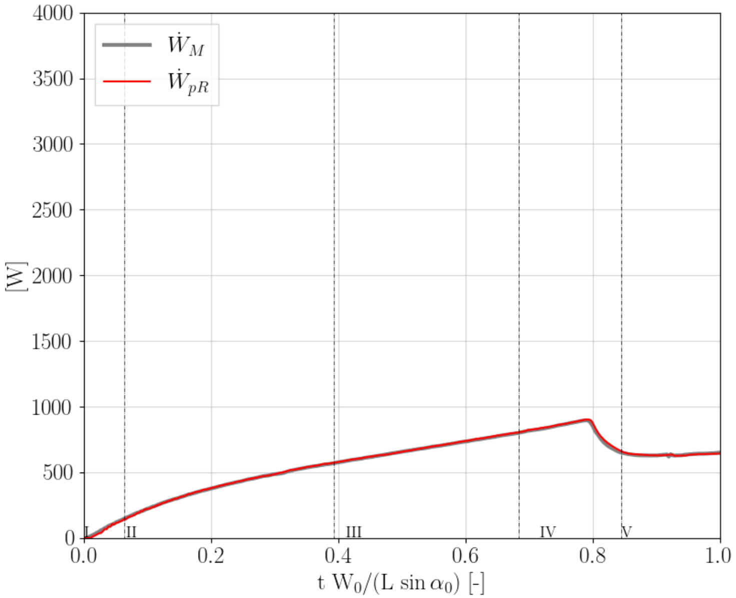

- Flexible plate
  - ➢ The mount transfers energy to the fluid and to the plate (kinetic and potential elastic energy) since the plate is deforming

Water
$$\frac{\partial}{\partial t}\iiint_{V_w} \rho \left(\frac{\|\boldsymbol{u}_w\|^2}{2}\right) dV_w = \iint_{S_{Wet}} p[v_n + \dot{\delta}_n]dS = W_{pR} + W_{p\dot{\delta}_n}$$

Structure
$$\dot{K}_{\dot{\delta}_n} + \dot{U}_{\varepsilon} - \left(W_{pR} + W_{p\dot{\delta}_n}\right) = W_M$$

$$v_n = \boldsymbol{v} \cdot \hat{n}$$
$$\delta_n = \boldsymbol{\delta} \cdot \hat{n}$$

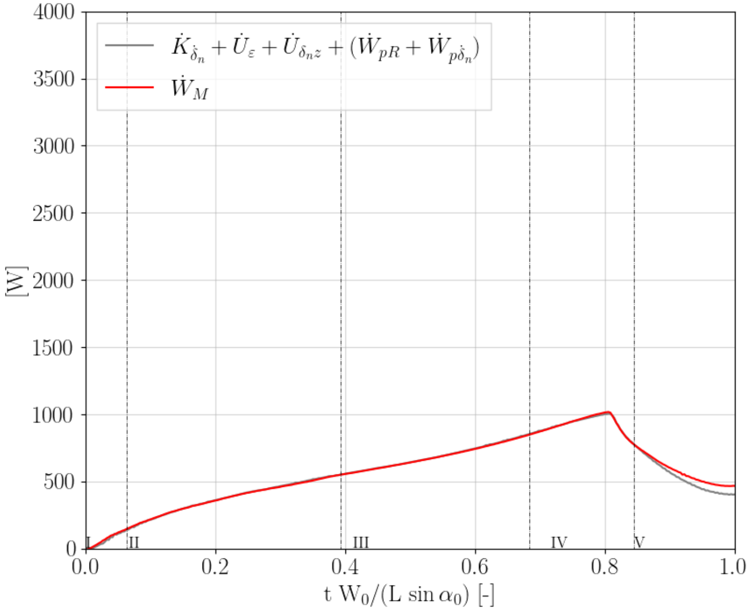

Conservation of Energy Analysis (8): Equation Difference

- The difference equation is satisfied
- The elastic potential energy almost equals the power provided by the pressure due to the flexibility
- The kinetic energy content is the smallest

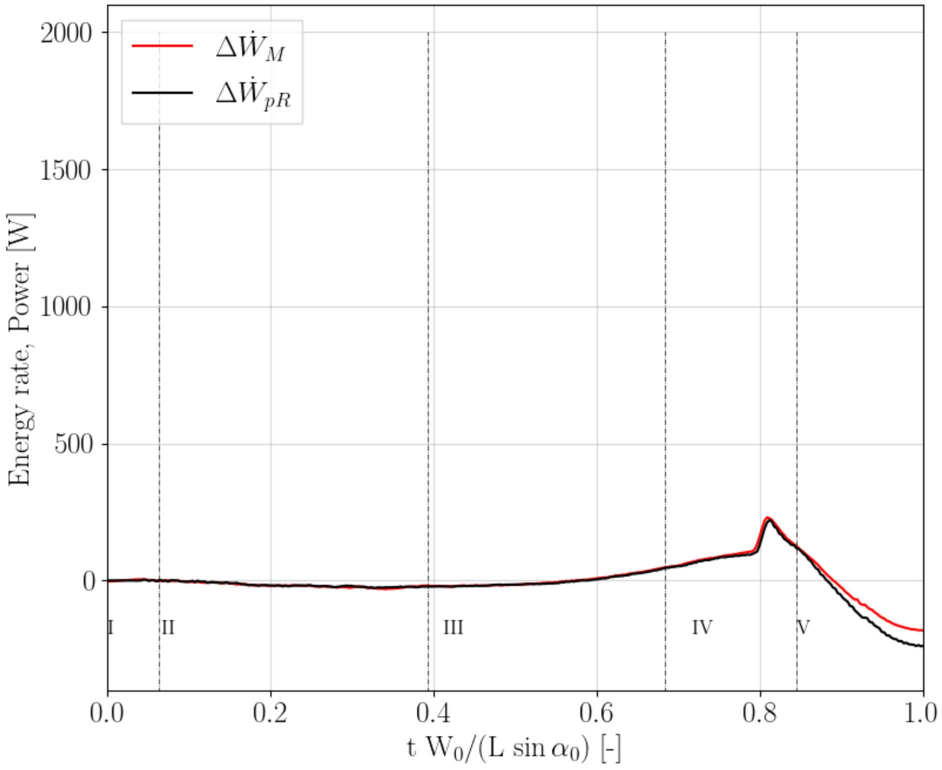

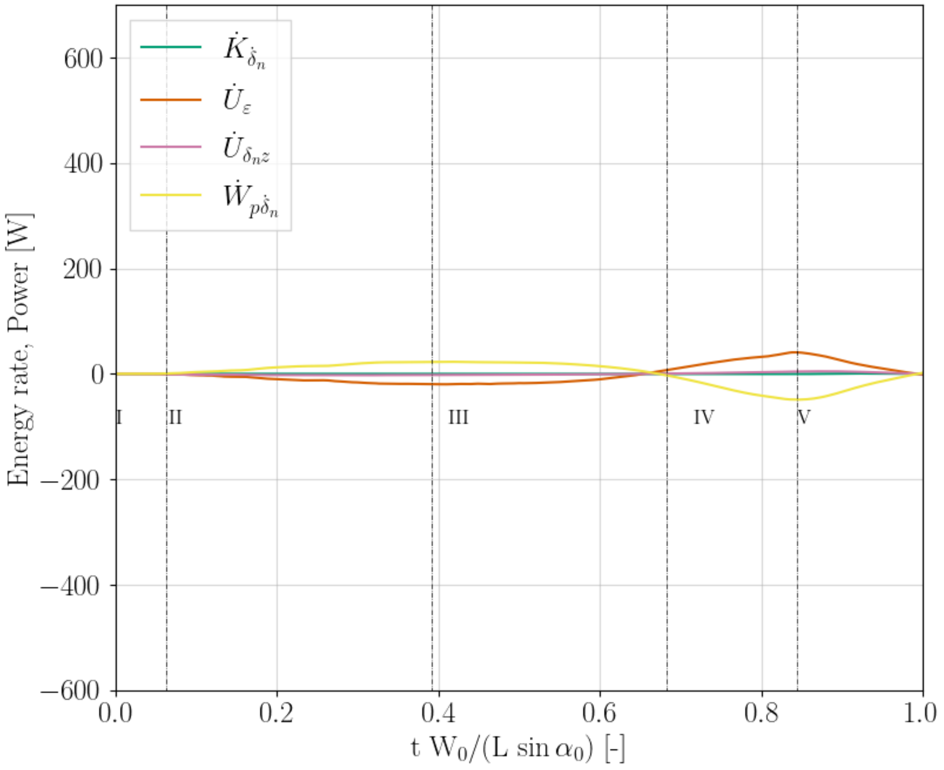

- For all the cases the ε_{xx}^2 strain contribution is the most important.
- The second most important term is $\varepsilon_{xx}\varepsilon_{zz}$ since for the T-bars the ε_{zz} component is the most important (due to their orientation)

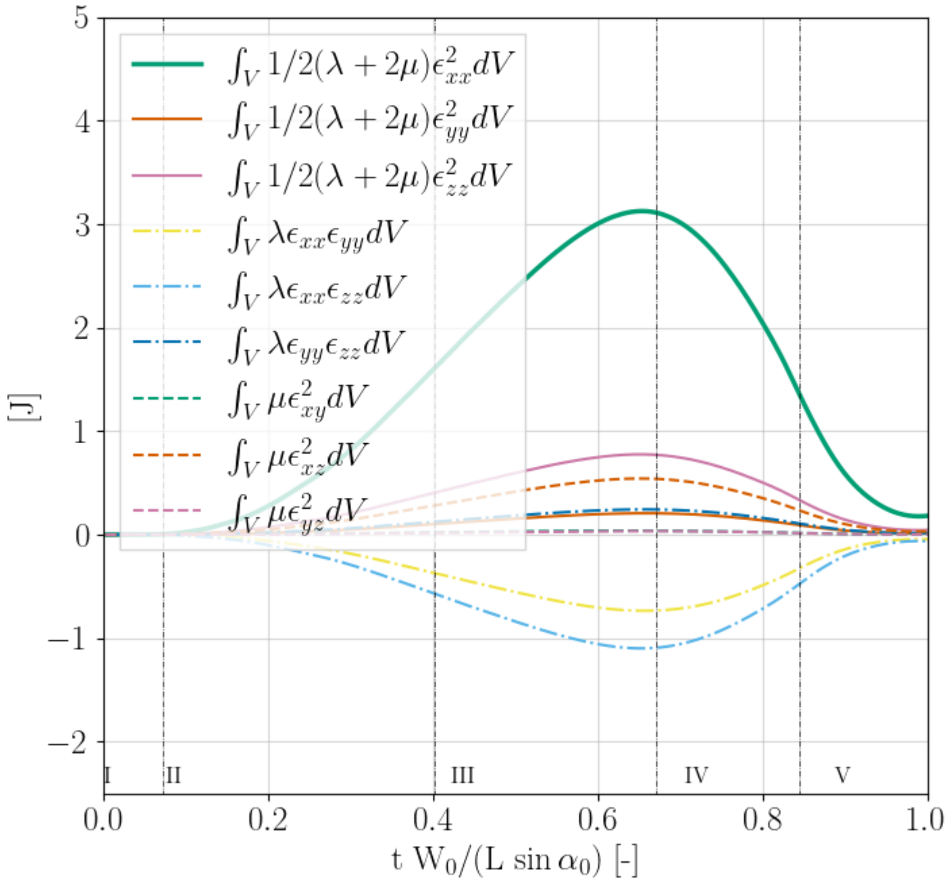

3. Conservation of Energy Analysis (11): Correlation Analysis

- A good correlation between Δp_{SR} and the elastic potential energy exists phase wise
- Δp_{SR} correlates well also with ΔW_{pR} and ΔW_M
- Δp_{SR} does not correlate well with the kinetic energy variation

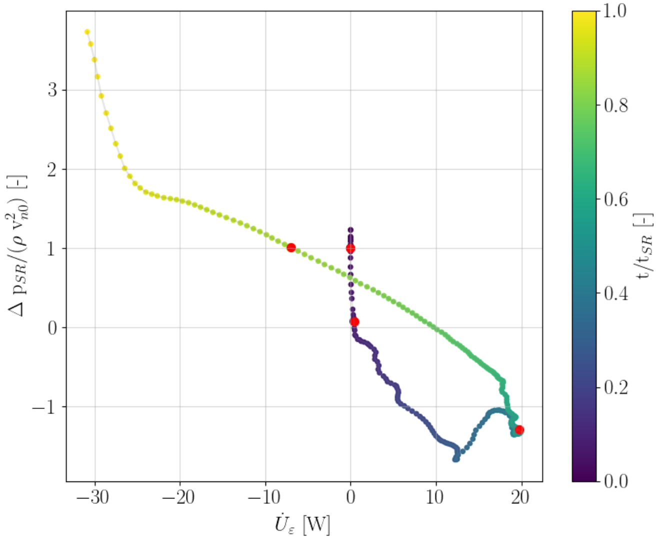

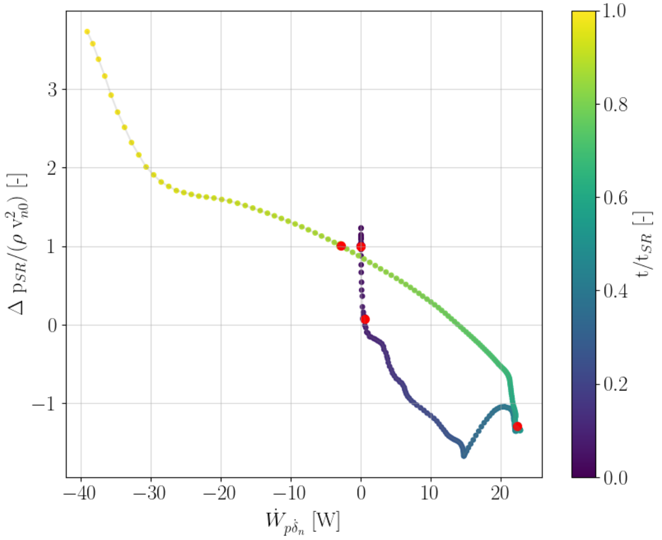

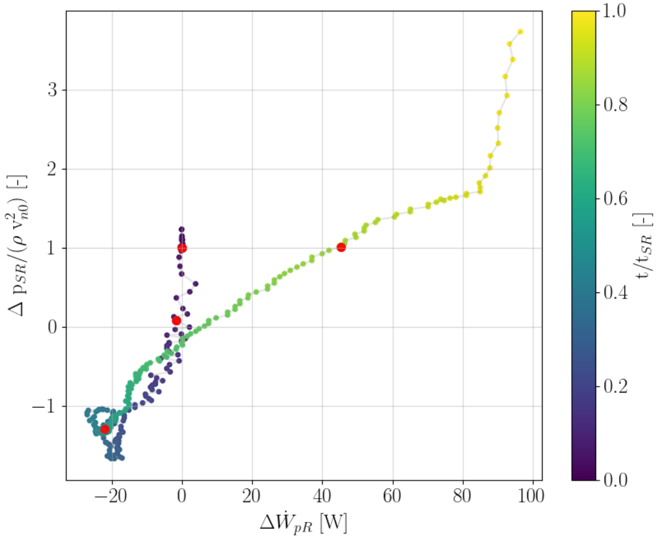

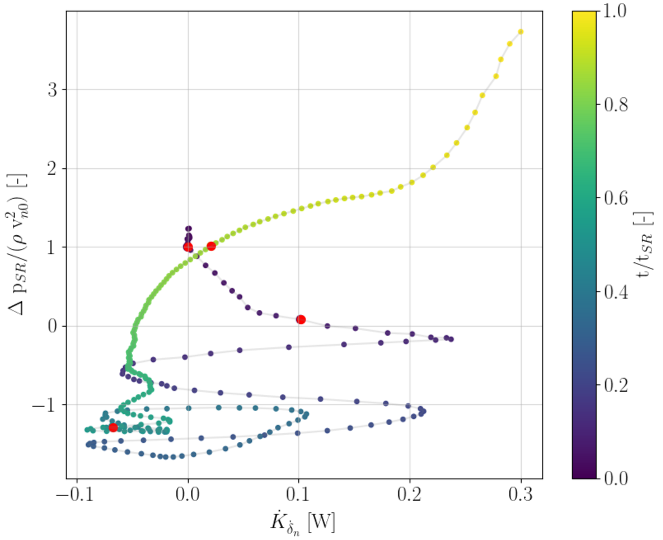

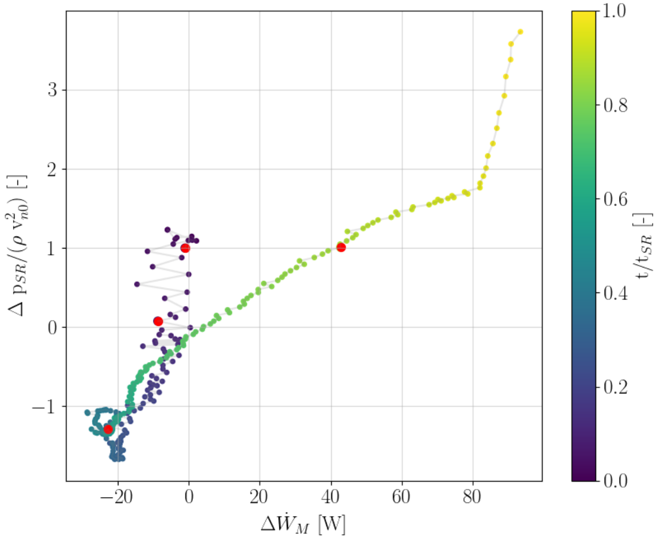

Backup slides – Energy conservation O.403

Conservation of Energy Analysis (5): Rigid and Flexible Plate

- Rigid plate
  - The mount transfers energy directly to the fluid since the plate is rigid

Water

$$\frac{\partial}{\partial t}\iiint_{V_w}\rho_w\left(\frac{\|\boldsymbol{u}_w\|^2}{2}\right)dV_w = \iint_{S_{Wet}(t)} p(v_n)dS = W_{pR}$$

Structure

$$-W_{pR} = W_M$$

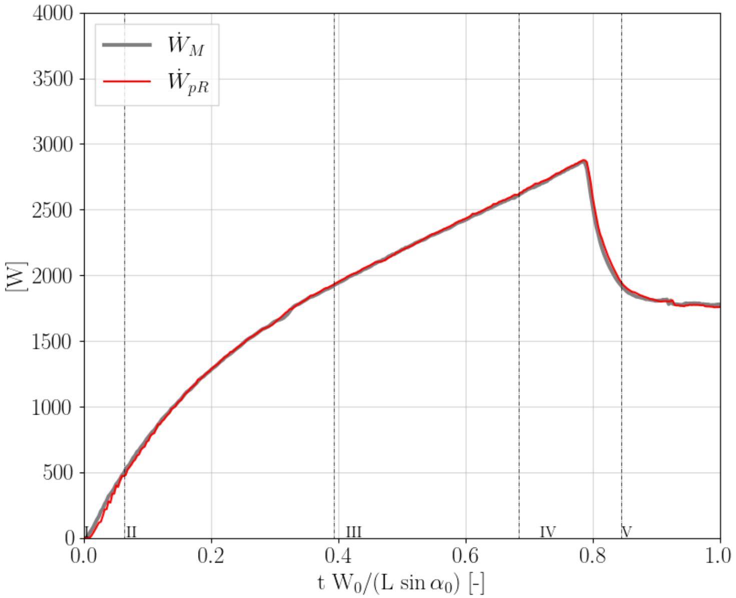

- Flexible plate
  - The mount transfers energy to the fluid and to the plate (kinetic and potential elastic energy) since the plate is deforming

Water

$$\frac{\partial}{\partial t}\iiint_{V_w}\rho\left(\frac{\|\boldsymbol{u}_w\|^2}{2}\right)dV_w = \iint_{S_{Wet}} p[v_n + \dot{\delta}_n]dS = W_{pR} + W_{p\dot{\delta}_n}$$

Structure

$$\dot{K}_{\dot{\delta}_n} + \dot{U}_\varepsilon - \left(W_{pR} + W_{p\dot{\delta}_n}\right) = W_M$$

$$v_n = \boldsymbol{v} \cdot \hat{n}$$
$$\delta_n = \boldsymbol{\delta} \cdot \hat{n}$$

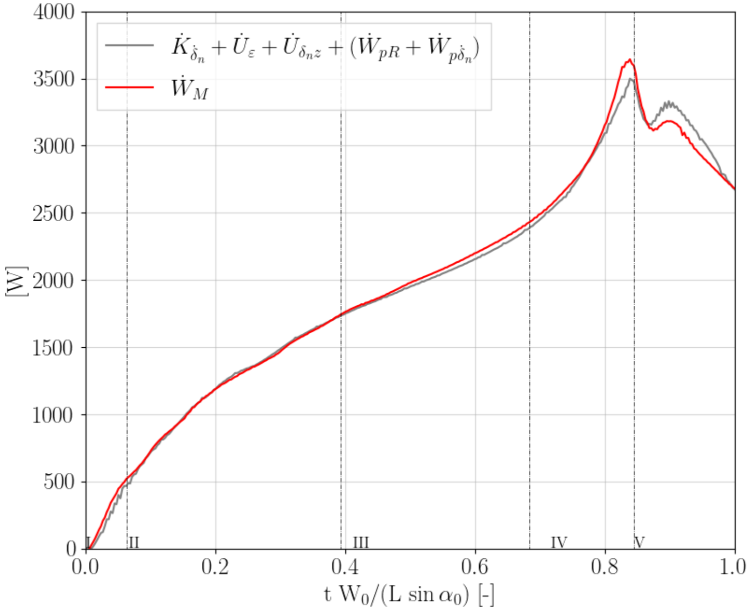

Conservation of Energy Analysis (8): Equation Difference

- The difference equation is satisfied
- The elastic potential energy almost equals the power provided by the pressure due to the flexibility
- The kinetic energy content is the smallest

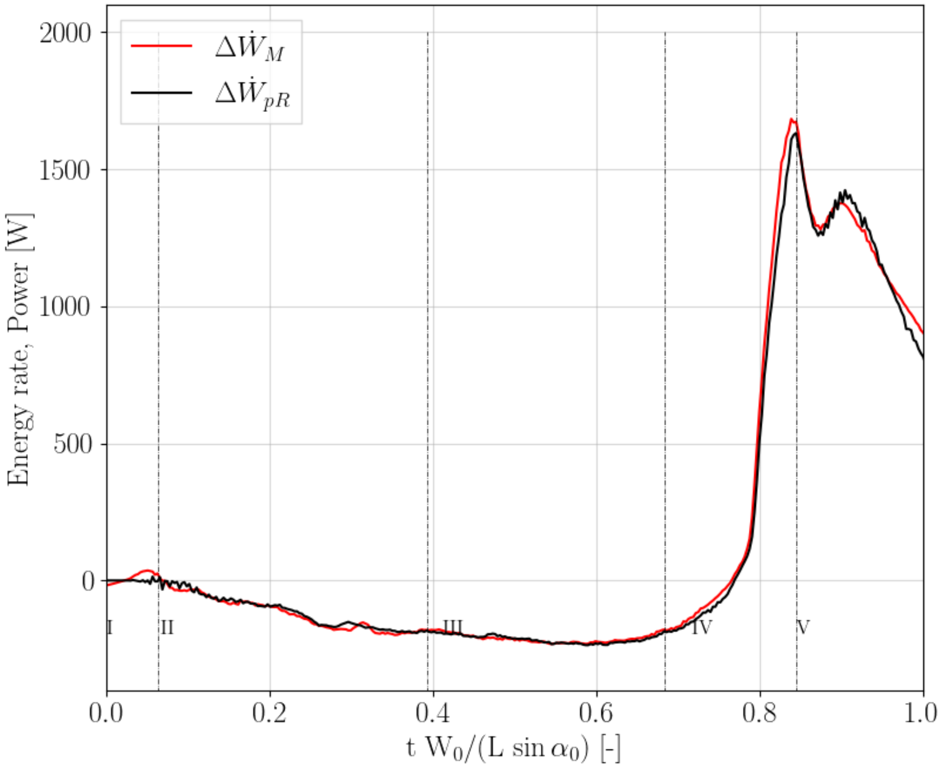

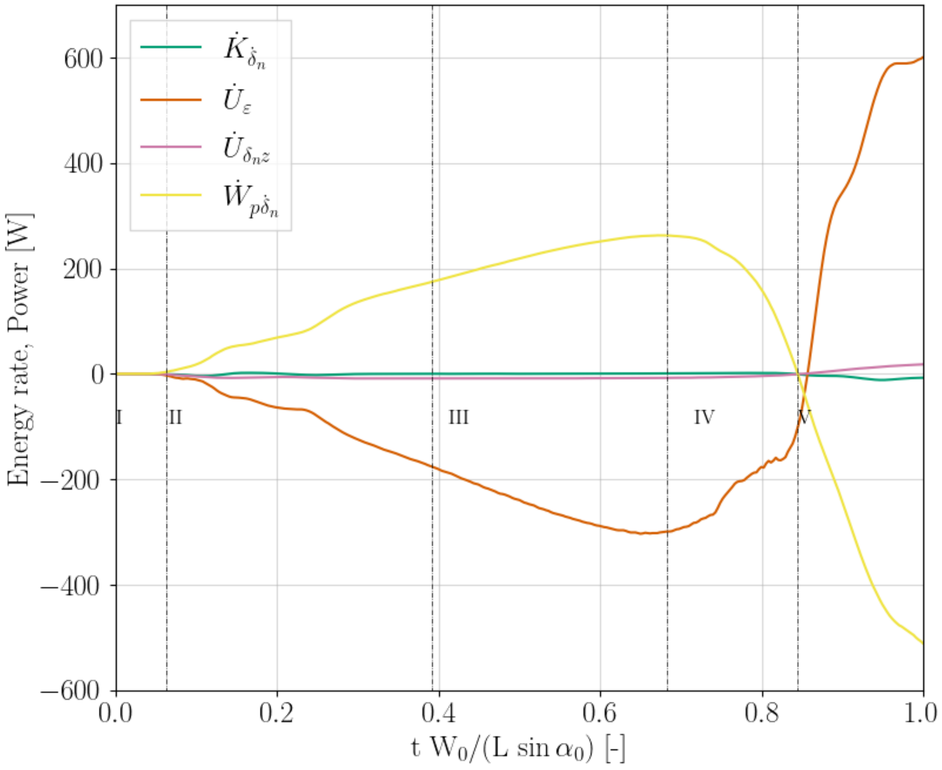

3. Conservation of Energy Analysis (10): Elastic Energy Components

- For all the cases the ε_{xx}^2 strain contribution is the most important.
- The second most important term is $\varepsilon_{xx}\varepsilon_{zz}$ since for the T-bars the ε_{zz} component is the most important (due to their orientation)

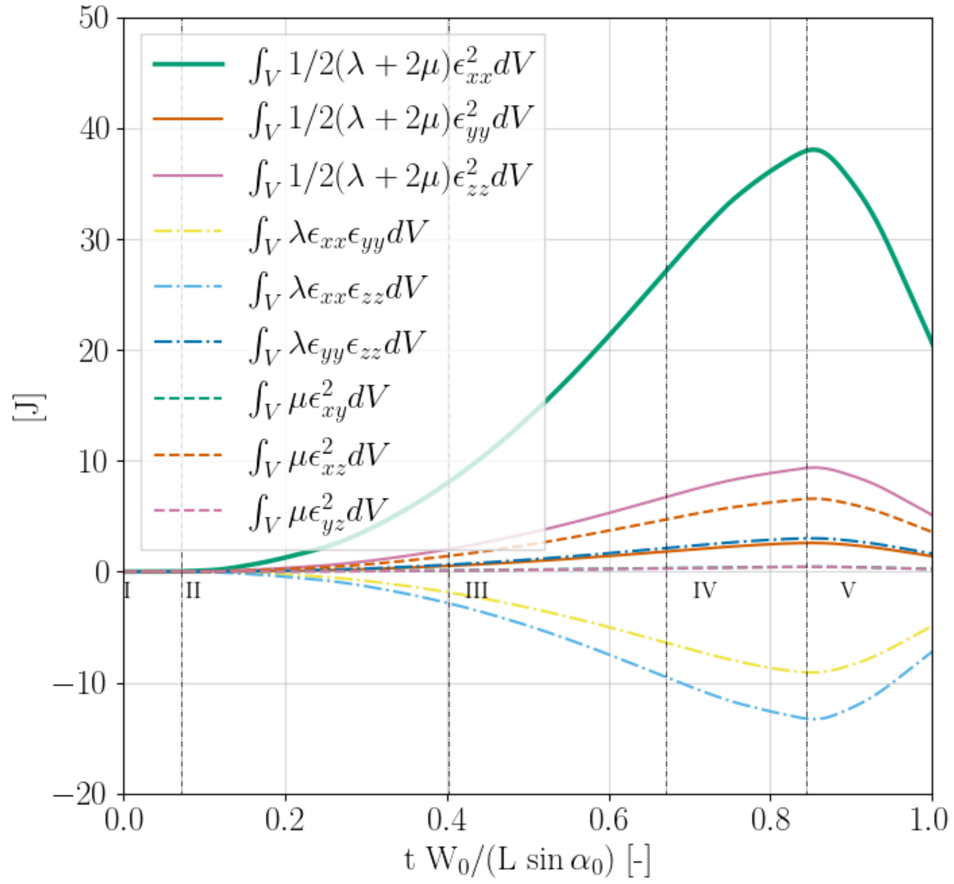

3. Conservation of Energy Analysis (11): Correlation Analysis

- A good correlation between Δp_{SR} and the elastic potential energy exists phase wise
- Δp_{SR} correlates well also with ΔW_{pR} and ΔW_M
- Δp_{SR} does not correlate well with the kinetic energy variation